

personal buildup for

Force Motors Limited Library



MTZ worldwide 2/2012, as epaper released on 18.01.2012
<http://www.mtz-worldwide.com>

content:

page 1: Energy Chains:. p.1

page 2: Cover Storyenergy Chains: Drives in Comparison. p.2

page 3: ???Johannes Winterhagen,? Editor-in-ChiefWiesbaden, 21 December 2011: ?FREEDOM REPLACES FEAR. p.3

page 4: Ulrich Spicher: Analysis of the Efficiency of Future Powertrains for Individual Mobility. p.4-11

page 12: Benjamin Bossdorf-Zimmer, Stephan Krinke, Tobias Löscher Horst: The Well-to-wheel Analysis - Measurable and Plannable Environmental Performance. p.12-17

page 18: Raymond Freymann, Jürgen Ringler, Marco Seifert, Tilmann Horst: The Second Generation Turbosteamer. p.18-23

page 24: Markus Schwaderlapp, Philipp Adomeit, Andreas Kolbeck, Matthias Thewes: Ethanol and its Potential for Downsized Engine Concepts. p.24-29

page 30: Mark Bischoff, Christian Eiglmeier, Torsten Werner, Stefan Zülch: The New 3.0-Litre TDI Biturbo Engine from Audi - Part 2: Thermodynamics and Calibration . p.30-37

page 38: Thomas Andreas, Christian Baumgarten, Christian Nisters, Harald Ortwig: Management System for the Efficient use of Gaseous Fuels. p.38-43

page 44: Hartmut Sauter, Detlef Mathiak, Jan Müller, Stephan List : Crankcase Ventilation - Inline Measurements of Oil Aerosols. p.44-47

page 48: Agostino Gambarotta, Andrea Ruggiero, Michele Sciolla, Gabriele Lucchetti: HiL/SiL System for the Simulation of Turbocharged Diesel Engines. p.48-53

page 54: Research Peer Review. p.54-55

page 56: Hans-Philipp Walther, Stéphanie Schlatter, Georg Wachtmeister, Konstantinos Boulouchos : Combustion Models for Lean-Burn Gas Engines with Pilot Injection. p.56-63

page 64: Dirk Goßlau, Peter Steinberg : Predictive Cooling System Control to Reduce Fuel Consumption. p.64-73

copyright

The PDF download of contributions is a service for our subscribers. This compilation was created individually for Force Motors Limited Library. Any duplication, renting, leasing, distribution and publicreproduction of the material supplied by the publisher, as well as making it publicly available, is prohibited without his permission.

MTZ

WORLDWIDE

02 February 2012 | Volume 73

TURBOSTEAMER of the Second
Generation

ETHANOL and its Potential for
Downsized Engine Concepts

PREDICTIVE Cooling System
Control

ENERGY CHAINS: DRIVES IN COMPARISON

COVER STORY

ENERGY CHAINS: DRIVES IN COMPARISON

4, 12 | Cars are still sold to a considerable extent on the basis of their average fuel consumption. This means that end customers base their decisions mainly on a car's local emissions. However, these do not at the same time reflect the energy balance or the sustainability of a powertrain concept. Therefore, the increasing diversity of powertrain designs in particular requires a holistic view of the energy chains involved.



COVER STORY

ENERGY CHAINS

- 4 Analysis of the Efficiency of Future Powertrains for Individual Mobility
Ulrich Spicher [KIT]
- 12 The Well-to-wheel Analysis – Measurable and Plannable Environmental Performance
Benjamin Boßdorf-Zimmer, Stephan Krinke, Tobias Lösche-ter Horst [Volkswagen]

INDUSTRY

ENERGY MANAGEMENT

- 18 The Second Generation Turbosteamer
Raymond Freymann, Jürgen Ringler, Marco Seifert, Tilmann Horst [BMW]

FUELS

- 24 Ethanol and its Potential for Downsized Engine Concepts
Markus Schwaderlapp, Philipp Adomeit, Andreas Kolbeck [FEV], Matthias Thewes [RWTH Aachen University]

DIESEL ENGINES

- 30 The New 3.0-l TDI Biturbo Engine from Audi – Part 2: Thermodynamics and Calibration
Mark Bischoff, Christian Eiglmeier, Torsten Werner, Stefan Zülch [Audi]

ENGINE MANAGEMENT

- 38 Management System for the Efficient Use of Gaseous Fuels
Thomas Andreas [Rotarex], Christian Baumgarten, Christian Nisters, Harald Ortwig [Trier University of Applied Sciences]

MEASUREMENT

- 44 Crankcase Ventilation – Inline Measurements of Oil Aerosols
Hartmut Sauter [Mahle], Detlef Mathiak [BMW], Jan Müller, Stephan List [Topas]

SIMULATION

- 48 HiL/SiL System for the Simulation of Turbocharged Diesel Engines
Agostino Gambarotta, Gabriele Lucchetti [University of Parma], Andrea Ruggiero, Michele Sciolla [Fiat]

RESEARCH

- 54 Peer Review

COMBUSTION

- 56 Combustion Models for Lean-burn Gas Engines with Pilot Injection
Hans-Philipp Walther, Georg Wachtmeister [TU München], Stéphanie Schlatter, Konstantinos Boulouchos [ETH Zürich]

COOLING

- 64 Predictive Cooling System Control to Reduce Fuel Consumption
Dirk Goßlau, Peter Steinberg [BTU Cottbus]

RUBRICS | SERVICE

- 3 Editorial
- 55 Imprint, Scientific Advisory Board

COVER FIGURE © Cliparea | Custom media / shutterstock

FIGURE ABOVE © [M] FoxPictures / shutterstock

FREEDOM REPLACES FEAR

Dear Reader,

You will almost certainly have set yourself some new objectives for the New Year. You may want to bring a specific development project to a successful conclusion in 2012. Or you may be looking for the first customer for what you believe is a highly innovative product line. Or perhaps you have other ideas.

There are good reasons for setting objectives, but they do also have their limits. Without them, we would be wandering around aimlessly and we would only be able to make progress by chance. Consequently, in January many companies start the annual process of agreeing on objectives. This involves putting in writing the contribution which each employee will make to achieving the corporate objectives and specifying the bonus that they will receive in return. But what concept of human nature lies behind these activities? Is it "homo economicus", the idea, long since discredited by research, of a person who only has an eye to his or her own interests?

The truth is quite different. People are motivated; they do not need to be motivated by someone else. People want to do meaningful work. They have ideas and they want to achieve good results when they put these ideas into practice. They support one another without expecting a reward in return.

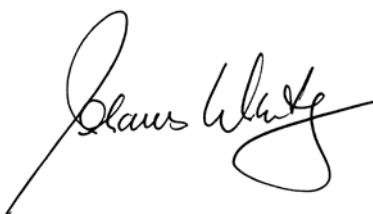
Developmental psychology research has shown without doubt that it is disastrous to give children material rewards when they learn new things. By doing this, teachers destroy the children's motivation and the result is a "What's in it for me?" attitude.

How is it that research results which have been so carefully verified have not found

their way into business practice? There is a suspicion that managers of dependent employees want to have power over people. Their employees remain in a state of dependency and fear, even if they could achieve better results by being set free.

It is likely that this problem will resolve itself. Skilled workers are in short supply in all the industrial countries. Any manager who wants to surround himself with the best people in his discipline will have to offer them freedom. In this rapidly changing world, it is acceptable for companies to be afraid of failing, but not for individual employees. Successful organisations will adapt their structures, working hours and remuneration to the needs of their people.

Bear this in mind when you are holding your meetings about annual objectives and ask your employees what they really want.



JOHANNES WINTERHAGEN, Editor-in-Chief
Wiesbaden, 21 December 2011





ANALYSIS OF THE EFFICIENCY OF FUTURE POWERTRAINS FOR INDIVIDUAL MOBILITY

A meaningful assessment of energy propulsion concepts for individual mobility must include the provision of energy as well as the entire vehicle. The Institute for Reciprocating Engines at the Karlsruhe Institute of Technology has produced an analysis that also takes into account the real operating conditions.



AUTHOR



PROF. DR.-ING. ULRICH SPICHER

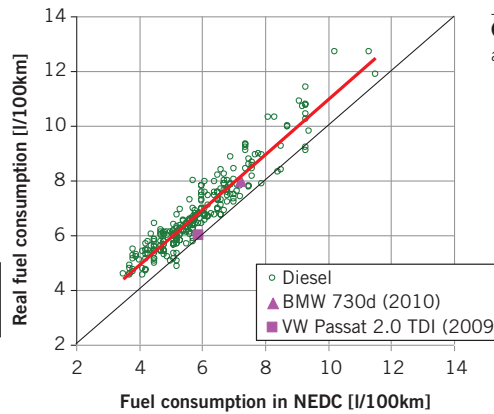
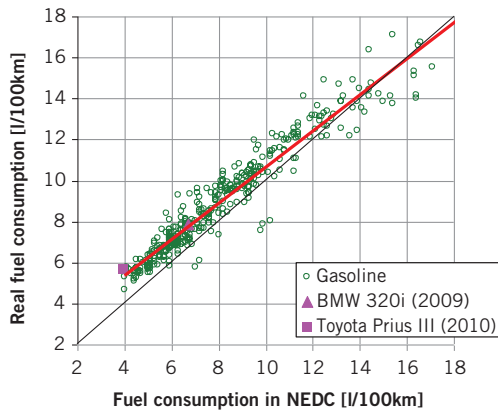
is Director of the Institute for Reciprocating Engines at the Karlsruhe Institute of Technology (KIT) (Germany).

MOBILITY AND ENERGY BALANCE

The development of future powertrains for passenger cars will strongly be determined by the kind of future mobility. In the public discussion, passenger cars with internal combustion engines (ICE) have been identified as major contributors to the greenhouse effect due to their exhaust emissions (carbon dioxide CO_2 , CO, HC, NO_x , particulates). Passenger cars are evaluated in standardized test cycles. In the EU, the New European Driving Cycle (NEDC) is used, in which only the energy content necessary for vehicle propulsion is considered as usable energy. For the operation of a vehicle, additional energy is necessary to fulfil the requirements of environment, safety and comfort, which cannot be neglected. Therefore, it is obvious that the energy balance as well as the efficiency analysis cannot be performed only for the powertrain subsystem, but instead for the total vehicle system including energy production (gasoline, diesel, electricity). Only through such considerations is a correct evaluation of the energy efficiency possible.

FUEL CONSUMPTION: TEST CYCLE AND ROAD DRIVING

For the NEDC, which is operated on a chassis dynamometer at an ambient temperature between 20 and 28 °C, the duration of the test is approximately 20 min and the total driving distance is nearly 11 km. The average speed during the cycle is 33.6 km/h. A medium-sized reference vehicle (so called C-class car) with a vehicle mass of 1700 kg, a rolling resistance coefficient of 0.012, an air resistance coefficient of 0.29 and a frontal area of 2.23 m² requires a power output of 4.96 kW at the wheels. Considering a power-train efficiency of $\eta_{\text{PT}} = 0.9$, the effective power output of the engine is $P_{\text{eff}} = 5.5$ kW. This yields to a total energy of 16.5 kWh for a driving distance of 100 km. In real traffic situations, the driving speeds are significantly higher than during the NEDC; this requires both higher engine power and more total energy. Driving at an average speed of about 60 km/h, which corresponds approximately to a real driving situation with average speeds between 50 and 70 km/h, depending on the driver



① Comparison of real fuel consumption and fuel consumption in NEDC

and the vehicle, a total energy of around 21 kWh per 100 km is necessary for the reference vehicle. In general, the fuel consumption on the road under real driving conditions is higher than the fuel consumption during the NEDC, ①. This evaluation considers new cars produced between 2008 until 2011, which were tested by German automobile magazines (Auto Motor Sport – AMS). The real fuel consumption was taken from the test reports as well as from some selected reference vehicles that were driven under real traffic conditions. The comparison of fuel consumption for the reference vehicles suggests that fuel consumption from the test reports can be approximated by the following correlation:

$$\text{Real fuel consumption} = 0.5 \cdot (\text{AMS test consumption} + \text{AMS fuel saving test consumption})$$

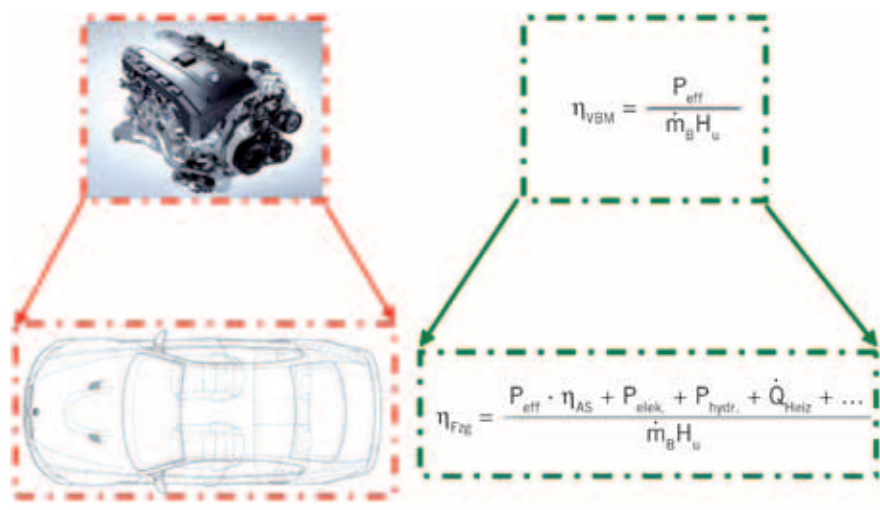
The values of fuel consumption from the AMS fuel saving mode were normally on the same level as those of the NEDC, while the overall fuel consumption in the test reports was always higher than the fuel consumption of the reference cars. The fuel consumption of the reference vehicle considered in this study was 6.2 l/100 km (62 kWh) with a Diesel engine and 8.5 l/100 km (74 kWh) with an SI engine. Therefore, just 2.1 l of Diesel fuel or 2.4 l gasoline are necessary for real driving of 100 km. The calculation of the efficiency of the powertrain in the system „tank-to-wheel“ results in a powertrain efficiency of 33.9 % for the Diesel engine and 28.2 % for the SI engine. Altogether, it can be seen from ① that the real fuel consumptions for the SI engine and for the

Diesel engine are typically 10 to 20 % higher than the fuel consumption in the NEDC. Sporadically, smaller or bigger deviations can be recognized, whereby Hybrid vehicles are conspicuous. For example, the Toyota Prius III-Hybrid with a real fuel consumption of 5.7 l/100 km shows an increase in fuel consumption of 46 % compared to the fuel consumption of 3.9 l/100 km in the NEDC. Due to these results, it can be concluded that the NEDC is not well-suited for the evaluation of hybrid vehicles.

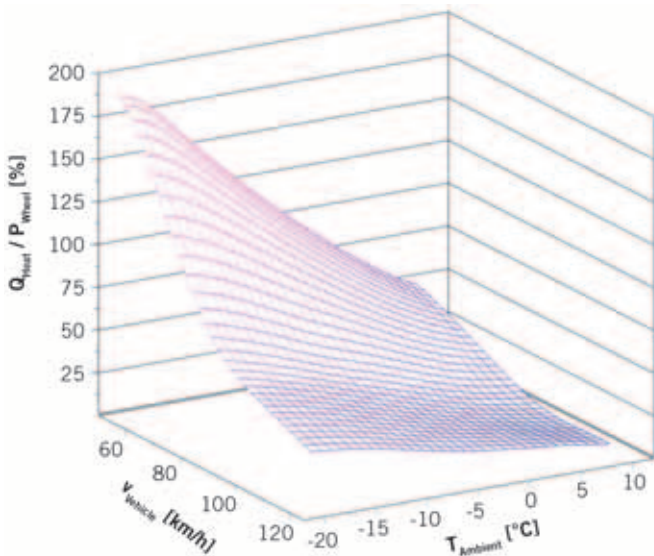
EXTENSION OF THE SYSTEM BOUNDARIES

Today, the passenger car is the symbol of individual mobility in almost all industrial countries on earth and has to fulfil manifold targets in addition to driving. Therefore, it is obvious that in addition to the

energy required for driving, all the other energy demands for safety, comfort and environment have to be considered in the evaluation of the efficiency of the energy use. This leads to an extension of the powertrain system “tank-to-wheel” to the system “well-to-wheel”, in which the production of the fuel, the portion of the fuel used for driving and the portion used to fulfil safety, comfort, and environmental requirements are considered. ② shows the differences between these two energy systems as well as the change of the efficiency equations. All energy conversions inside the car have to be considered for the evaluation of the efficiency of the system “vehicle”. This is pointed out in the equation for efficiency with the extension from the system “engine” to the system “vehicle”, ② (right). This is similar to energy evaluation of buildings, in which not only the heating



② Extension of system boundaries



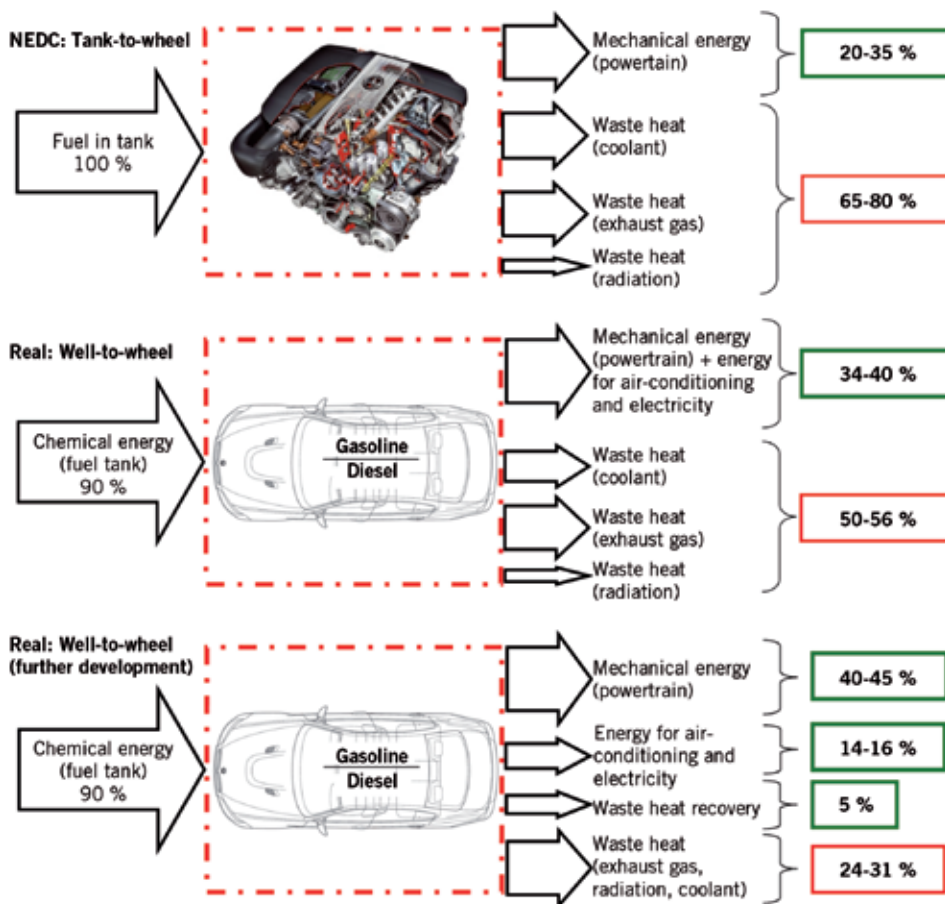
③ Relation of heating energy to power at wheels

power for auxiliary equipment in the vehicle. This propulsion energy is considered in the efficiency of the powertrain, while the energy for auxiliary units is considered as energy loss. For example, the auxiliary unit “alternator” delivers the electric energy for the entire car. This energy should be considered when evaluating the total efficiency. The heat in the cooling water and the exhaust as well as the heat radiation is normally considered as a loss in the energy balance. However, a part of this heat loss can be used for heating the cabin of the vehicle for comfort. Therefore, in a correct energy balance of the total energy system “vehicle”, this part of the engine heat loss has to be considered in the efficiency balance. This leads to the equation of the total efficiency of the energy balance for the system “vehicle”, shown below on the right of ②.

Independent of the powertrain, the warming or cooling of the vehicle’s interior requires either heating energy or cooling energy which has to be delivered to the cabin. ③ shows the correlation of the

equipment is considered as a criterion for the energy efficiency of the building, but also the insulation quality of the building itself, including heating losses through walls, windows, roof, etc.

In internal combustion engines, the chemical energy of the fuel is converted to heat and then to mechanical energy. The mechanical energy is used for propulsion via the powertrain as well as for

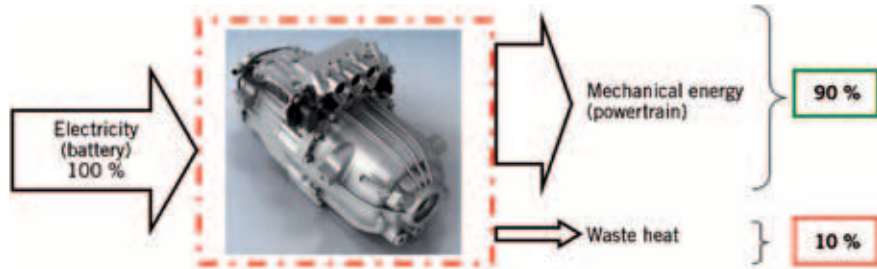


④ Comparison of efficiency with „tank-to-wheel“ and „well-to-wheel“ evaluation

heating energy needed for warming the cabin and the power needed for driving the reference car, depending on the driving speed as well as on the ambient temperature. Considering a driving speed of 60 km/h, the ratio of heating power to driving power is 64 % for an ambient temperature of 0 °C. At an ambient temperature of 10 °C, the ratio increases to 106 % and at 20 °C to 152 %.

Investigations with a Diesel engine in [1] have shown that during part load (city driving) with high exhaust gas recirculation (EGR) rates, up to 38 % of the energy of the fuel used is delivered as heating energy to the cooling water. This heating energy decreases to 20 % of the fuel energy with increasing load and reduced EGR-rates or without EGR. The heat loss which is transferred to the cooling water can be used for heating the passenger cabin, which results in a positive effect of comfort for the passengers. Considering only the energy balance system “powertrain”, this positive energy contribution is defined as a loss. With the evaluation of the energy balance system “vehicle”, the energy for cabin heating is considered in the efficiency of the system, because the cabin heating energy is available without any additional fuel.

Comparing the efficiency of the powertrain in the NEDC (“tank-to-wheel”) with the energy balance of the system with the boundaries “well-to-wheel”, the appropriate values are shown in ④. For the “tank-to-wheel” method in the NEDC the efficiency of the powertrain of the reference car is 29.5 %. Depending on both the car and the powertrain, current cars have powertrain efficiencies between 20 to 35 %.



⑤ Efficiency of electric powertrain (battery-to-wheel: „tank-to-wheel“)

Thus, the total energy loss is 65 to 80 %. For the evaluation of the system “well-to-wheel”, the energy for oil production, oil refining and transport of the fuel to the tank has to be considered, too. The energy used for that can be assumed to be approximately 10 % of the total energy content of the crude oil [2]. Thus, the energy content of the fuel in the tank is 90 % of the primary energy. Therefore, the value of the efficiency of the powertrain and all other efficiencies, which have to be considered in the total energy balance system “well-to-wheel”, must be reduced by 10 %, or multiplied with the factor 0.9.

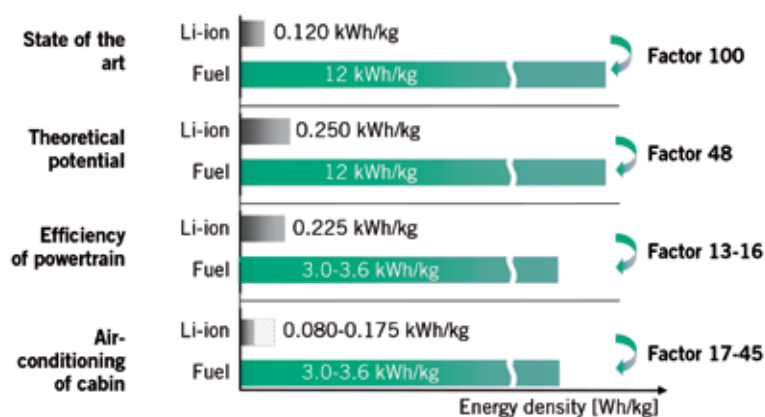
Depending on ambient temperature and requirements on comfort, safety, and environment, the engine efficiency of a car with an ICE as a powertrain is significantly higher than the engine efficiency of only the powertrain. The average powertrain efficiency is about 25 % (SI engine) and 30 % (Diesel engine) under real world driving conditions, while the average engine efficiency, related to the total energy balance system “tank-to-wheel” including vehicle” is between 38 % (SI engine) and 45 % (Diesel engine) for the

driving speed 60 km/h with an annual averaged ambient temperature in Germany of about 10 °C. Considering the loss of 10 % for fuel production, the real engine efficiency for the total energy balance system “well-to-wheel” is about 34 % (SI engine) and about 40 % (Diesel engine) under averaged driving and ambient conditions for a medium-sized car. With other ambient conditions and smaller or bigger cars and slower or faster driving these efficiency values increase or decrease.

Significant potential exists to improve the engine efficiency of ICE. It is expected in research and development of ICE, that the powertrain efficiency with the SI engine can be improved to at least 40 % and with the Diesel engine to at least 45 %. In addition, research and development is being carried out to utilize the waste heat and convert it to electric energy for auxiliary units, for boosting, for heating, and for the power-train itself. Analyses in [3] have shown that an improvement of up to 5 % in the total efficiency of the system “powertrain and vehicle” can be achieved. Therefore, total efficiencies of the system “well-to-wheel” of 54 % (SI engine) and 61 % (Diesel engine) at averaged operating conditions (ambient temperature 10 °C, averaged driving speed of about 60 km/h, medium-sized car) are possible.

EFFICIENCIES WITH ELECTRIC POWERTRAIN

Currently, electric mobility is favoured and politically advocated as a future powertrain solution for vehicles. The main advantages are apparently both the low energy requirement for electric driving and the low environmental pollution by CO₂ emissions. With the principle of “tank-to-wheel”, only the energy conversion from the battery in the car to the



⑥ Comparison of energy density (Fuel; Lithium-ion battery)

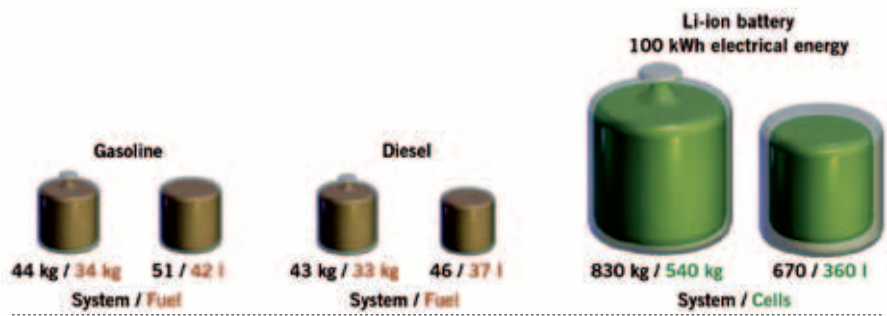
wheels is considered, ⑤. Electric motors have very good efficiencies of about 90 %, while the heat loss is only about 10 %. This leads to the general opinion that the electric powertrain is significantly superior compared to an ICE powertrain.

Extending the boundaries from “tank-to-wheel” to “well-to-wheel”, the loss of energy for the production of electricity, delivery to the electrical outlet, and charging of the battery have to be considered. Additionally, the energy required for the auxiliary units has to be considered. A further amount of energy is necessary for the transportation of the very heavy battery in the car during driving (significantly higher mass of the vehicle). Considering the reference car (C-class) for a comparison, an energy amount of about 21 kWh per 100 km (equivalent to 2.1 l Diesel or 2.4 l gasoline) is necessary for driving the car, either with an ICE or with an electric motor, because for both powertrains, the mass of the car is assumed to be the same. However, the mass of the electrically driven car is indeed higher due to the battery. Furthermore, the energy amount for real world driving with changing ambient conditions has to be considered.

Air-conditioning of the car cabin has a big influence on the energy requirements, ③. Heating the cabin requires additional energy of 8 kWh (0.8 l Diesel or 0.95 l gasoline). This corresponds to about 40 % of the energy needed to drive the car 100 km at a speed of 60 km/h with an ambient temperature of 10 °C (annual average temperature in Germany). This additional energy for heating the cabin is directly included in the fuel consumption of an ICE without additional fuel, while this heating energy has to be provided by the battery with an electric powertrain. To supply the vehicle with electric energy for both safety and comfort functions (about 10 % of the energy for driving), the addition of nearly 2 kWh has to be considered. Therefore, altogether energy of about 31 kWh (21 kWh + 8 kWh + 2 kWh) is necessary for driving the reference car over a distance of 100 km, either with an ICE powertrain or with an electric powertrain.

ENERGY STORAGE

The storage of electric energy in the battery is exceptionally important for electric driving. It is expected that energy density of



⑦ Energy storage in vehicle (500 km range of driving)

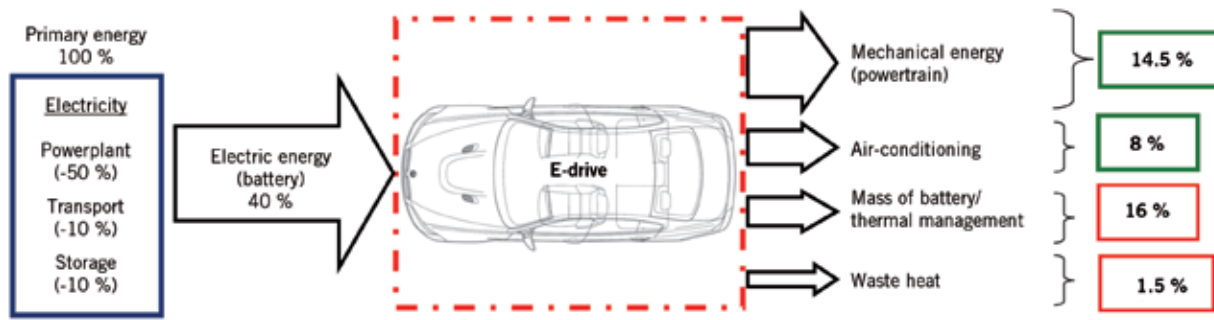
Lithium-ion batteries will be significantly improved in the future. ⑥ shows the state of the art as well as the theoretical limits of this battery technology regarding energy density compared to fossil fuels (gasoline, Diesel). A comparison of the energy density of gasoline and Diesel (approximately 12 kWh/kg) with that of modern, state-of-the-research cells for Lithium-ion batteries [4], which is about 0.12 kWh/kg shows that the energy density ratio between fossil fuels and these batteries is about 100:1. Considering the theoretical potential, which is expected to be 0.25 kWh/kg [4], the relation will be 48:1 and still on a very low level in comparison to gasoline and Diesel. Due to the efficiencies of the different power-trains, the ratio is reduced to 16:1 with the Diesel engine ($\eta_A = 30\%$) and to 13:1 with the SI engine ($\eta_A = 25\%$) compared to the electric motor ($\eta_A = 90\%$). This ratio becomes worse again (17:1 to 45:1), when the energy for air-conditioning the cabin is considered, depending on the ambient conditions.

Additionally, the mass of the battery has to be considered. ⑦ shows a comparison of different energy storage systems for passenger cars with a driving range of 500 km [5]. This driving range is expected from most of the customers (more than 90 %) who normally use vehicles. The comparison of the systems shows that a Lithium-ion battery needs energy of 100 kWh (NEDC-conditions) for driving 500 km, whereby due to the further developments the theoretical energy density of this battery technology will be reached. However, the required mass of the battery cells is more than 500 kg. In addition, due to the mass of the thermal management device for the battery, the mass increases to more than 800 kg. As already mentioned, under real world operating con-

ditions, a higher energy of 155 kWh is necessary, which requires an additional increase of the battery mass. Considering the additional energy for the transport of such a battery (55 kWh with 100 kWh and 75 kWh with 155 kWh), both the mass of the battery and the energy rise to total masses and energy amounts of about 1100 kg with 155 kWh and about 1450 kg with 230 kWh.

“WELL-TO-WHEEL” ANALYSIS

⑧ shows the result of a “well-to-wheel”-analysis (as in ④). Depending on the primary energy used for the power generation (20 % renewable, 20 % nuclear power; 60 % black and brown coal, natural gas) [6], the efficiency of power generation in a fossil fuel power plant can be estimated to be approximately 50 %. Due to the fact that nuclear power and renewable energy is considered as free of emissions, only the electricity from power plants with fossil energy carriers is considered in the further calculations. With the assumption of 10 % loss of energy for both electricity transport and charging the battery, the efficiency up to the battery in the car decreases to 40 %. A big portion of the energy stored in the battery (about 16 %) has to be used for the transportation of the battery itself and the equipment for its thermal management, which means a further reduction of efficiency. The energy requirement for air-conditioning and auxiliary units (comfort and safety) is around 8 % and has to be considered as a positive effect with an increase of efficiency. That means that just 16 % of the primary energy remains for the powertrain. The result is a total efficiency of 22.5 % for a car with an electric motor (14.5 % efficiency of the powertrain and



8 „Well-to-wheel“-analysis of electric powered vehicle with 500 km range of driving

8 % for air-conditioning and for functions of both safety and comfort). Altogether, with 17.5 % of the primary energy for battery transport and thermal management of the battery as well as heat loss and 60 % energy loss due to power generation and delivery to the car, the total amount of energy loss in efficiency is about 77.5 %.

IMPACT ON THE ENVIRONMENT

Because political and public discussions about future powertrains for passenger cars are mainly focussed on the so-called greenhouse effect and the related CO₂ emissions, the analysis has to include the influences on the CO₂ emissions. From analyses of the energy economical situation in [6] and the determined correlation from this report, it can be summarized that passenger cars in Germany produced about 105 Million t CO₂ in 2010. Power generation caused a total of 320 Million t CO₂ in 2010. The total amount of electricity in 2010 was about 600 TWh. This leads to emissions of 530 g CO₂/kWh. This calculation considers the energy mix in Germany, consisting of 40 % power generation without CO₂ emissions (renewable, nuclear power) and 60 % power generation from fossil energy carriers (black coal, brown coal, natural gas). The emission of

CO₂ from power generation in coal power plants is about 880 g CO₂/kWh.

The calculation of the CO₂ emissions from passenger cars in Germany results in following: With an annual driving distance of about 600 billion km and the fuel consumption of the reference car of 8.5 l per 100 km with gasoline and 6.2 l per 100 km with Diesel fuel and a share of SI engines to Diesel engines of 70:30 [7], the emission is 323 g CO₂/kWh. The factor between these two values is 1.6, which means that in Germany more harmful climate emissions are produced by power generation than by passenger cars for a given energy content.

CONCLUSION

An objective assessment of different concepts for powertrains of passenger cars must be the basis of the structure of future individual mobility. Considering both energy efficiency and CO₂ emissions, the ICE powertrain is already today superior compared to an electric powertrain. Furthermore, the individual benefit, the comfort and the costs with ICE is of big advantage. This will not change during the next decades, because the total change of power generation to renewable

power generation will need much longer than expected in the public discussion. The reason is that not only the electric energy of today has to be produced; a significant amount of additional electric energy for mobility will be necessary. Due to this correlation it is obvious that the further development of SI engines and Diesel engines is still the best solution to reduce greenhouse emissions and costs. Additionally, there is a big potential by using new fuels made from biomass for the ICE, the so called „tailor-made-fuels“.

REFERENCES

- [1] Donn, Chr.; Zulehner, W.; Ghebru, D.; Spicher, U.; Honzen, M.: Experimental Heat Flux Analysis of an Automotive Diesel Engine in Steady-State Operation and During Warm-Up, SAE 2011-24-0067
- [2] Schaub, G.; Turek, Th.: Energy Flows, Material Cycles and Global Development. Springer-Verlag, ISBN 978-3-642-12735-9
- [3] Span, R.; Eifler, W.: Nutzung der Motorabwärme durch Kreisprozesse. FVV Abschlussbericht zum Vorhaben Nr. 1009, Issue R553-2011
- [4] Ogumi, Z.: State-of-the-Art of Rechargeable Batteries for Vehicles. SAE/JSAE 2011, Kyoto Keynote-Speech, September 2011
- [5] Thiesen, L. P.: Strategie für das Elektrozeitalter, Elektromobile Vielfalt. Begleitheft zur Einführung des Opel Ampera, April 2011
- [6] Fahl, U.; Blesl, M.; Thöne, E.: Energiewirtschaftliche Gesamtsituation. BWK Das Energie-Fachmagazin Bd. 63 (2011) No. 4
- [7] <http://www.kba.de>, 2011

12th Stuttgart International Symposium



Automotive and Engine Technology

VEHICLE TECHNOLOGY

Aerodynamics, new vehicle concepts, driving dynamics and driver assistance systems

VEHICLE POWERTRAIN

Hybrid technology, alternative fuels, spark-ignition and diesel engines, engine management and modelling

VEHICLE ELECTRONICS

Electric vehicles, software and design, modelling and simulation

13 and 14 March 2012
Stuttgart | Germany

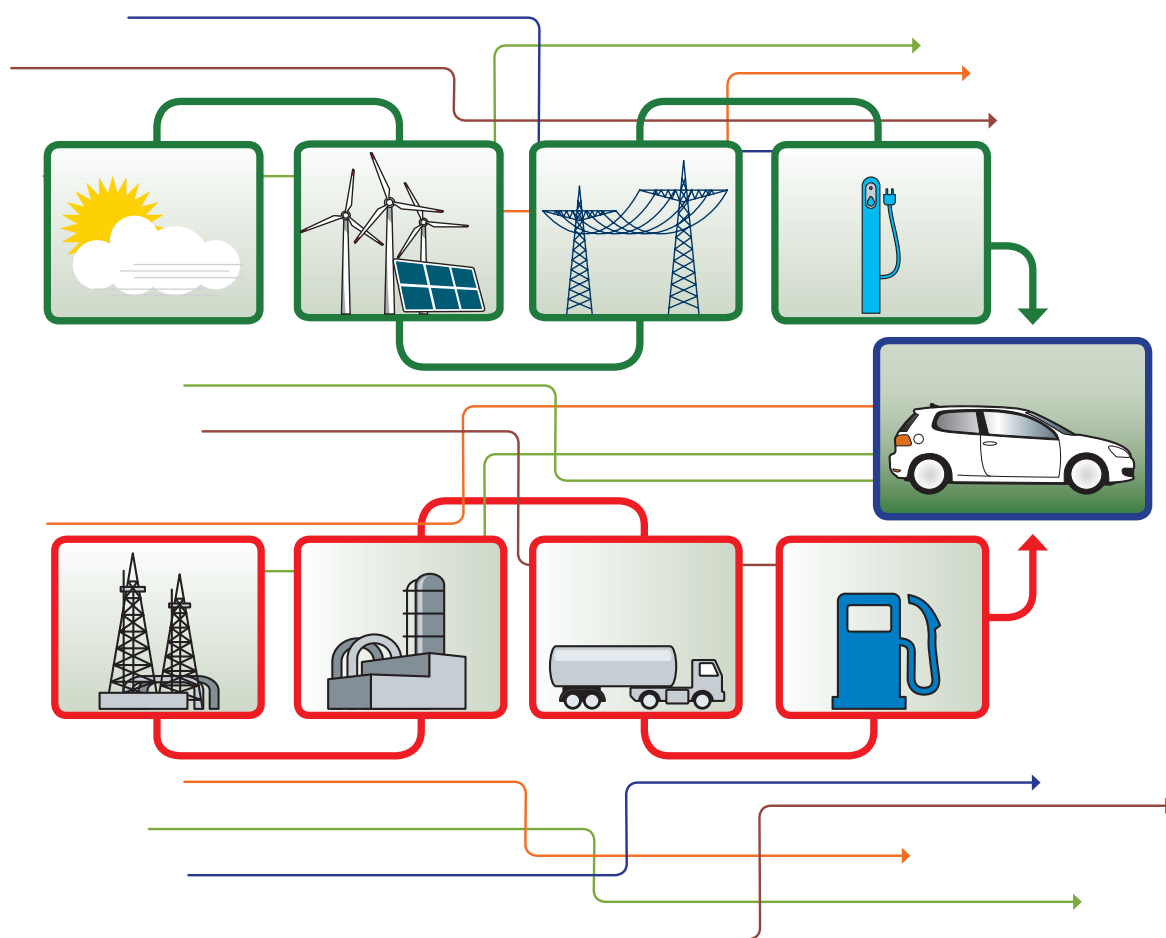


ATZ live
Abraham-Lincoln-Straße 46
65189 Wiesbaden | Germany

Phone +49 (0)611 / 7878 – 131
Fax +49 (0)611 / 7878 – 452
ATZlive@springer.com

PROGRAM AND REGISTRATION
www.ATZlive.com

THE WELL-TO-WHEEL ANALYSIS MEASURABLE AND PLANNABLE ENVIRONMENTAL PERFORMANCE



Climate change and resource depletion present a major challenge for the automotive industry. As oil reserves dwindle, so other resources capable of providing energy for the mobility sector are being sought, and alternative powertrain solutions are taking on a new significance. At the same time the efficiency and greenhouse gas emissions of the different types of vehicle can no longer be measured simply by focusing narrowly on powertrain performance but only by looking at the complete energy chain from resource to road. VW has created a “well-to-wheel” analysis to provide support in developing a sustainable fuel & powertrain strategy.

AUTHORS



BENJAMIN BOSSDORF-ZIMMER
is responsible for Environmental Analysis of Powertrains & Fuels at Volkswagen Group Research (Environmental Affairs Product) in Wolfsburg (Germany).



DR. STEPHAN KRINKE
is Head of Environmental Affairs Product at Volkswagen Group Research in Wolfsburg (Germany).



DR. TOBIAS LÖSCHE-TER HORST
is Head of Powertrain Research at Volkswagen Group Research in Wolfsburg (Germany).

FOCUS

In such an analysis, vehicles and powertrains are assessed with reference to sustainable resource use and reduced CO₂ emissions, taking into account the fact that the efficiency of a vehicle powertrain is not determined just by the efficiency of the engine but also – particularly in light of the increasing diversity of available fuels and energy sources – by the efficiency of the upstream energy production and supply chain. To make such a comprehensive assessment of the efficiency and CO₂ emissions of a powertrain system, the energy chain must be analysed in its entirety – from energy source, or well, to wheel.

WELL-TO-WHEEL

This well-to-wheel study is based on standardised methodology and data, and on systematic environmental and powertrain research analyses and simulations carried out by Volkswagen. It looks both at internal combustion engines and also at fully or partially electrified powertrains, in both cases with reference to a C-segment vehicle. The trends which emerge from this study are also relevant in principle for powertrain concepts used in other vehicle segments. The following fuels were considered:

- : petrol
- : diesel
- : natural gas/biogas
- : LPG
- : biofuels (petrol/diesel)
- : electricity
- : hydrogen.

In the case of electric vehicles, several different well-to-tank pathways for the

electricity (or hydrogen) were considered, ❶. Other pathways exist, in addition to those depicted, but were not examined in the study.

THE CRITERIA

The following criteria are key to ensuring comparability:

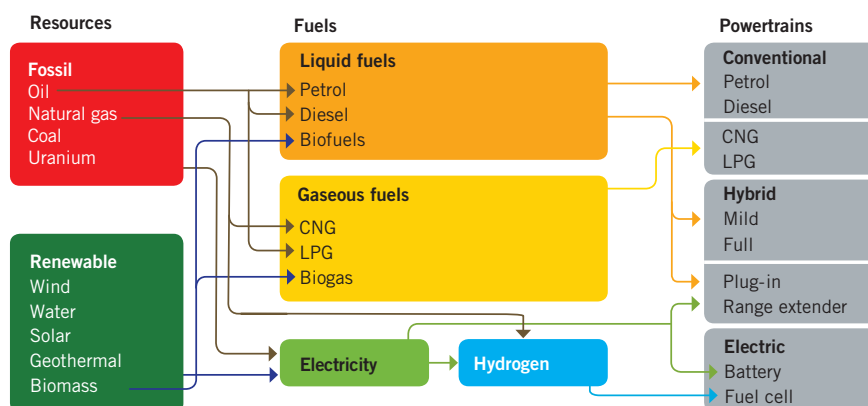
- : identical vehicle class (in this case C-segment)
- : similar engine power
- : similar minimum range (in this case 160 km)
- : all values based on same driving cycle (in this case “New European Driving Cycle”).

The inherent differences between the various powertrains result in variations in customer-related benefits such as range and infrastructure. However, this does not conflict with the objectives of the study, where the focus is on ensuring a uniform evaluation framework.

In evaluating the energy and environmental profile of the various powertrains and fuels, the study looks at the entire energy chain starting with extraction of the resource. The manufacture and recycling of vehicles, or vehicle powertrains, is not considered. The CO₂ profile is quantified in terms of emissions of carbon dioxide and also of other greenhouse gases, expressed in the form of CO₂ equivalents (CO₂eq) [1].

Energy efficiency is calculated by measuring the amount of primary energy resources required at the front end of the energy chain to move a vehicle 100 km at the output or back end of the chain. The study focuses not only on production of the final fuels or final energy – i.e. the processes at the refineries where petroleum-based

❶ Energy chains for powertrain concepts examined in the study



fuels are produced and at the power stations where electricity is produced – but also looks at extraction, processing and transport processes. All peripheral plant and equipment (e.g. compressors, etc.) is also taken into account. By applying the efficiency approach [2], renewable and fossil-based fuels become comparable on the basis of energy efficiency.

For biofuels, for example, the energy chain begins with the initial biomass (sowing, fertilisation, harvesting, transport, processing, etc.). For wind power on the other hand, it begins with the harvested electricity.

The energy and environmental profiles for a given energy pathway are quantified using data from the “European Life Cycle Database”, supplemented by data supplied by the Gabi Life Cycle Assessment software [3,4].

CO₂ AND ENERGY EFFICIENCY OF POWERTRAINS AND FUELS

② shows (top) the well-to-wheel profiles of conventional, ICE-based powertrain concepts. These are calculated by adding

together the direct emissions from current-design production vehicles (naturally aspirated petrol engine (MPI), twincharger petrol engine (TSI), diesel engine (TDI)) and the additional impacts from the fuel production and supply (“well-to-tank”) process. The environmental profile calculation for the production and supply of petroleum-based fuels is based on an analysis of conditions in the European refining industry.

The specific refinery emissions for a given end energy product are calculated on the basis of the energy consumed in manufacturing each single product. Similarly, the specific energy demand is calculated on the basis of oil consumption.

Such a calculation approach matches fuel production and delivery inputs fairly and accurately to the specific end product. This approach shows for example that petrol has higher energy inputs than, say, diesel. Conventional petrol and diesel powertrains are also assessed in conjunction with various levels of hybridisation. Increasing levels of hybridisation progressively reduce fuel consumption and therefore improve well-to-wheel performance.

Depending on electricity mix and battery size, further hybrid concepts not shown in ② are possible (in particular plug-in and range extender concepts).

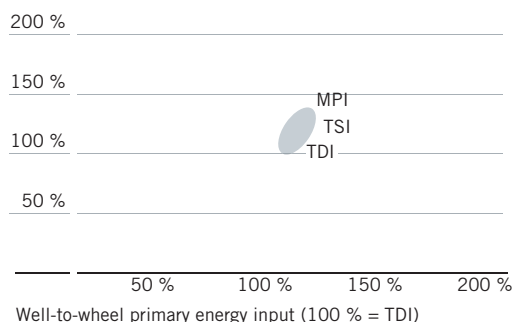
Use of gas-based fuels (natural gas (CNG) and LPG) impacts the energy chain in two ways: not only is the well-to-tank pathway for gas fuels less energy-intensive than the pathways for petroleum based fuels, but also the emissions from the vehicle itself (“tank-to-wheel” phase) are relatively low. This results in a good overall CO₂ profile for gas-powered vehicles based on TSI petrol engines.

ELECTRIC POWERTRAINS

② (bottom left) shows the results of a well-to-wheel analysis for battery (BEV) and fuel-cell powered (FCEV) electric vehicles. The influence of regional factors on CO₂ and energy performance is greater for electricity production than for fuel production. For battery-powered electric vehicles therefore, various different regional electricity mixes were taken into account. Operating a battery electric vehicle on Chinese electricity produces higher car-

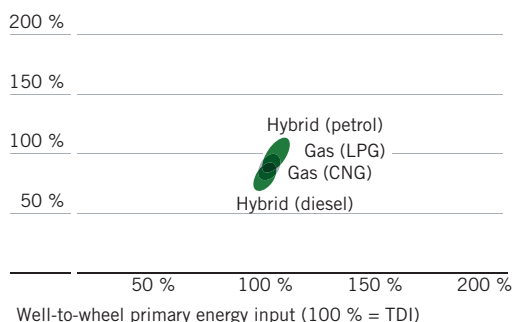
Conventional powertrains

Well-to-wheel CO₂eq (100 % = TDI)



Gas and hybrid powertrains

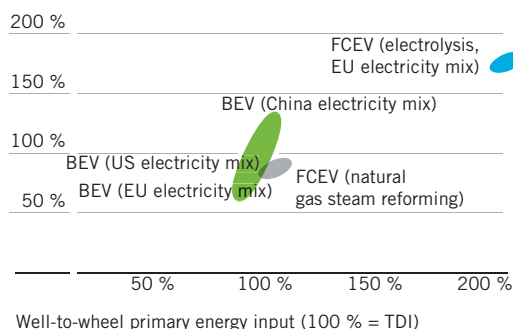
Well-to-wheel CO₂eq (100 % = TDI)



② Well-to-wheel performance of different types of powertrain and fuel

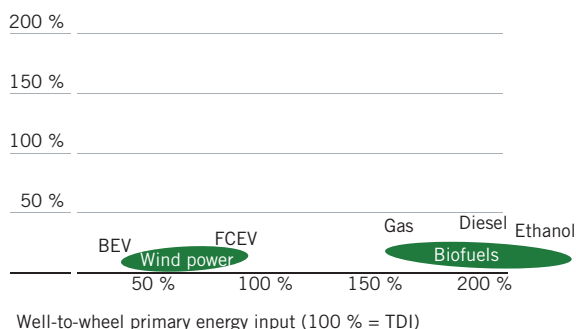
Electric powertrains

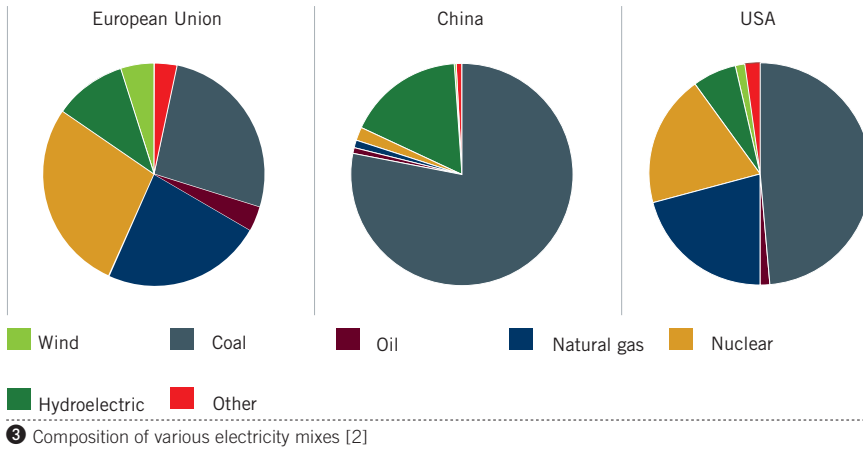
Well-to-wheel CO₂eq (100 % = TDI)



Renewable energy

Well-to-wheel CO₂eq (100 % = TDI)





bon dioxide emissions, due to the relatively CO₂-intensive plants used to produce the power, compared with operating such a vehicle on the EU electricity mix, ③. The following criteria are the main factors influencing the efficiency and CO₂ emissions of the power industry in different world regions:

- : power generation technology
- : age/capacity utilisation of the regional plant stock
- : energy sources used (gas, coal etc.)
- : use/rate of combined power and heat production.

As well as providing the driving power for battery electric vehicles, electricity is also used as the energy source for electrolysis of hydrogen. If the electricity used to produce H₂ is generated using the current EU mix, ② (EU), the CO₂ and energy profile of the fuel cell vehicle is sobering. This solution does, however, offer benefits if surplus electricity can be used which would otherwise go to waste, or if the electricity is generated renewably, ② (bottom right). In this case fuel cells represent a genuinely viable alternative – particularly for long-range mobility. As a transitional scenario, it is also possible to produce hydrogen by means of natural gas steam reforming – a process widely used in industry.

Subject to these conditions, a fuel-cell vehicle can offer a well-to-wheel performance similar to that of conventionally powered vehicles. Renewable energy can likewise be used in battery electric vehicles. In an overall comparison, the well-to-wheel performance of a BEV powered by renewable electricity is the best of any of the powertrains considered in the study.

BIOFUELS

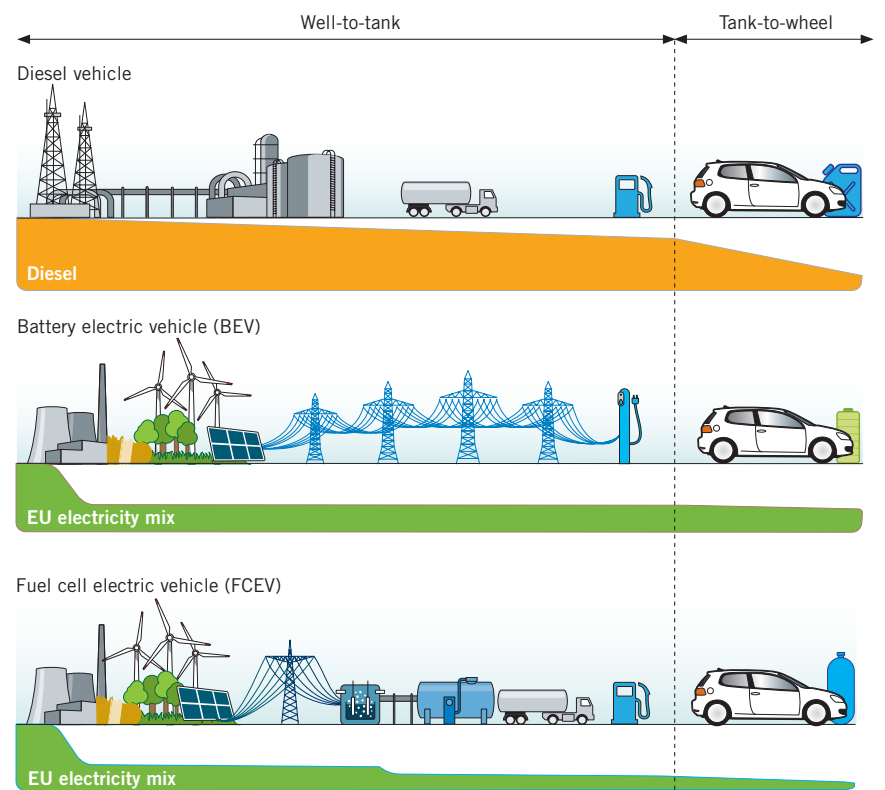
One possible future fuel option for internal combustion-based powertrains is bio-fuels. If such fuels are produced using biomass residues (e.g. straw, wood residues), significant advantages can be achieved in terms of well-to-wheel CO₂ emissions. The fewer the stages in the process of converting biomass into fuel, the greater the efficiency of the energy chain. For example biogas, used in a natural gas vehicle, has

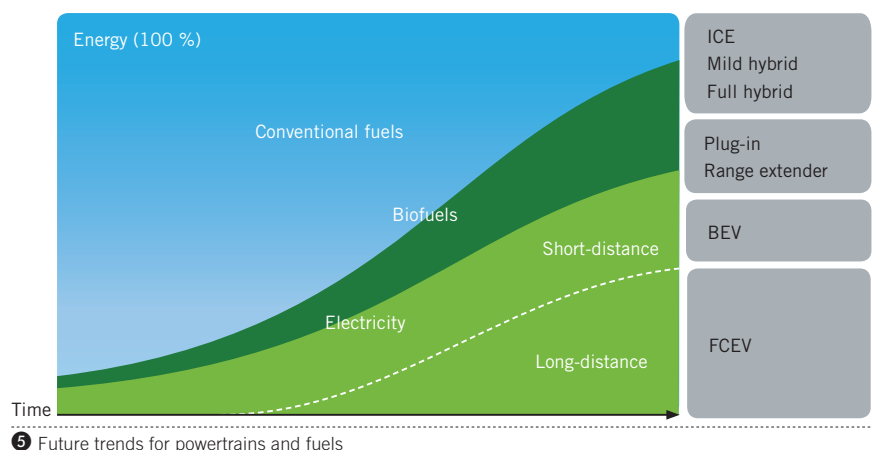
slight efficiency advantages compared with liquid biofuels.

THE ROUTE TO SUSTAINABLE MOBILITY

All these drive systems are capable of meeting high standards in terms of CO₂ and energy efficiency. ④ presents a clear picture of the efficiency profiles of the energy chains for the various powertrains and fuels. In the case of internal combustion-based powertrains, efficiency losses and CO₂ emissions are concentrated mainly in the driving phase, i.e. the “tank-to-wheel” phase. In the case of fuel-cell and electric vehicles on the other hand, emissions and energy losses occur mainly at the fuel production and delivery stage, i.e. in the “well-to-tank” chain. In this case the choice of upstream energy chain has important implications. In fact the choice of electricity mix or of hydrogen production route is more significant in terms of well-to-wheel performance than, for example, modifications to the efficiency of the powertrain.

Ultimately, sustainable mobility can only be achieved through end-to-end opti-





misation of the energy chain. Well-to-wheel analysis is an important step in identifying the relevant action areas here. As far as the automotive industry is concerned, continuous improvement of vehicle and powertrain technologies will remain a key task into the future.

The energy production and delivery chain is taking on increasing significance in light of resource depletion and the increasing diversity of available powertrains and fuel types. Biofuels can make a contribution in this context. However, their availability is limited.

The market introduction of electric vehicles must be coupled with the intro-

duction of renewable energies. Only in this way will electrically powered vehicles ultimately be able to make a substantial contribution to improving CO₂ performance and energy efficiency in the mobility sector.

CONCLUSION

Electric drive, in conjunction with renewable electricity, is paving the way for sustainable mobility. Fuel-efficient internal combustion engines – particularly in combination with biofuels – are likewise making a contribution. 5 shows possible future trends for differ-

ent automotive fuels and associated powertrain systems. In this context, the only way a full transition to renewable energy can be achieved, over time, is through large-scale adoption of electric drive. The long-term aim will be to use such energy in both short-distance and long-distance mobility.

Well-to-wheel analysis is a necessary and appropriate tool for quantifying the CO₂ emissions and energy consumption of powertrain systems and fuels along the entire energy chain. It provides a way of making environmental performance measurable and strategically plannable.

The well-to-wheel study has been audited by TÜV Nord CERT GmbH and certified as compliant with DIN ISO 14040 [5].

REFERENCES

- [1] Guinée, J. B.; Lindeijer, E.: Handbook on Life Cycle Assessment: Operational guide to the ISO standards. Dordrecht: Kluwer Academic Publishers 2002
- [2] International Energy Agency: „World Energy Outlook 2010“. Paris: IEA Publications, 2010
- [3] Joint Research Center (JRC) of the European Commission: European Life Cycle Database. Ispra: JRC, 2010
- [4] PE International: Life Cycle Assessment database of GaBi Software. Stuttgart: PE International, 2011
- [5] International Organization for Standardization: ISO 14040: Environmental Management – Life Cycle Assessment – Principles and Framework. 2nd ed. Geneva: International Organization for Standardization, 2006

FROM KNOWLEDGE
TO SUCCESS
VIA NEWS,
INFORMATION,
INSIGHTS AND
EXPERIENCES.



**ATZ AUTOTECHNOLOGY. THE PUBLICATION
THAT MOVES THE AUTOMOTIVE WORLD.**

Make the connection to international automotive progress with **ATZ autotechnology**, along with highlights from automotive engineering, production, electronics and engine development. Also read international and FISITA news, interviews and Global Viewpoint. 6 times per year, free of charge.

Register now at: www.ATZautotechnology.com

ATZ autotechnology



THE SECOND GENERATION TURBOSTEAMER

Waste heat recovery is the key to further reductions in fuel consumption and exhaust emissions. In 2005, the potential of this approach was demonstrated for the first time with the BMW Turbosteamer. With the second generation, the system design has been thoroughly simplified to enable efficient vehicle integration.

AUTHORS



PROF. DR.-ING. HABIL. RAYMOND FREYMANN
is Director of BMW Forschung und Technik GmbH in Munich (Germany).



DIPL.-PHYS. JÜRGEN RINGLE
is Group Manager of the Thermal Energy Conversion Team at BMW Forschung und Technik GmbH in Munich (Germany).



DR. DIPL.-PHYS. MARCO SEIFERT
is Manager of the Research Project "Turbosteamer" at BMW Forschung und Technik GmbH in Munich (Germany).



DIPL.-ING. TILMANN HORST
is Ph.D. Student in the Thermal Energy Conversion Group at BMW Forschung und Technik GmbH in Munich (Germany).

USE OF WASTE HEAT FOR EFFICIENCY INCREASE

The global increase of population and industrialisation leads to a rising demand for personal mobility. Since anthropogenic emissions have already reached a critical level, highly efficient and environmentally friendly powertrains are of great significance. In recent years, the BMW Group has already achieved a huge increase in efficiency through the fleet-wide introduction of EfficientDynamics technologies such as direct fuel injection, fully variable valve timing, turbo charging, brake energy recovery or the Auto Start Stop function [1].

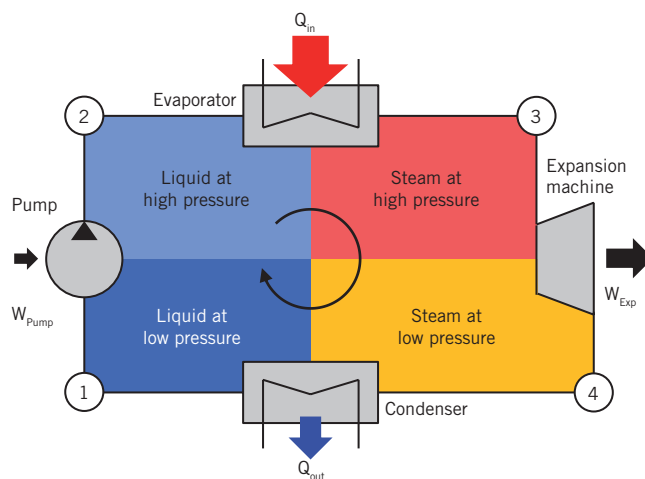
Nevertheless, even modern internal combustion engines only convert about one third of the chemical energy contained in the fuel into mechanical work. The remaining two thirds is lost as waste heat and is, therefore, the largest unused energy source in a vehicle today. In conclusion, many ongoing projects focus on the recovery of this waste heat as an important part of BMW EfficientDynamics in the future.

The BMW Turbosteamer, which recovers waste heat by means of a steam cycle, is part of these efforts, alongside exhaust gas heat exchangers for accelerated warming-up, thermoelectric generators and thermal insulation of the engine [2]. The second generation of Turbosteamer, which enables efficient and compact waste heat recovery in the powertrain of cars, is presented in the following sections.

SYSTEM DEVELOPMENT

The challenge in the development of the Turbosteamer is to transfer the principle of two-stage energy conversion, which is well established in stationary applications for power generation, to a car. It is essential to adapt the process control of the steam process to the general conditions and restrictions of mobile use.

The Rankine cycle is the standard cycle for describing the thermodynamic processes taking place in the components of the Turbosteamer [3]. In the first stage of the Rankine cycle, a working fluid is compressed by supplying mechanical work to a pump (W_{Pump} , 1 \rightarrow 2). The fluid is fed into a heat exchanger where it is heated, evaporated and superheated by a waste heat source (Q_{in} , Evaporator, 2 \rightarrow 3). The superheated steam is then sent into



① Principle of a waste heat recovery system based on the Rankine cycle

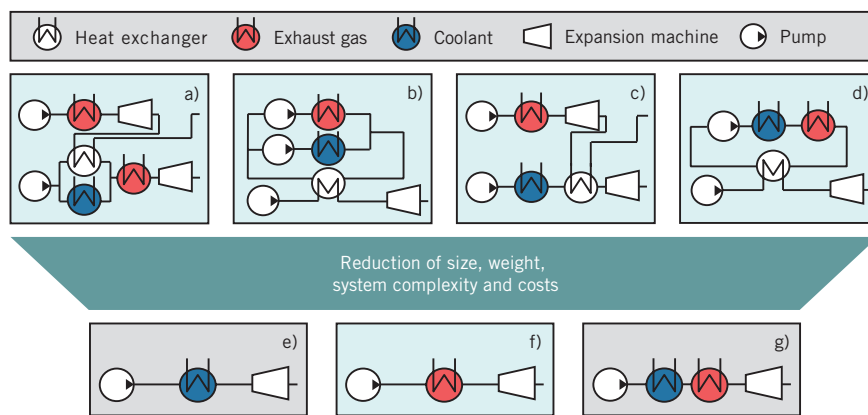
an expansion machine where it delivers mechanical energy (W_{Exp} , $3 \rightarrow 4$). The following heat rejection in a second heat exchanger leads to a saturated liquid at the suction side of the pump and thus closes the cycle (Q_{out} , Condenser, $4 \rightarrow 1$). Due to the distribution of the waste heat to two media (coolant and exhaust gas) in the car, many different system layouts regarding the heat addition are possible. These vary in the level of heat utilisation, in the number of required system components and in the number of fluid cycles, ②.

Hence, the main design task is to find a system layout that allows for maximum

energy recovery from the waste heat of the engine. This target was pursued as a “maximum approach” with the first generation of Turbosteamer. In order to demonstrate the full potential of waste heat recovery, both heat sources (exhaust and coolant heat) were exploited. For this purpose, a high temperature fluid cycle which retrieved heat from the exhaust system was used as the primary energy provider. The coolant heat and the residual heat of the high temperature process and the exhaust gas were recovered by an additional low temperature cycle, ② (a). On the test bench, this system achieved an additional power

output of up to 15 % based on the then current BMW four-cylinder gasoline engine [4]. In principle, other system layouts with two fluid cycles (amongst others, with intermediate cycles and heat conducting thermo-fluids) are possible, ② (b-d and further configurations). These are, however, associated with high system complexity and are thus generally not feasible for mobile applications.

In order to develop the Turbosteamer concept in the direction of series production, the activities following the initial publication [4] focused on system layouts with only one fluid cycle, ② (e-g), because these offer much better cost-benefit ratios. While it is possible to exploit different heat sources using only one fluid cycle, the efficient conversion of the coolant heat would require a significant increase of its temperature level [5]. Hence, the system layout chosen for the second generation Turbosteamer is a single-loop system for the recovery of exhaust gas heat, ② (f).

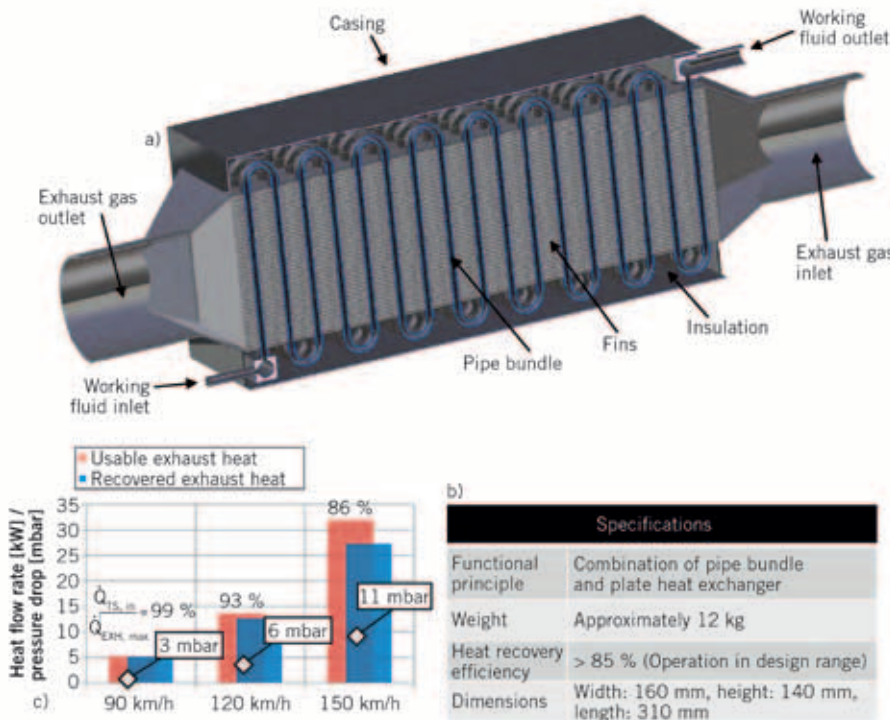


② Possible system layouts of a waste heat recovery system for cars

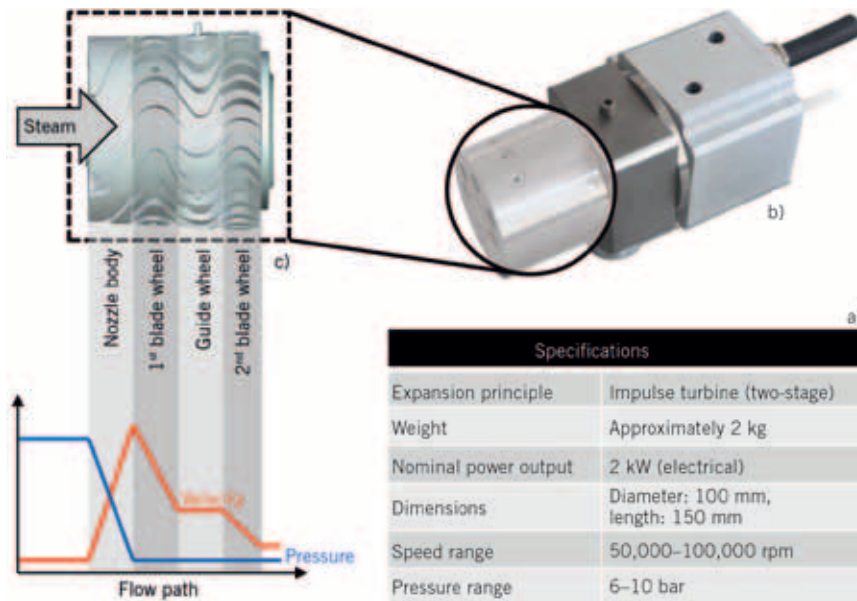
DEVELOPMENT OF THE KEY COMPONENTS

The feasibility of a specific system layout depends heavily on the development of vehicle-compatible components. It is essential to recreate the standard cycle as efficiently as possible. The components used in earlier applications of the Rankine cycle are generally not suitable for implementation in a car due to weight and space restrictions, differing nominal power output, dynamic requirements and cost considerations. This is especially the case for the key components of the system, the exhaust gas heat exchanger (EHX) and the expansion machine. Therefore, the development of these components will be discussed in more detail below.

The goal of the heat exchanger development is to maximise the heat input from the exhaust gas while taking into account the space available within the vehicle (BMW 5 Series, see cover illustration). Because the realisation of good heat transfer in a constrained space generally leads to high pressure losses, a conflict with efficient engine operation occurs [6]. The expansion machine has to convert as much of the energy stored in the high-pressure steam as possible into mechanical work. Losses in this component dramatically reduce the overall efficiency of the system



③ Construction (a), specifications (b) and performance (c) of the newly developed exhaust gas heat exchanger



④ Specifications (a), construction (b) and functional principle (c) of the newly developed turbine-generator unit

and thus lead to an increased heat load in the condenser and the heat sink [3].

③ shows the construction (a) and the specifications (b) of the newly developed EHX. The optimisation of the heat transfer surfaces of the gas and fluid passages have lead to a very compact and light EHX which is adapted to the underbody geometry of the current BMW 5 Series. The heat transfer surfaces of plate or pipe bundle heat exchangers generally have equal sizes on the gas and fluid side. However, the heat transfer coefficient on the gas side only reaches about a tenth of the value for the fluid side in this application [7]. Based on these findings, the cho-

sen design is a combination of pipe bundle and plate heat exchanger, which has resulted in a drastically increased heat transfer area on the gas side.

In the course of system simplification, various principles for steam expansion, power generation and coupling with the powertrain were once again evaluated. A turbine combined with an electric generator was identified as the most appropriate concept due to its high power density, ④ (a). The design as an impulse turbine leads to a significant reduction of losses through leakage flow in comparison to a scaled down reaction turbine as is generally used in power plants [8]. An advantage over

volumetric expansion machines is the possibility to run without lubrication. The resulting compact turbine-generator unit is depicted in ④ (b).

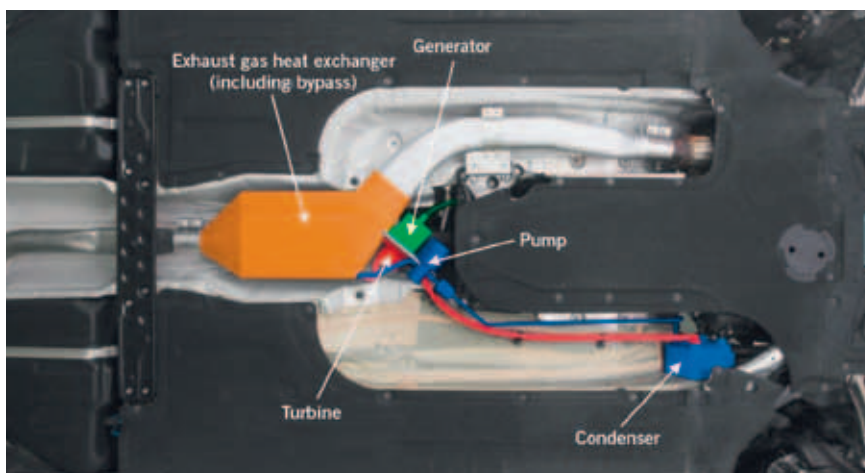
The functional principle of the turbine is shown in ④ (c): The high-pressure steam enters the machine over a variable cross section in which its potential energy is converted into kinetic energy. The resulting vapour streams impinge on the first blade wheel where they are deflected and thus generate a torsional moment on the turbine shaft. Following another deflection in the guide wheel, the remaining kinetic energy is transferred to the second blade wheel. Afterwards, the cooled and expanded steam exits the machine.

VEHICLE INTEGRATION CONCEPT

The geometrical and functional integration of the system into a vehicle provides a huge challenge. With regard to the first series application, an “add-on” application based on an existing vehicle and powertrain concept was chosen. With an additional weight of only 10 to 15 kg and considerably reduced system volume compared to the first generation [4], underbody integration is feasible.

In ⑤, the implementation is presented in the form of a mock-up to illustrate the possible integration into a BMW 5 Series. The exhaust gas heat exchanger including bypass is integrated in the underbody of the vehicle and is thus positioned behind the catalytic converter. In order to keep the system as compact as possible, the turbine-generator unit and pump are also positioned here. The condenser has a position near the engine because it is integrated into the vehicle cooling system.

Apart from the geometrical integration, the functional interactions between the existing powertrain and the Turbosteamer have to be taken into consideration. On the one hand, the operating range is limited by the exhaust gas backpressure occurring in the heat exchanger. On the other hand, heat addition to the cooling system through the condenser may only occur when a sufficiently large cooling capacity is available. Due to the strong dependence of thermal conditions on the vehicle speed, the electrical power output of the turbine-generator unit is also very variable. This has to be brought in line with an equally diverging power demand of the on-board electrical system.



⑤ Mock-up of the Turbosteamer add-on system integrated into the underbody of the current BMW 5 Series

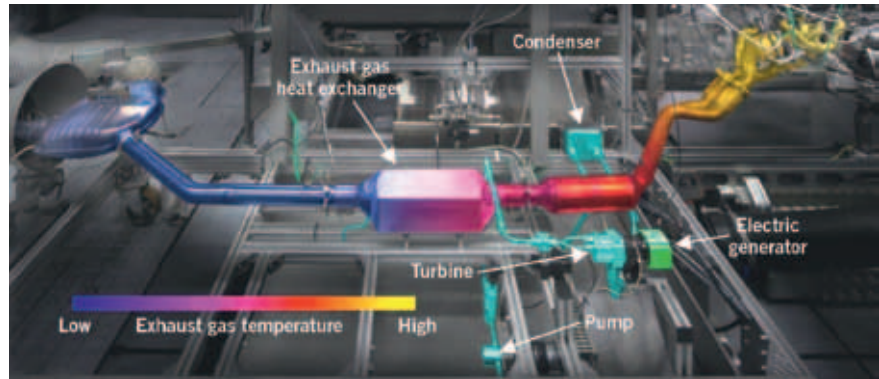
Based on the knowledge of the system behaviour, the interactions regarding heat absorption and rejection, as well as the coupling with the on-board electrical system, the operating range and strategy have been defined. Simulations and test bench measurements lead to the conclusion that an add-on system that reaches its nominal power output at a vehicle speed of 150 km/h gives the best cost-benefit ratio.

EXPERIMENTAL STUDIES

In order to test the newly developed components and investigate their dynamic behaviour, the system was operated on an engine test bench. ⑥ shows the test bench setup where a direct injection lean burn engine was used as a heat source. Here, all components that were already shown in ⑤ are present.

FUNCTIONAL DEMONSTRATION OF THE KEY COMPONENTS

③ (c) shows three examples of measurement results for the EHX. The plot compares the maximum heat flow rate that can, in theory, be recovered from the exhaust gas stream (\dot{Q}_{max}) to the heat flow rate that is transferred to the working fluid (\dot{Q}_{in}) at different vehicle speeds [5]. In addition, the resulting exhaust gas backpressure is depicted. These results show that the heat exchanger recovers over 85 % of the maximum achievable



⑥ Turbosteamer setup on the engine test bench

heat flow rate through the whole operating range. At low speeds, almost the entire usable fraction of the exhaust heat is recovered. At 11 mbar, the maximum exhaust gas backpressure that occurs at the operating point of nominal power output (2 kW) is very low. These results demonstrate that the space available for the heat exchanger is optimally utilised.

The turbine-generator unit has also been tested in conjunction with the other system components. At the system's design point (120 km/h) 600 W of electrical energy was generated. The maximum power output was more than 1 kW, which underlines the capability of the chosen expansion principle chosen. Overall, the efficiency remained below the estimations for an optimised turbine. Hence, the improvement of this component is the focus of further development.

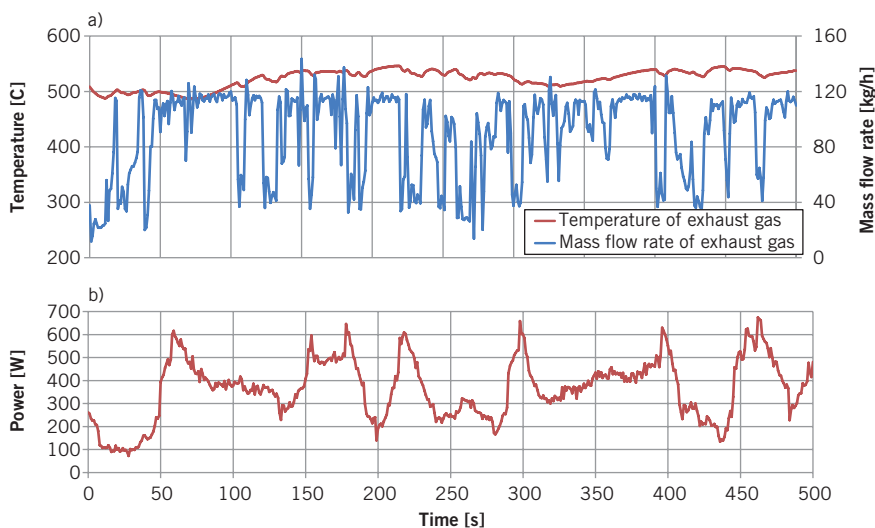
DYNAMIC OPERATION

During real operation, the exhaust heat emitted by the engine is subject to fast dynamic changes. ⑦ (a) shows the behaviour of exhaust gas temperature and mass flow rate for a driving profile example on the motorway at up to 130 km/h. While the exhaust gas temperature shows a very slow response, the mass flow rate reacts immediately to changes in the engine load. Hence, the exhaust heat flow is also subject to sudden changes. A control system was developed for the test bench setup in order to guarantee the safety of the components and optimal operation of the system at all times. In this context the non-linearity of the EHX and the operating characteristics of the turbine presented major challenges.

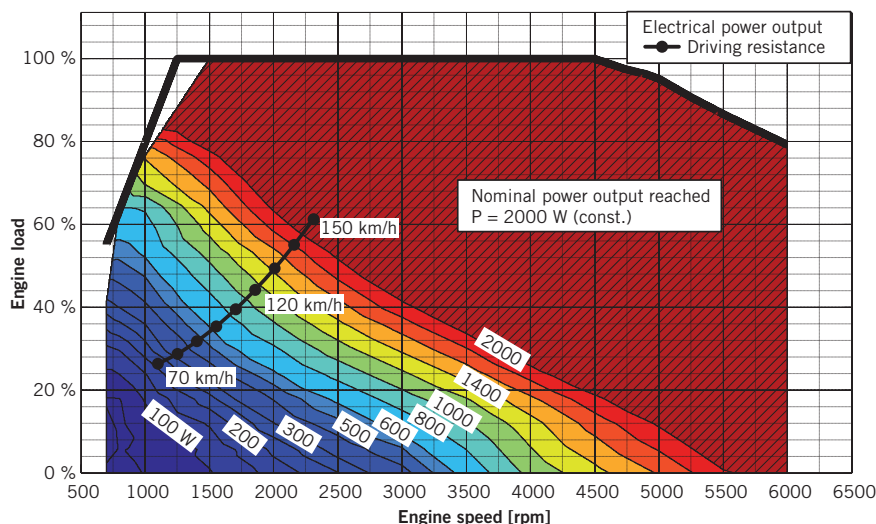
⑦ (b) shows the turbine power output measured during the driving cycle. With a maximum value of 700 W, the power could already provide a significant load reduction of the on-board generator. Furthermore, it was proved that an exhaust heat recovery system consisting of the presented components can be operated dynamically.

SYSTEM POTENTIAL

The key parameters for improving the system's efficiency are the increase of the evaporation pressure and improvement of the expansion efficiency. Based on these considerations and prognoses for the achievable turbine efficiency, an operating map of the system was created. ⑧ shows the electrical power output of the Turbosteamer as a function of speed and load for a modern turbocharged four-cylinder gasoline engine. In addition, the driving resist-



⑦ Behaviour of exhaust gas temperature and mass flow rate (a) and turbine power output (b) during a test of dynamic operation



8 Performance prediction and operating range of the optimised Turbosteamer add-on system in the current BMW 5 Series with turbocharged four-cylinder gasoline engine

ance curve for a current model of the BMW 5 Series is plotted.

Up to a vehicle speed of approximately 150 km/h, where the system's nominal power output of 2 kW is reached, the entire exhaust gas stream is directed through the EHX. By opening the bypass channel above this speed, the EHX only recovers the fraction of the heat that is required for the generation of the nominal power output (crosshatched area). Between 70 and 150 km/h, the system reaches 3 to 5 % of the engine power output at the respective operating points. Assuming typical efficiency characteristics of the on-board generator, an average reduction of the mechanical engine load of approximately 6 % within the Turbosteamer's operating range is achieved. Accordingly, a similar reduction in fuel consumption can be expected.

THANKS

The authors would like to thank Dr.-Ing. Christian Schmidt, Manager of the Department Efficient Dynamics Powertrain Research at BMW Forschung und Technik GmbH, for his support and promotion of the work leading to this publication.

SUMMARY AND OUTLOOK

The results show that the BMW Group has made great progress towards the series production of a vehicle-compatible waste heat recovery system based on the Rankine cycle. With the implementation of an expansion machine with very high power density (impulse turbine) and the development of a compact and backpressure-optimised exhaust gas heat exchanger, the second generation Turbosteamer has been considerably miniaturised in comparison to its predecessor. With a weight of only 10 to 15 kg and significantly reduced volume, the system can be integrated into the underbody of a BMW 5 Series as an add-on component, ⑤.

Once in series production, the system will be able to completely cover the power demand of the on-board electrical system during journeys on country roads and motorways. In combination with intelligent heat management optimised for waste heat recovery, an increase in fuel efficiency by up to 10 % is conceivable. Even greater consumption savings may be possible when today's add-on approach is transformed into a fully integrated system designed to maximise the combined efficiency of the engine and waste heat recovery system. Thus, future powertrain concepts with two-stage energy conversion in analogy to stationary gas and steam power plants can be realised.

REFERENCES

- [1] Langen, P.; Reissing, J.; Kliezt, M.: Hochentwickelte Antriebe – kein Widerspruch zur Profitabilität. 19. Aachener Kolloquium Fahrzeug- und Motorentechnik, 2010
- [2] Neugebauer, S.; Eder, A.; Liebl, J.; Seifert, M.; Strobl, W.: Analysieren, Verstehen und Gestalten – ein Gesamtansatz zur konsequenten Vermeidung von Wärmeverlusten. 15. Aufladetechnische Konferenz, Dresden, 2010
- [3] Moran, M. J.; Shapiro, H. N.: Fundamentals of Engineering Thermodynamics. 3rd Edition, Jon Wiley & Sons, 1998
- [4] Freymann, R.; Strobl, W.; Obieglo, A.: Der Turbosteamer: Ein System zur Kraft-Wärme-Kopplung im Automobil. In: MTZ 69 (2008), No. 5, P. 404-412
- [5] Seifert, M.; Ringler, J.; Guyotot, V.; Freymann, R.: Potenzial der Abwärmerückgewinnung mittels eines Rankine-Prozesses beim PKW. 12. Tagung „Der Arbeitsprozess des Verbrennungsmotors“, Graz, 2009
- [6] Zellbeck, H.; Roß, T.; Risse, S.: Abgasturboaufladung – Abgasnachbehandlung – Rekuperation – Effiziente Nutzung der Energie im Abgas. In: CO₂ – Die Herausforderung für unsere Zukunft, ATZ/MTZ-Konferenz Energie, 2010
- [7] VDI-Gesellschaft Verfahrenstechnik und Chemieingenieurwesen: VDI-Wärmeatlas. Berlin: Springer, 2005
- [8] Menny, K.: Strömungsmaschinen. Hydraulische und thermische Kraft- und Arbeitsmaschinen. 5th Edition, Wiesbaden: Teubner, 2006



ETHANOL AND ITS POTENTIAL FOR DOWNSIZED ENGINE CONCEPTS

The intense discussion of e-mobility has withdrawn the public attention from alternative fuels – which appears inadequate when the properties and potentials of ethanol fuels for combustion engines are considered. FEV and RWTH Aachen University investigated to which extent this alternative fuel could be conducive to CO₂ reduction.

AUTHORS



DR.-ING. MARKUS SCHWADERLAPP
is Executive Vice President of
FEV GmbH in Aachen (Germany).



DR.-ING. PHILIPP ADOMEIT
is Executive Engineer Thermo-
dynamics at FEV GmbH in
Aachen (Germany).



DIPL.-ING. ANDREAS KOLBECK
is Head of the Department of
Advanced Diesel Passenger Car
Engine at FEV GmbH in Aachen
(Germany).



DIPL.-ING. MATTHIAS THEWES
is Research Assistant at the Institute
for Combustion Engines at RWTH
Aachen University in Aachen
(Germany).

POTENTIALS OF ETHANOL

Ethanol is one of the most established alternatives to fossil fuels. Ethanol is a renewable fuel due to its production from biomass. It enables a close carbon cycle, since a part of the CO_2 , which is generated during production and combustion, is withdrawn from the atmosphere by the growth of the biomass. Today's mass production processes yield a CO_2 reduction of approximately between 35 % [1] and up to 72 % [2, 3], depending on the production process and the climatic conditions. The prognosis for future production processes of ethanol based on lignocellulose predicts values above 80 %.

BIOFUEL ETHANOL

The substitution of fossil fuels by bio-fuels has caused a remarkable increase of the world wide ethanol production in the last decade, ①. However the energetic contribution of ethanol to the worldwide provided energy content of liquid fuels is merely 1 % [4]. Current prognoses assume that the availability of ethanol will grow by a factor of three in the next 20 years [7].

Especially the production of ethanol of the so-called "1st generation" with the feedstock of sugarcane, corn, crop and sugar beet potentially competes with the food production. Ethanol of the "2nd generation" with lignocellulose feedstock remains in a potential competition on land usage, unless by-products of the food production, such as wheat straw, are

exploited. Up to now, the production processes of the "2nd generation" have not been realized in large scale facilities.

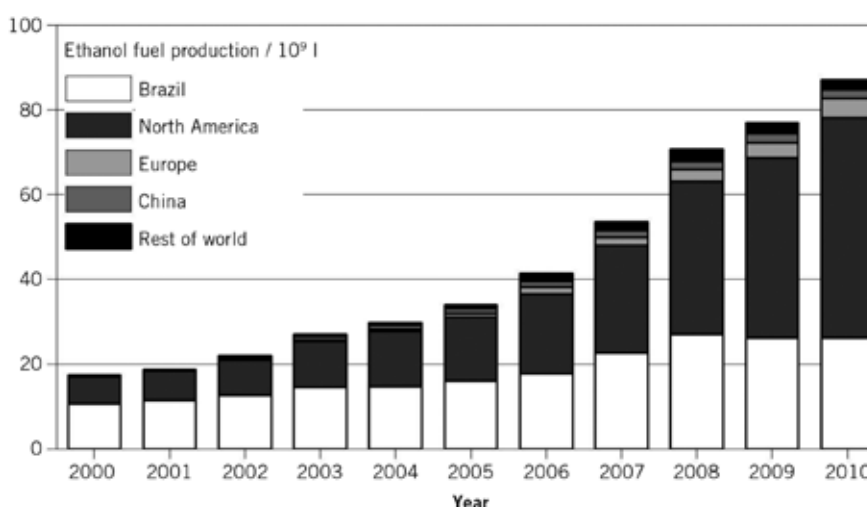
Today's fuel specifications allow a limited blending fraction of ethanol into gasoline. For fuels with specifications with minor ethanol content the octane-grades of fuels have not been increased [5,6].

An alternative procedure is the blending of ethanol in so-called splash blends. In this case ethanol is added to gasoline fuel with conventional RON, which increases the octane-grade of the blend. In combination with an adapted engine design the splash blends enable to deploy an additional potential to reduce CO_2 emissions, which will be examined in the present contribution for both gasoline and Diesel engines.

EFFECT OF ETHANOL BLENDS ON GASOLINE AND DIESEL COMBUSTION SYSTEMS

The present investigations are performed with three different test engines, whose specifications are displayed in ②. Engines A and C are conventional engines with enhanced peak pressure capability, whereas engine B is a single cylinder research engine with substantially increased torque and peak pressure capability.

The knock resistance and the high heat of vaporisation of ethanol enable to increase the efficiency of the SI combustion system. The results of full load operation in ③ are obtained with increased compression ratios C.R. The upper C.R. limit



① Production quantity and world wide distribution of the production of ethanol [2]

| TEST ENGINE | | A | B | C |
|---|--------------------|---------------------------------------|--|-------------------------------|
| COMBUSTION SYSTEM | | SI DI | SI DI | CI DI |
| CYLINDER DISPLACEMENT | [cm ³] | 448 | 364 | 390 |
| STROKE | [mm] | 87 | 82.5 | 88.3 |
| BORE | [mm] | 81 | 75 | 75 |
| MAX. MEAN EFF. PRESSURE | [bar] | 22.4 (effective) | 40 (indicated) | 35 |
| SPECIFIC POWER | [kW/l] | 90 (effective) | ~ 120 | 85 |
| COMPRESSION RATIO | 1 | 9.3 to 11.5 | 7 to 13.5 | 15 |
| VALVES / CYLINDER | | 4 | 4 | 4 |
| MAX. PEAK PRESSURE | [bar] | 145 | 190 | 220 |
| INJECTION SYSTEM | | Piezo-actuated injector (R. Bosch) | Piezo-actuated injector (Continental) | Piezo CR system (R. Bosch) |
| MAX. RAIL PRESSURE | [bar] | 200 | 200 | 2000 |
| BOOST PRESSURE | [bar] | 2.3 (absolute) | max. 3.8 (absolute) | max. 3.8 (absolute) |
| MAX. EXHAUST TEMPERATURE BEFORE TURBINE | [°C] | 950 | 1050 | 830 |

② Technical specifications of the test engines

is reached when standard deviation of the IMEP in the critical range for vehicle jerking up to 3000 rpm becomes equal to that obtained with RON95 in the base engine. The E20 Match Blend with the same RON as the base gasoline RON95 does not allow increase to the C.R., whereas E20 Splash Blend enables an increased C.R. by 2.2 units. Due to the higher C.R. and the reduced enrichment requirement the engine efficiency with E20 Splash Blend is improved between 6.1 % and up to 39 % compared to operation with RON95 gasoline.

The combustion behaviour of E85 with the identical compression ratio reveals, that an enrichment for component protection is completely avoided for high ethanol blending rates. Simultaneously the engine design has to allow for substantially increased peak firing pressures. By operation with E85 the engine efficiency is further improved, reaching peak values of 39.1 % in the speed range of optimum efficiency at 3000 rpm, which is significantly above the efficiency of 29.4 % achieved with RON95 gasoline operation. With E20 Splash Blend a remarkable efficiency of 36.9 % is obtained.

Due to the large knock resistance with maximum Ethanol content (E100) the compression ratio can be substantially increased by five units, ③ for test engine B. Even under these conditions the maximum indicated efficiencies can still be

reached at full load. This indicates that engine concepts with considerably enhanced degree of downsizing or C.R. of up to 15 are required to fully utilize the potential of E100.

In overall it is seen that a systematic adaptation of the engine design to the specific properties of ethanol splash blended gasoline fuels enable to gain a substantial potential for further CO₂ reduction.

After the discussion of ethanol blends for gasoline engines, in the following the ethanol fuel blending for Diesel engines and its specific potentials shall be considered. When utilizing ethanol blends in Diesel engines the fuel properties mainly affect the emission level, especially the particulate emissions. As seen in ④ a blending of 30 % of E85 into Diesel fuel enables an almost soot-free combustion even at the highest investigated part load point 14.8 bar IMEP. This can be attributed to the increased oxygen content of the fuel and the lowered evaporation curve, which are beneficial to both improved mixture formation and soot oxidation conditions. During these test runs the efficiency of combustion has been maintained at a constant level by controlling the centre of combustion to a constant value.

The high resistivity of ethanol against auto-ignition, which has a positive effect for gasoline engine operation, is disadvantageous for Diesel engine operation in low

part load conditions. The cetan number of a Diesel blended with 40 % E85 is insufficient to ensure auto-ignition at part load of 4.3 bar IMEP. Even with 30 % E85-blending increased HC emissions and a deteriorated engine efficiency are observed, so that under the present engine operation conditions the 30 % E85-blending can be regarded as beyond the upper limit of E85 blending to Diesel fuel.

For rated power operation a comparable performance can be obtained with all blending grades. Both indicated mean effective pressure and engine efficiency remain at a nearly constant level, exhibiting a certain tendency of decreasing particulate emissions with growing E85 content.

In overall the results show that the potentials of blending E85 into Diesel are fully exploited at a maximum blending grade of 20 %. The Diesel combustion system can handle this level of blending in the complete map of operation without substantial changes to the engine hardware.

REQUIREMENTS OF ETHANOL BLENDS ON THE CALIBRATION OF GASOLINE AND DIESEL ENGINES

The altered fuel properties resulting from ethanol blending requires a corresponding adaptation of the engine calibration. A reliable detection of the ethanol blending rate can be undertaken either directly by a

sensor, or indirectly by the mixture deviation and the resulting AFR controller correction. Based on this the engine controls can be adapted by calibration for different ethanol contents and use of corresponding interpolation functionality in the control algorithms.

One important aspect of the SI engine calibration for high ethanol contents is the control of the cold start and warm-up operation, and the corresponding counter-measures regarding excessive oil dilution. The high heat of evaporation and the increased fuel quantity cause a strong cooling of the in-cylinder charge, which massively deteriorates the mixture formation during cold start. This can be compensated by a high enrichment factor for ethanol blending up to 85 %. For direct injection SI-engines the required enrichment can be reduced by a late injection into the compression stroke with higher in-cylinder charge temperature. Furthermore, additional measures to ensure the cold start can be used, such as air or fuel-preheating and low pressure injection [8, 9].

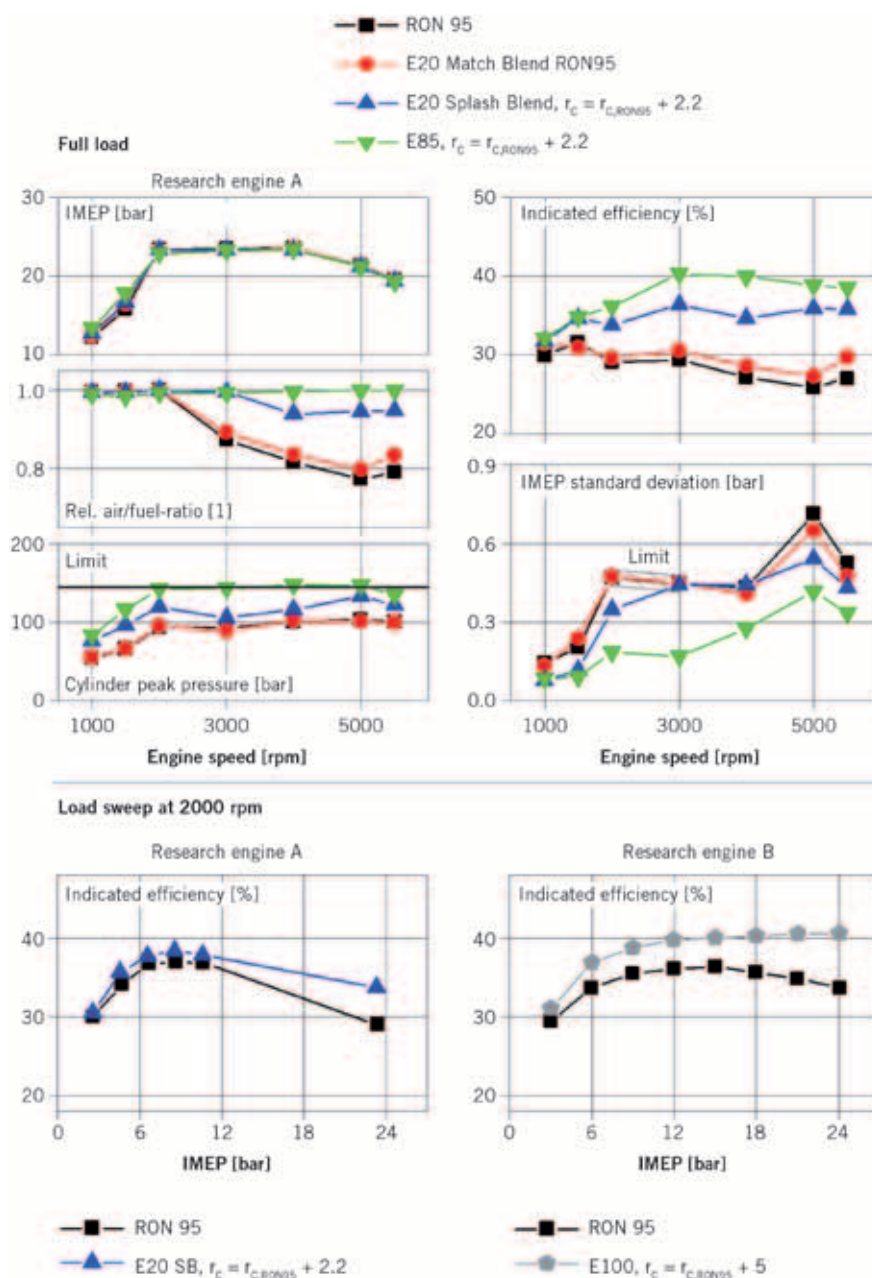
Due to the high enrichment factors with E85 repeated cold starts frequently cause a substantially increased fuel entrainment into the engine oil, as seen in the results shown in ⑤. Furthermore the water vapour concentration in the exhaust gas is increased by high ethanol blending grades, which in turn causes a dilution of the engine oil with water. When the diluted oil is sufficiently heated up during engine operation, a rapid evaporation of the ethanol from the engine oil occurs. This leads to a significant fuel concentration in the intake air duct, coming from the crank case ventilation. This effect can require an optimization of the CCV introduction duct to ensure a homogeneous distribution to all cylinders and a sufficient safety against local freezing. Regarding the calibration, a functionality for the detection of the ethanol evaporation process is required, which adaptively enlarges the limits of the AFR controller during this time.

To account for the case that no satisfactory oil dilution levels can be ensured during the engine operation, an additional model for the oil dilution state is required, which in case of need requests engine heat-up operation from the driver.

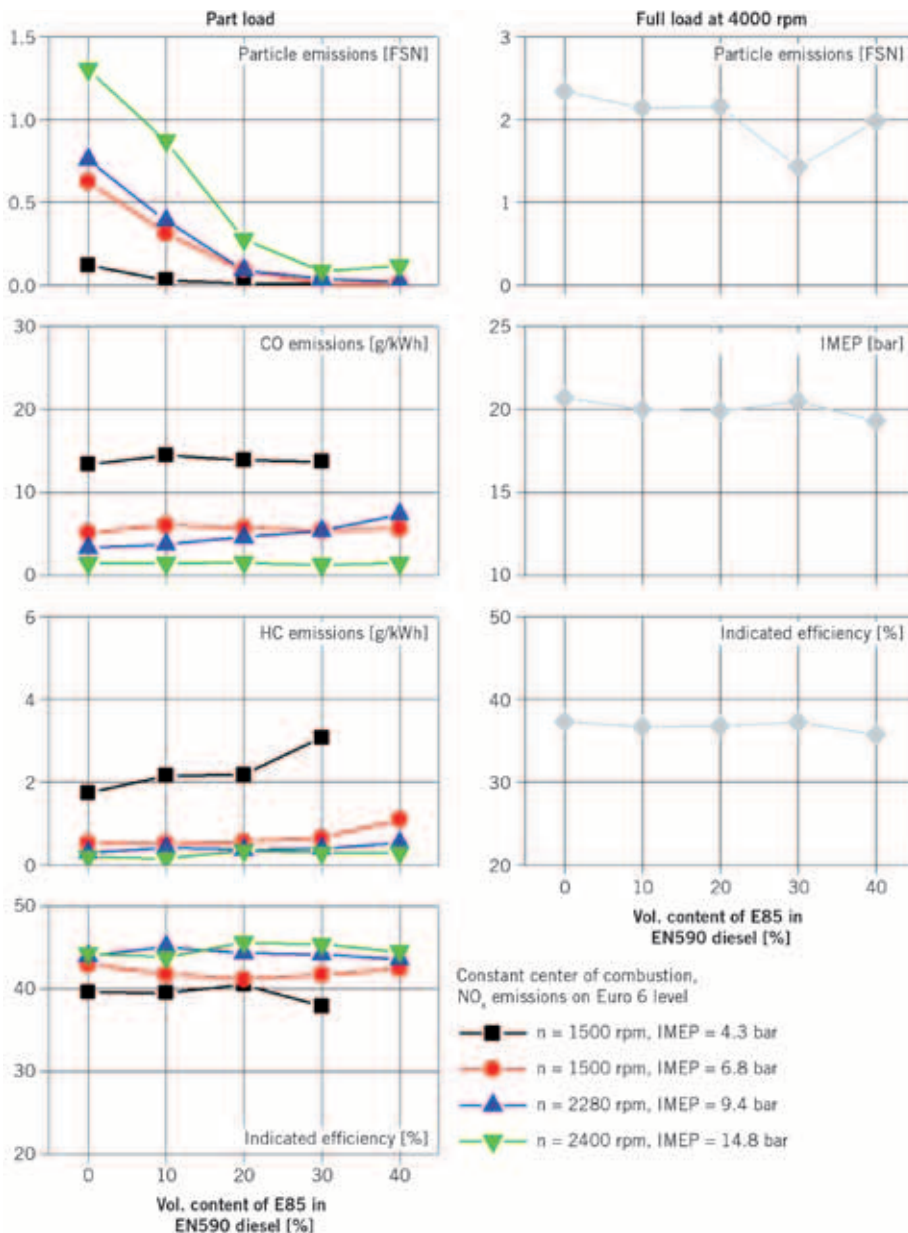
In order to operate the Diesel engine with different fuel blends, adapted control concepts are required, which provide com-

pensation for the effect of the reduced Cetan number on the combustion process. Here model based control concepts are preferred as they contribute substantially to reduce the calibration efforts. As an example ⑥ shows the concept structure of the cylinder pressure guided closed loop control of the centre of combustion. The in-cylinder pressure is measured by a pressure transducer and analysed in the control unit. The diminishing Cetan number with increased E85 blending

causes deviations in the combustion rate, which are compensated by controlling the begin of injection BOI in order to maintain a constant centre of combustion. A similar control concept is used for the air path in order to control the nitrogen oxide emissions to the levels prescribed by emission legislation. In overall it can be stated, that the techniques and tools required for the calibration of gasoline and Diesel engines for variable ethanol fuel blending are basically available.



③ Gasoline engine results in full and part load operation, comparing results of E20 Match Blend, E20 und E85 Splash Blend and E100 with adapted compression ratios to those of conventional RON95, load sweeps at 2000 rpm



④ Effect of the E85 blending rate to Diesel fuel on the part and full load engine performance and emissions

EVALUATION OF THE CO₂ POTENTIAL

To determine the potential for reduction of CO₂ emissions by ethanol blending a evaluation of the performance in the NEDC of the test engines A and C is undertaken for different vehicle classes ranging from mid sized passenger car to sport utility vehicles. Since the efficiency gain by increased compression ratio of the SI-engine improves with engine load, more CO₂ reduction can be achieved by ethanol blending with vehicles with higher driving resistance. As shown in ⑦ the CO₂ advantage with E20 splash blend

ranges from 3.9 to 4.9 %. With increasing ethanol fraction the gradient of the CO₂ reduction flattens out, since the C.R.: increase does not grow linearly with the ethanol fraction. Furthermore the improvement of engine efficiency is not linearly depending on the compression ratio. Considering the dependency of the efficiency on engine load for high ethanol fractions, ③, a further potential for CO₂ reduction can be expected by enhanced downsizing, provided that future charging systems will be capable to enable enhanced boosting levels with a satisfactory transient response.

For the Diesel engine ethanol blending does not result in a direct improvement of the engine efficiency, ④. However an indirect advantage arises from the prolonged regeneration intervals which are achieved by the significant reduction of particulate emissions with increased ethanol blending. This effect already becomes effective at comparably small ethanol fractions.

On the base of the engine results presented here, it can be concluded that once an ethanol blending of approximately 25 % in gasoline fuel is reached, it is feasible for the overall CO₂ reduction to simultaneously increase the blending of ethanol in Diesel fuel up to a maximum of 8 to 10 %.

OUTLOOK

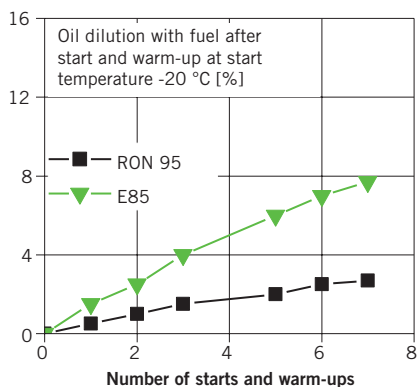
The blending of ethanol as a splash blend into gasoline and Diesel fuels provides a high additional potential for CO₂ reduction, when the engines are adapted for the specific fuel properties. For the downsized SI-engine ethanol splash blending enables to increase the compression ratio due to the improved knock resistivity, which directly improves engine efficiency. Therefore bio-ethanol can deliver an additional contribution by an improved combustion process of up to 6 % for conventional SI-engines and of up to 10 % for E100 to the CO₂ reduction by the fuel itself.

The application of ethanol blends to Diesel engines mainly enables to massively reduce particulate emissions and thereby allows for prolonged regeneration intervals of the exhaust aftertreatment system. Thus ethanol blending in comparably smaller fractions can also contribute to a reduction of the CO₂ emissions.

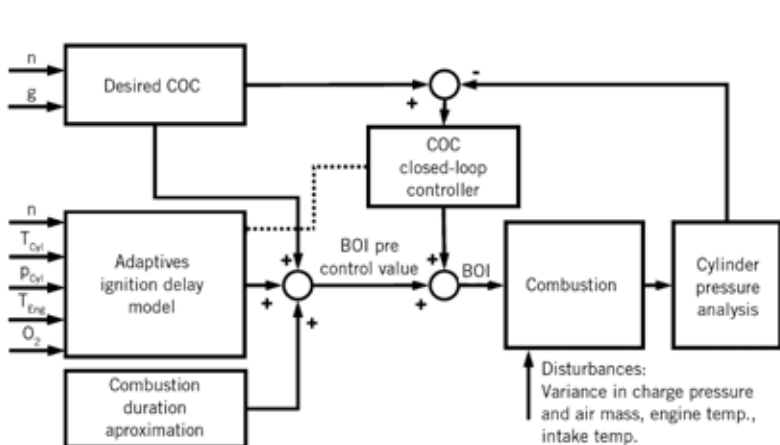
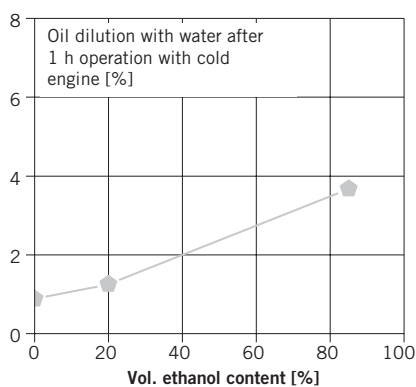
In overall bio-ethanol reveals a significant potential for CO₂ reduction in addition to the partially closed carbon cycle during the production from biomass. The key factor for the intensified use of ethanol is the availability of efficient “2nd generation” production processes. In short and medium terms the enforced use of alternative fuels such as ethanol is expected to enable more CO₂ reduction in transportation than the electro-mobility.

REFERENCES

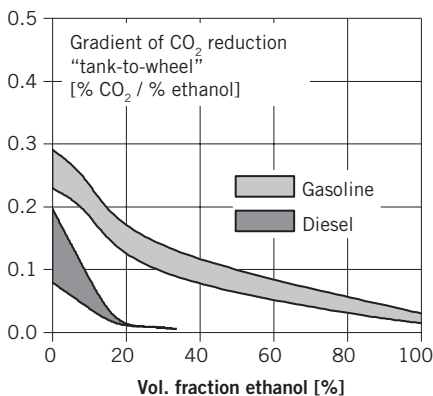
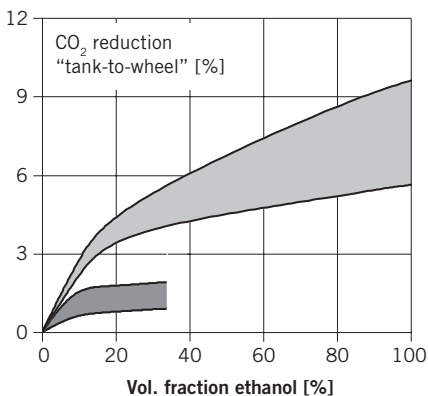
- [1] European Commission: Renewable Energy Directive 2009/28/EC RED, 23.04.2009
- [2] Renewable Fuel Standard Program (RFS2) Regulatory Impact Analysis, United States Environmental Protection Agency, <http://www.epa.gov/>



5 Oil dilution with ethanol blended gasoline



6 Model based closed loop control of the centre of combustion of the Diesel engine



7 Reduction of CO₂ emission with adapted gasoline and Diesel engines in the NEDC

otaq/renewablefuels/420r10006.pdf, (downloaded 09.03.2010)

[3] Energy Information Administration (EIA), International Energy Statistics, Biofuels Production, Fuel Ethanol, 2000-2009,

[4] <http://ethanolrfa.org/pages/World-Fuel-Ethanol-Production>, (downloaded 06.10.2011)

[5] Energy Information Administration (EIA), International Energy Annual Energy Review 2009, DOE/EIA-0384(2009), Release Date: August 19, 2010

[6] Energy Information Administration (EIA), International Energy Outlook 2011, DOE/EIA-0487(2011), Release Date: September, 2011

[7] F.O. Licht: World ethanol and biofuels report, Agra Europe, London, 2006

[8] Ballauf, J.: 2,0l TFSI Flexible Fuel Motor im Audi A4, 19. C.A.R.M.E.N.-Symposium 2011, Straubing, 2011

[9] Hadler, J.; Szengel, R.; Middendorf, H.; Sperling, H.; Gröer, H.-G.; Tilchner, L.: Der 1.4 l 118 kW TSI für E85 Betrieb – die Erweiterung der verbrauchsgünstigen Ottomotorenlinie von Volkswagen, 32. Internationales Wiener Motoren-symposium 2011, Wien, 2011

THANKS

The investigations of the test engine A have been performed within the scope of the FVV-Vorhaben Nr. 942, „Alternative Kraftstoffe DI-Ottomotoren – Untersuchung und Bewertung von alternativen Kraftstoffen für den Einsatz in modernen DI-Ottomotoren“. The investigations with test engine B have been conducted as part of the Cluster of Excellence „Tailor-Made Fuels from Biomass“, which is funded by the Excellence Initiative by the German federal and state governments to promote science and research at German universities. The Diesel engine investigations have been undertaken in the BEAUTY (Bio-Ethanol engine for Advanced Urban Transport by Light Commercial & Heavy-Duty Captive Fleets) project, funded by the EU within the „Seventh framework programme“.



THE NEW 3.0-L TDI BITURBO ENGINE FROM AUDI

PART 2: THERMODYNAMICS AND CALIBRATION

The new 3.0-L V6 TDI biturbo engine from Audi, with two-stage turbocharging in an innovative V-specific arrangement, four-valve technology and piezo common rail injection system has a power output of 230 kW and a maximum torque level of 650 Nm. The engine complies with the Euro 5 emissions standard and sets a new benchmark in terms of emotional driving pleasure and fuel efficiency in the upper mid-size class. The efficiency measures of the second-generation V6 TDI monoturbo have also been adopted. The thermodynamics, calibration and exhaust aftertreatment of the new engine are described below. The first part of the article in MTZ 1 covered the structural and mechanical elements.

AUTHORS

**DIPL.-ING. MARK BISCHOFF**

is Test Engineer Thermodynamics and Calibration V6 TDI biturbo at Audi AG in Neckarsulm (Germany).

**DR.-ING. CHRISTIAN EIGLMEIER**

is Head of Thermodynamics and Calibration V6 TDI biturbo at Audi AG in Neckarsulm (Germany).

**DIPL.-ING. TORSTEN WERNER**

is Test Engineer Thermodynamics and Calibration V6 TDI biturbo at Audi AG in Neckarsulm (Germany).

**DIPL.-ING. STEFAN ZÜLCH**

is Head of Thermodynamics and Calibration V-Diesel Engines at Audi AG in Neckarsulm (Germany).

DEVELOPMENT OBJECTIVES

The development objectives of thermodynamics, calibration and exhaust aftertreatment were already defined in an early stage of the project, in order to position the engine as a benchmark in its competitive field:

- : outstanding power delivery and sporty top-end performance
- : smooth, harmonious acceleration characteristics under all conditions, especially in the turbocharger changeover range
- : very good dynamic responsiveness at all engine speeds, including when starting off
- : compliance with Euro 5 exhaust standard
- : adoption of all the efficiency measures from the second-generation V6 TDI monoturbo.

The essential development measures to achieve the objectives of the new high-performance V6 TDI biturbo engine are set out below. The engine was based on the second-generation V6 TDI monoturbo, which was introduced to the market by Audi in 2010 [1].

FUEL SYSTEM

The new V6 TDI biturbo features a Bosch CRS 3.3 fuel injection system with 2000 bar maximum rail pressure. The stroke of the CP 4.2 high-pressure pump has been increased by 6 % to meet the increased fuel demand in comparison with the basic engine. The piezo servo injectors with eight-hole injector nozzles use an internally labeled ZK needle seat with so-called i-Midi blind hole for the first time.

The harmful volume which is of relevance for the formation of HC emissions has been reduced by around 32 % by means of these measures. To achieve the maximum power output of 230 kW, the hydraulic flow has been increased by 14 % in relation to the basic engine.

COMBUSTION PROCESS

To ensure outstanding starting characteristics and free-revving power delivery from the V6 TDI biturbo, the gas flow and the combustion process have been adapted for the high-performance concept. Along with the injector configuration, the key development points were:

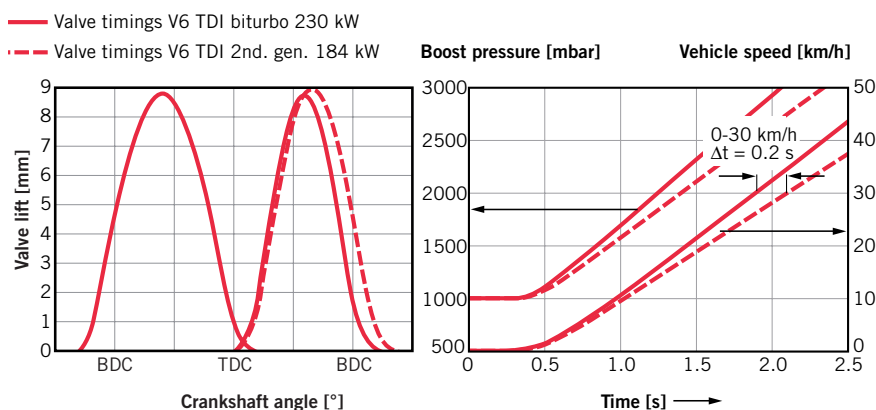
- : compression ratio and piston design
- : valve timing
- : intake port design.

The geometric compression ratio of the V6 TDI biturbo has been reduced from 16.8:1 (basic second-generation V6 TDI) to 16.0:1 by enlarging the piston bowl for the purpose of increasing power output.

The intake and exhaust valve timing in conjunction with the two-stage turbocharger have been optimized with the aid of one-dimensional gas flow simulation and verified by means of test-rig and vehicle trials. It proved to be effective in this respect to shorten the intake event length by 23° (measured at 1 mm valve lift) compared with the basic engine.

Several effects had positive consequences in this case:

- : 1 to 2 % increase in volumetric efficiency at low engine speeds and hence an immediate improvement in starting characteristics from a standstill, ❶. In the vehicle this resulted in an improve-



❶ Optimization of drive-off dynamics by modification of valve timing

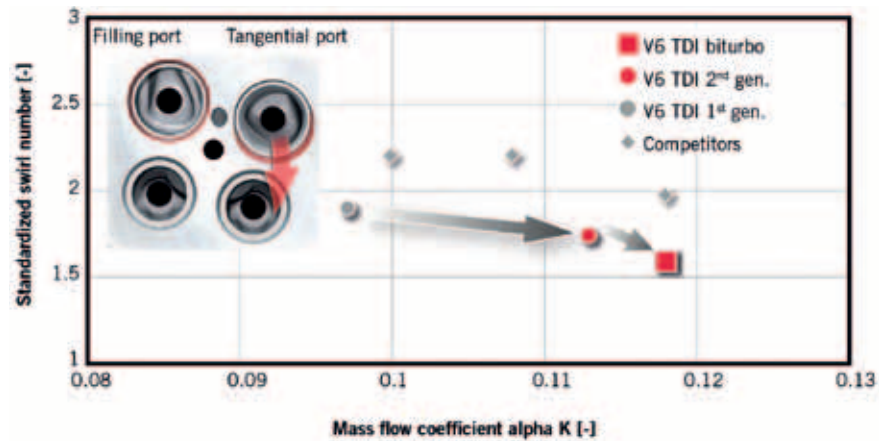
ment of 0.2 s in the acceleration figures from 0 to 30 km/h. Boost pressure build-up was considerably improved.

- At nominal power output there was another improvement in performance, as the scavenging-related disadvantage of the short camshaft was overcompensated by means of modified swirl level (combustion) and the greater efficiency of the turbocharger assembly.
- The effective compression ratio has actually been increased at low engine speeds in the V6 TDI biturbo in comparison with the basic engine, even though the geometric compression ratio has been reduced. This means that the cold-start capability at extremely low temperatures still complies with Audi standards.

The design of the intake ports has also been modified for the V6 TDI biturbo. In order to achieve further improvement in the charge, the filling ports are provided with a chamfer running around the port instead of a seat swirl chamfer, ②. The seat swirl chamfer is now only implemented in the tangential port. The improvement in charge thus enhances the turbocharging capability of the unit. It delivers top flow coefficients, including when compared to the competition. The slight reduction in the level of swirl can be compensated in the partial load range by means of the central swirl flap. The all-round chamfer on the charge port of the V6 TDI biturbo was implemented by modifying one machining stage (seat swirl chamfer) in engine manufacture without forfeiting the synergies with the 3.0 TDI base unit. The low swirl level of the V6 TDI biturbo and the injection system are perfectly matched, and together with the improved charge they lead to efficient combustion.

TURBOCHARGING

The charger system of the V6 TDI biturbo is comprised of a small high-pressure (HP) turbocharger and a large low-pressure (LP) turbocharger, arranged sequentially. The wide spread of the two turbocharger sizes enables outstanding dynamic responsiveness at low engine speeds and optimum power delivery at high revs. This sporty configuration places high demands on the operation of the engine in the changeover range, which has to be driven through without the driver noticing.

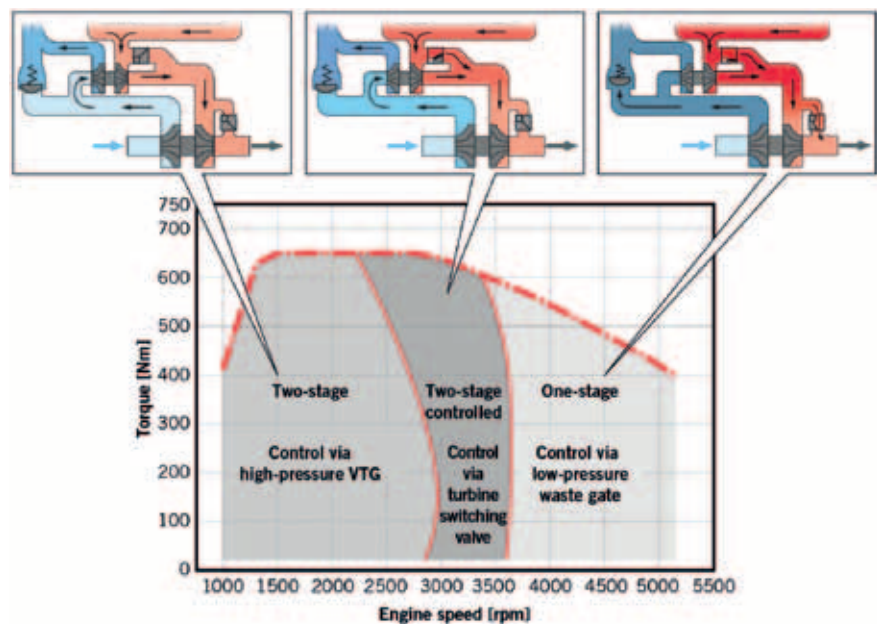


② Modified inlet ducts: swirl and mass flow coefficient

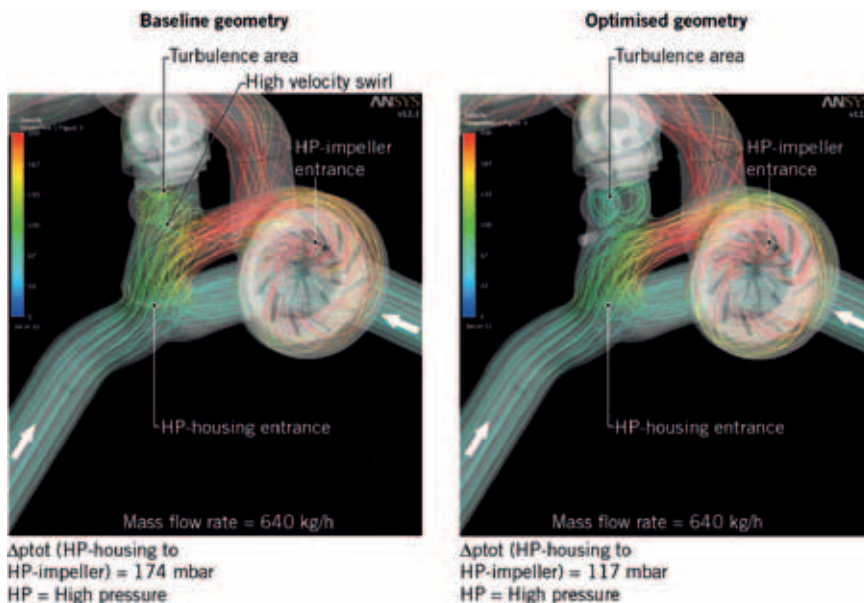
The boost pressure control by means of the three actuators for the variable turbine geometry VTG (HP turbocharger), the turbine switching valve and the wastegate (LP turbocharger) is model-based. The basis is the Volkswagen Group's own boost pressure control system, which is already used for the four-cylinder inline TDI biturbo [2]. The functions have been extended for use in the V6 TDI biturbo, as this is the first time that a high-pressure turbocharger with VTG has been used. At the same time some additional measures have been implemented for the suppression of turbocharger noise in dynamic driving mode.

③ shows the operating modes of the turbocharging assembly in the engine map. At engine speeds below 2300 rpm the pneumatically activated turbine switching valve is closed and the entire exhaust gas flow passes through the HP turbine. The boost pressure is regulated by means of the VTG of the relatively small HP turbocharger. The self-regulating compressor bypass valve is closed. Outstanding responsiveness is achieved in this way at low engine speeds.

In the engine speed range from 2300 to 3400 rpm, the turbine switching valve is slightly opened in order to divert part of the exhaust gas flow past the HP turbocharger.



③ Operating modes of the turbocharging system in the engine map



④ Optimization of flow to high-pressure turbine

As a result the large LP turbocharger receives more exhaust gas energy in order to precompress the intake air. As a result of the high pressure difference across the valve, even the smallest increases in the cross section of the opening lead to a significant rise in the exhaust enthalpy at the large turbocharger. Despite this, even and harmonious acceleration is achieved in the transition phase, underlining the considerable effectiveness of the model-based boost pressure regulation.

At engine speeds above 3400 rpm the turbine switching valve is completely opened and the required boost pressure is regulated by means of the wastegate of the LP turbocharger. The configuration of the large LP turbocharger enables outstanding top-end performance and high power output across a wide rev range. This enhances the sporty character of the engine and offers potential for future performance improvements. In changed operating conditions such as heat, cold or high altitude, the aforementioned operating ranges are shifted. The model-based boost pressure control system responds to this by adjusting the activation of the turbochargers in order to guarantee the driver the optimum driving experience.

To achieve outstanding responsiveness it is important that the gas flow to the HP turbocharger is good at low revs. In the course of the development process the flow characteristics in the HP turbine housing

were investigated with the aid of CFD simulations. The pressure losses were reduced and the strength of the housing was increased at the same time, ④.

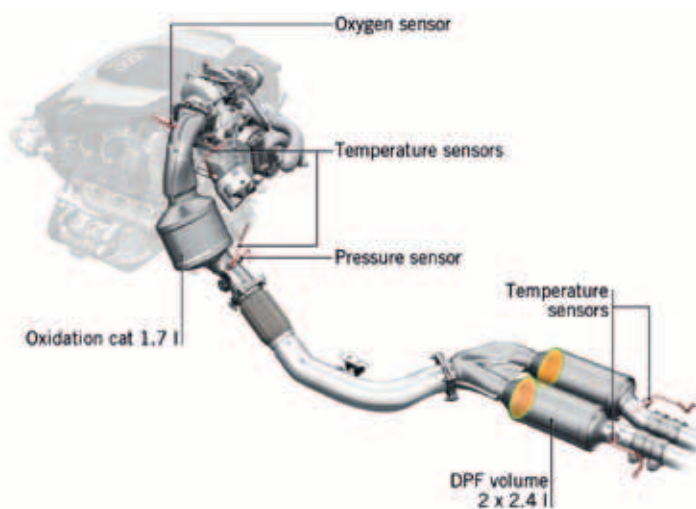
EXHAUST SYSTEM

The defined goals for the design of the exhaust system were:

- : low exhaust back-pressure for high performance and torque, low fuel consumption and imperceptible switching between the two turbochargers
- : early catalytic converter light-off
- : adequate DPF volume for low DPF regeneration periods.

The high power target and the associated high exhaust gas volumetric flow required the back pressure to be optimized throughout the exhaust system. In two-stage turbocharging, low exhaust back pressure is relevant not only in the nominal power range but also in the controlled switching range between the two turbochargers [4]. With the wide spread in the configuration between HP and LP turbochargers it is however an important factor to ensure that the changeover is imperceptible for the driver. It must also be considered that a further increase in exhaust back pressure may occur, depending on the loading of the particulate filter. For that reason the exhaust system has been opened up throughout for the V6 TDI biturbo in the Audi A6 and A7.

⑤ shows the exhaust system layout. The single-duct, oval oxidizing catalytic converter is located on the bulkhead side of the engine. It has a volume of 1.7 l and a cell density of 400 cpsi. To ensure effective reduction of heat loss, the turbine housing of the low-pressure turbocharger and the exhaust system upstream of the oxidizing catalytic converter are equipped with integral insulation. This ensures early catalytic converter light-off. To provide an ideal balance between the exhaust back pressure, the DPF volume and the package, the particulate filters are configured in a two-channel layout in the underbody. As the prop-shaft associated with the standard Audi four-wheel drive system runs in the middle above the particulate filters, it proved beneficial to separate the particulate filters into two round units arranged in parallel. In this way it was possible to



⑤ Exhaust system

achieve a total DPF volume of 4.8 l with low pressure losses. Like the oxidizing catalytic converter, the particulate filter (substrate: aluminium titanate) with a cell density of 300 cpsi has a precious metal coating, which is zoned in the direction of flow and assists soot burn-off.

Soot burn-off is calculated by the engine management system by way of the temperature sensors downstream of the oxidizing catalytic converter and the particulate filters. In order to achieve even loading of the twin particulate filters, the design of the Y-piece ahead of the DPFs was optimized by means of CFD calculation. The even loading and burn-off of the two particulate filters has been confirmed by numerous vehicle tests.

EXHAUST EMISSIONS

The new V6 TDI biturbo fitted in the Audi A6 and A7 is designed to meet the currently applicable Euro 5 emissions standard. Owing to the additional thermal masses of the two-stage turbocharging system, primary attention was given to achieving catalytic converter light-off after engine start. In order to achieve an effective increase in temperature inside the diesel engine, combustion in the expansion phase can be extended by means of systematic post-injections. This feature is already used in series production for the particulate filter application.

A catalytic converter heating function has been developed for the V6 TDI biturbo,

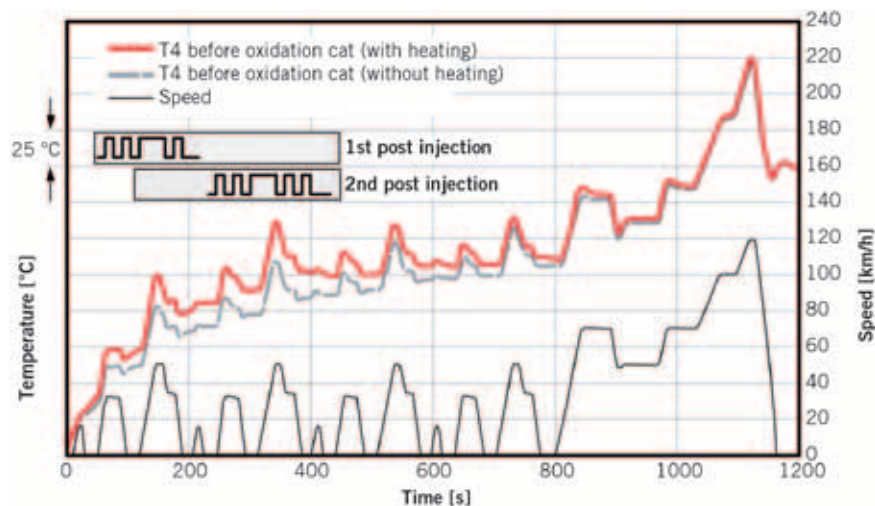
which delivers an effective increase in temperature after a cold start by means of close coupled and hence combusting post-injections. Additional software developments were necessary to coordinate the different operating modes. Shortly after cold-starting, when combustion stability has been achieved, the first combusting post-injection is also activated, ⑥. After a further stabilization phase a second combusting post-injection is added, leading to extended combustion, which enables a temperature increase of 25 K compared with basic mode without catalytic converter heating. Heating mode is deactivated on reaching the target temperature downstream of the oxidizing catalytic converter.

EXHAUST AFTERTREATMENT

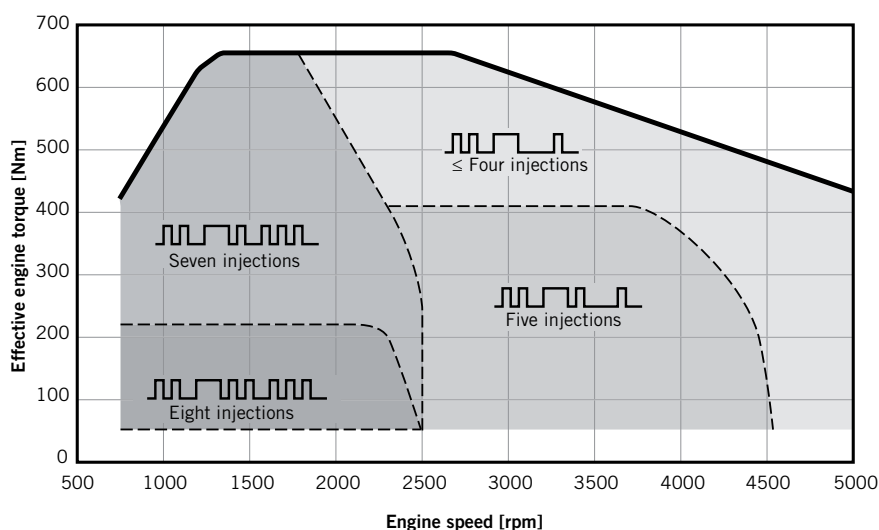
As a result of the special arrangement of the twin particulate filters with a Y-junction, additional software was necessary in relation to the particulate filter models for soot accumulation and soot burn-off. The regeneration intervals are determined by the most heavily laden DPF and the regeneration period is determined by the DPF with the slowest burn-off.

The second-generation V6 TDI already featured a triple post-injection strategy in order to increase the temperature in low-load operation, ensuring safe, rapid soot burn-off in all driving conditions, including in stop-and-go traffic [1]. For this, two close coupled and hence combusting post-injections are generated. The third, delayed post-injection generates the exothermic energy by means of the oxidizing catalytic converter.

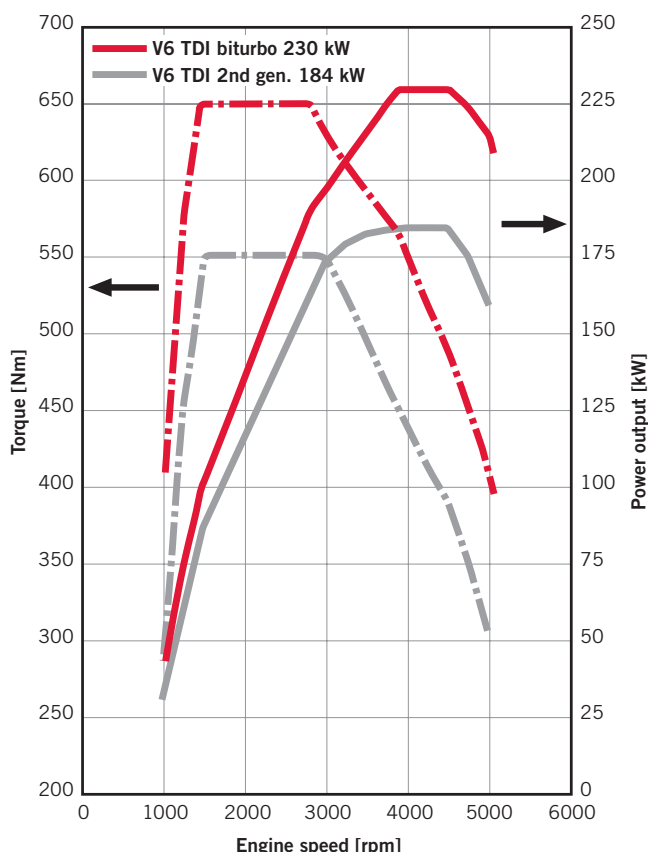
For the first time in the new V6 TDI biturbo, Audi is employing an enhanced fuel injection strategy which distributes the post-injection quantities of the previous third, remote post-injection across as many as three partial quantities. The number of possible partial quantities is continuously calculated by the engine management system and maximized by means of necessary minimum quantities. This results in as many as eight partial injections per combustion cycle during particulate filter regeneration, ⑦. The most significant advantages of this injection strategy are to be found in the engine speed range up to 2500 rpm: Soot burn-off is assured even when operating under light loads with high post-injection quan-



⑥ Heating measures for early cat light-off



⑦ Number of injections in map including particulate filter regeneration



8 Full load diagram

ties. As a result of the combination of the V6 TDI biturbo with the eight-speed torque-converter automatic transmissions and high gear ratios, for a high proportion of the time the eightfold injection mode is run in DPF regeneration, taking into account the customer's actions.

If the customer has a dynamic, sporty driving style, additional measures are taken in order to guarantee reliable soot burn-off even in these demanding driving situations. After rapid pedal movements by the driver are detected, the system switches to faster thermostat coordination in order to guarantee that the target temperature is still reached.

PERFORMANCE AND FUEL CONSUMPTION

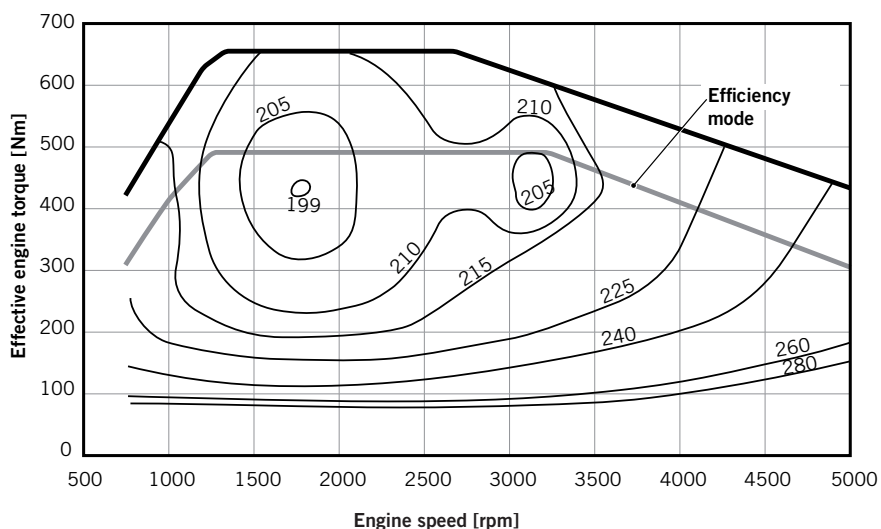
The new V6 TDI biturbo represents the addition of a high-performance V6 diesel engine delivering 230 kW and 650 Nm of torque [5] to the diesel engine range of the A6 and A7. The low weight of the engine also means that the overall vehicle combines plenty of driving pleasure and a sporty nature with low fuel consumption. The

maximum torque of 650 Nm is available across a wide rev range from 1450 to 2800 rpm, 8. As a result of the configuration of the LP stage, maximum power output is available from 3900 to 4500 rpm. This broad performance plateau enables excellent top-end performance and full-



load upshifts at 5200 rpm with no break in pulling power. Compared with the basic V6 TDI engine, the shift points are therefore up to 300 rpm higher. This gives the whole vehicle an especially emotional driving experience.

With the V6 TDI biturbo very good fuel consumption figures have been achieved across the entire engine map, even at full throttle, 9. At the optimum point it achieves 199 g/kWh consumption, which is outstanding for this power category. There is another low point in the engine map, which is characteristic of two-stage turbocharging, at 205 g/kWh. The turbo-charger configuration results in a broad map range with specific fuel consumption below 240 g/kWh. Should the customer want to make further fuel savings, the efficiency mode can be selected in the so-called Audi drive select. Torque and power output are then reduced by approximately 25 % and the gearshift engine speeds are lowered in order to run the engine in the optimum map ranges. In the new Audi A6 a fuel consumption figure of 6.4 l/100 km (169 g/km CO₂) is achieved with this high-performance diesel engine, 10. In addition to the standard start/stop system, the eight-speed automatic transmission also contributes to good customer-related fuel consumption with its high overall gear ratios.

The development goal of a sporty character has been implemented to optimum effect, even when starting off. The excellent performance of the second-generation



9 Map of effective specific consumption [g/kWh]

| | | | |
|---|-------------------------|---|------------------------|
|  | |  | |
| | Audi A6 V6 TDI 2nd gen. | Audi A6 V6 TDI 2nd gen. | Audi A6 V6 TDI biturbo |
| Transmission | Automatic, front | | Automatic, four-wheel |
| Emission class | Euro 5 | | |
| Max. engine power | kW | 150 | 180 |
| Max. engine torque | Nm | 400 | 500 |
| CO ₂ emissions NEDC | g/km | 133 | 156 |
| Acceleration 0-100 km/h | s | 7.2 | 6.1 |
| Maximum speed | km/h | 238 | 250 (governed) |

V6 TDI has once again been significantly improved. The A6 with V6 TDI biturbo accelerates from 0 to 100 km/h in only 5.1 s, a benchmark value within its direct competitors.

SUMMARY

With the V6 TDI biturbo, Audi has launched its most powerful series-production six-cylinder diesel engine to date. The engine enables the C-series models to achieve outstanding levels of sporty driving performance, together with impressive fuel economy. The two-stage turbocharging system has been accommodated in the restricted space available with no need for compromise in terms of thermodynamics. The components relevant to gas flow and the combustion process have been upgraded

for the V6 TDI biturbo on the basis of the second-generation V6 TDI. In the course of functional development and application, the expectations of a high-performance engine with regard to responsiveness and acceleration from a standstill have been implemented to optimum effect. At the same time a key objective was compliance with the Euro 5 emissions standard. Audi has thus also established a sound foundation for the further development of its engine range in compliance with increasingly stringent emissions regulations.

REFERENCES

[1] Bauder, R.; Kahrstedt, J.; Zülch, S.; Fröhlich, A.; Streng, C.; Eiglmeier, C.; Riegger, R.: Der 3.0 l V6-TDI der zweiten Generation von Audi – konsequente Weiterentwicklung eines effizienten Antriebs [The second-generation 3-litre V6 TDI from Audi – systematic further development of an efficient power plant]. 19th Aachen Colloquium Automobile and Engine Technology, 2010

[2] Pott, E.; Rudolph, F.; Thomforde, C.; Ziesenis, J.: Die neuen Dieselmotoren der Volkswagen Transporter-Baureihe [The new diesel engines in the Volkswagen Transporter model line]. 18th Aachen Colloquium Automobile and Engine Technology, 2009

[3] Eiglmeier, C.; Bauder, R.; Fröhlich, A.; Gabel, K.; Helbig, J.; Marckwardt, H.; Zülch, S.: The new 3.0-litre V6-TDI engine with Dual-stage Turbocharging in the Audi A6 and A7. 20th Aachen Colloquium Automobile and Engine Technology, 2011

[4] Ebinger, T.: Untersuchung der zweistufigen Aufladung beim PKW-Dieselmotor [Investigations of dual-stage-turbocharging at diesel engines for passenger cars]. Dissertation, University of Stuttgart, 2010

[5] Bauder, R.; Eiglmeier, C.; Eiser, A.; Marckwardt, H.: Der neue High Performance Diesel von Audi, der 3.0 l V6-TDI Biturbo [The new high-performance diesel from Audi, the 3.0 l V6 TDI biturbo]. 32nd International Vienna Motor Symposium, 2011

10 Comparison of performance and fuel consumption of the V6 TDI in the Audi A6

THANKS

The following people also assisted in the production of this article:

- : Dr.-Ing. Tanja Ebinger, Test Engineer in Department Pre-Development – V Diesel Engines
- : Dr.-Ing. Klaus Gabel, Fluid Dynamics Engineer in Department Pre-Development – V Diesel Engines
- : Dr.-Ing. Walburga Kerschbaumer, Fluid Dynamics Engineer in Department Pre-Development – V Diesel Engines
- : Dipl.-Ing. Gerald Reidick, Test Engineer in Department Thermodynamics and Calibration – V Diesel Engines.

12th Stuttgart International Symposium



Automotive and Engine Technology

VEHICLE TECHNOLOGY

Aerodynamics, new vehicle concepts, driving dynamics and driver assistance systems

VEHICLE POWERTRAIN

Hybrid technology, alternative fuels, spark-ignition and diesel engines, engine management and modelling

VEHICLE ELECTRONICS

Electric vehicles, software and design, modelling and simulation

13 and 14 March 2012
Stuttgart | Germany



ATZ live

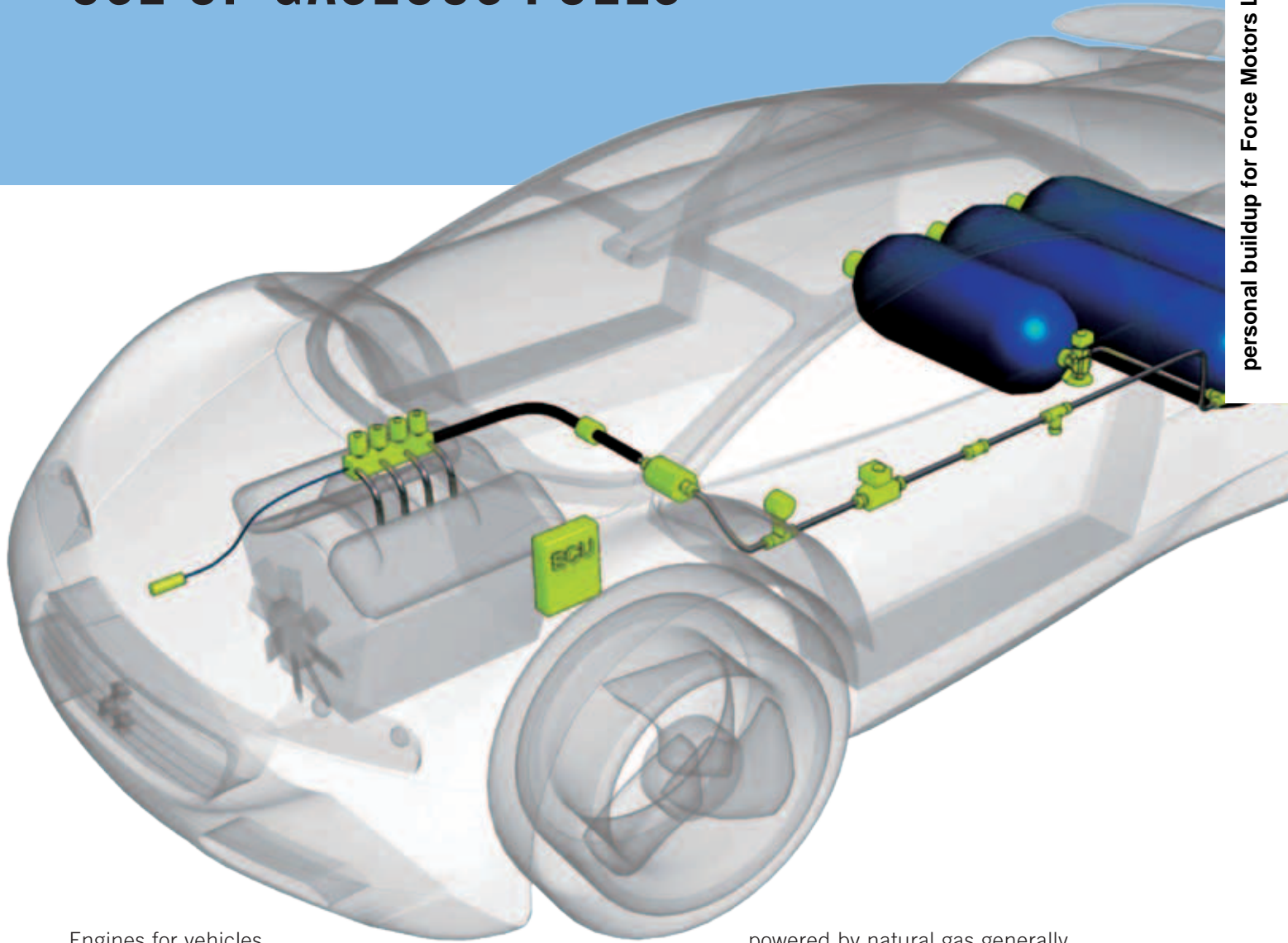
Abraham-Lincoln-Straße 46
65189 Wiesbaden | Germany

Phone +49 (0)611 / 7878 – 131
Fax +49 (0)611 / 7878 – 452
ATZlive@springer.com

PROGRAM AND REGISTRATION

www.ATZlive.com

MANAGEMENT SYSTEM FOR THE EFFICIENT USE OF GASEOUS FUELS



Engines for vehicles use purely mechanical gas management systems. The gaseous fuel is fed to the injection valves via a mechanical constant pressure regulator. Key factors that have a strong influence on fuel consumption and emissions, such as the temperature, quality and moisture content of the gas, are not taken into consideration. Rotarex, in collaboration with Trier University of Applied Sciences, has developed a mechatronic gas management system that allows map-based control of the mass flow into the gas distributor pipe.

AUTHORS



DR.-ING. THOMAS ANDREAS
is Manager of the Research and Development Department of the Rotarex Group in Lintgen (Luxembourg).



CHRISTIAN BAUMGARTEN
(B. Eng.) is Scientific Assistant at the Fluid Power Laboratory/Division of Trier University of Applied Sciences (Germany).



CHRISTIAN NISTERS
(B. Eng.) is Scientific Assistant at the Fluid Power Laboratory/Division of Trier University of Applied Sciences (Germany).



PROF. DR.-ING. HARALD ORTWIG
is Head of the Fluid Power Laboratory/Division at Trier University of Applied Sciences (Germany).

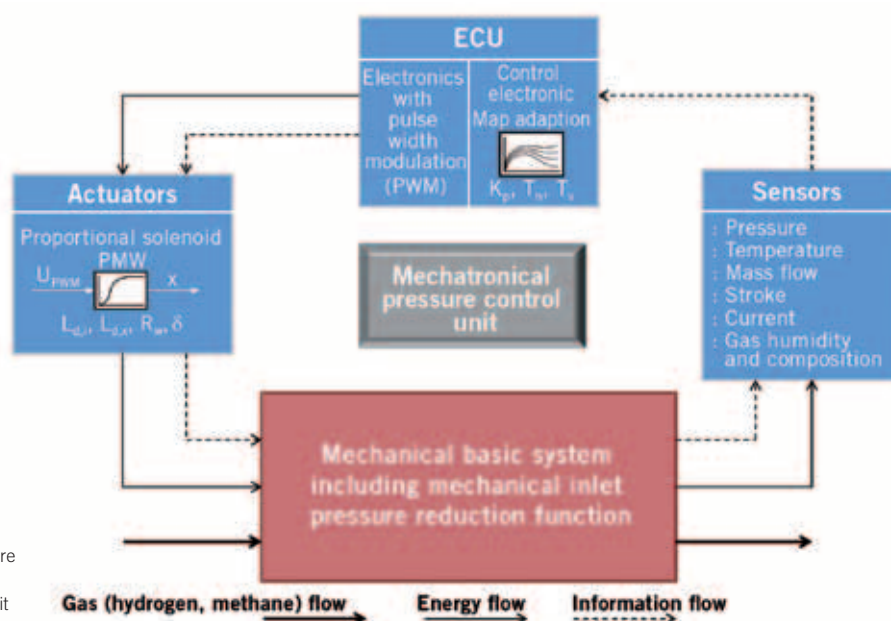
MOTIVATION

Motor vehicles of the future will no longer be operated exclusively with conventional fossil fuels, because fossil fuel reserves are indisputably finite. The worldwide climate debate further strengthens the need for the creation of a transport sector dependent on renewable forms of energy. The use of gaseous fuels is one of many alternative solutions discussed that have great potential for the future. A long-term solution is fortified regeneratively produced hydrogen, which is implemented by on-board fuel cells that generate electrical propulsion energy.

The widespread introduction of this energy source will, however, take some time. Methane (CNG technology) can play the role of a bridging function as a new fuel in the context of a sustainable energy supply of gaseous fuels for the transport sector. Sources of methane gas are natural gas, biogas, and in future also synthetic methane (electrolytic hydrogen is produced from renewable power sources and is then converted into pure methane by the addition of excess CO_2).

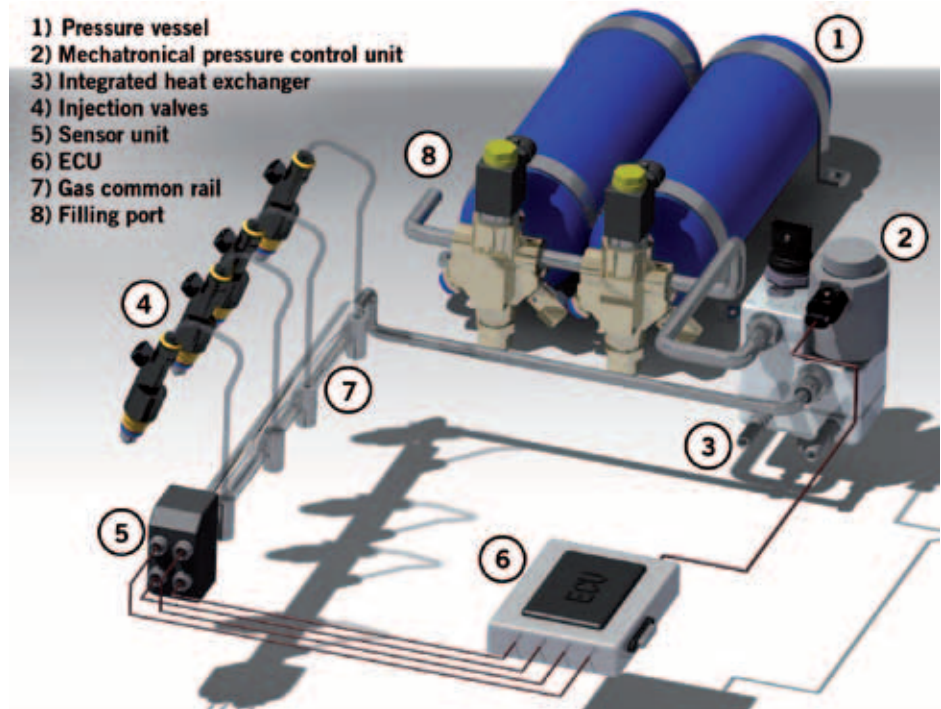
A great advantage of methane compared to other alternative fuels is the relatively high storage density and thus the achievable vehicle range. Current monovalent CNG vehicle developments (i.e. vehicles that start and run exclusively on methane) from different manufacturers already have ranges of about 500 km (medium size cars, over 100 kW engine power), although in these cases use is still made of purely conventional gas management systems in which the gaseous fuel is introduced via a mechanical constant pressure regulator to the gas common rail. In these purely mechanical gas management systems, however, no consideration is given to important factors such as gas temperature, air quality and humidity. Furthermore, the dosage of the gaseous fuel is very difficult because the only free parameter available is the variation in the opening times of injectors. Due to the limited dynamics of these valves a precise dosage of fuel is extremely difficult, but this would be very important for increasing the fuel efficiency of the motor vehicle, especially in the partial load range.

① Functional structure of the mechatronic pressure regulator unit

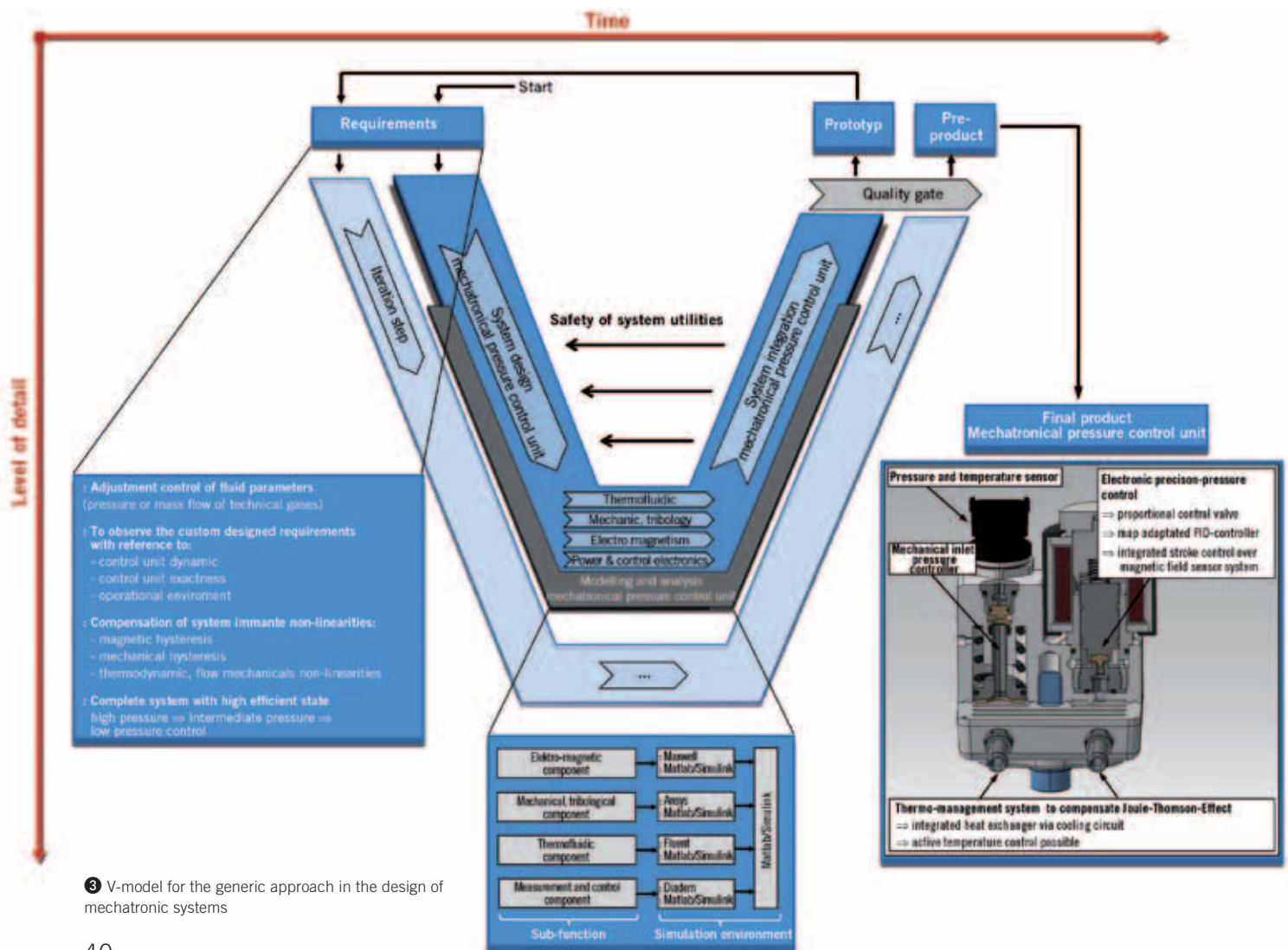


MECHATRONIC VERSUS MECHANICAL

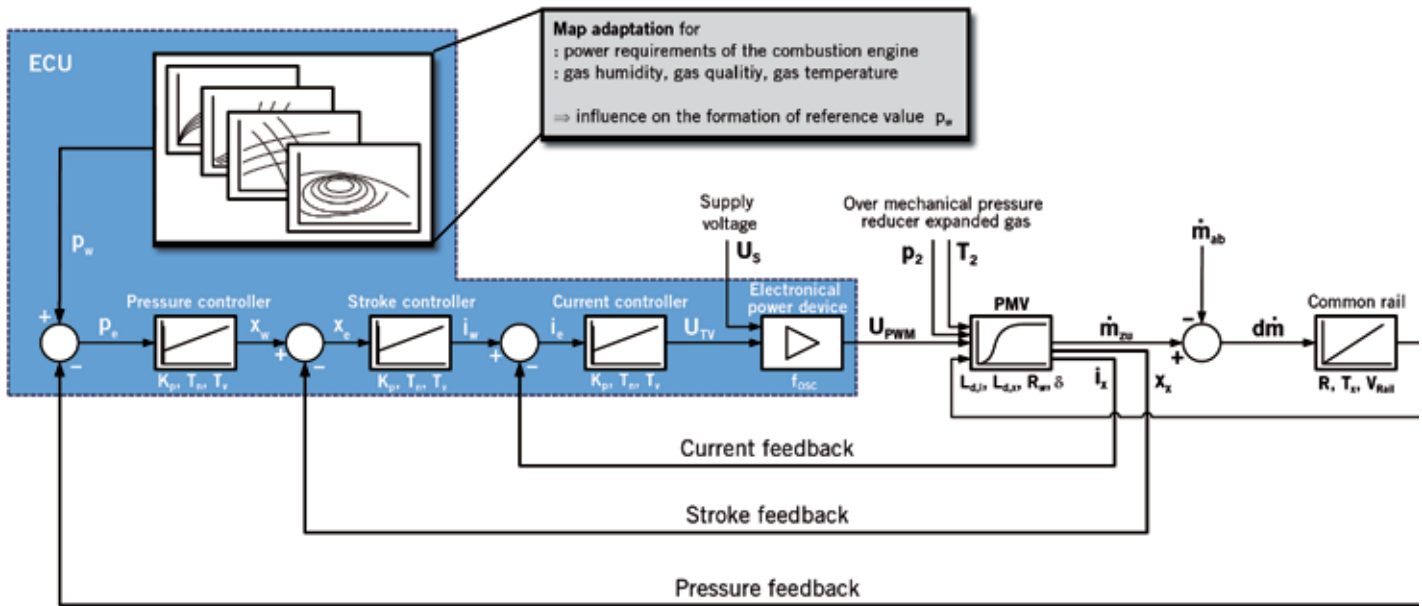
The mechatronic gas management system, ①, combines all relevant system components in one housing and compared to a purely mechanical system has tremendous advantages, since the mass flow into the gas common rail can be dynamically dosed. Via the sensor unit all physical states of the gas are recorded and processed in the ECU, and in this way the manipulated variable (variable common rail pressure) is influenced multidimensionally via corresponding maps. The injectors meter the gas sequentially via selective cylinders into the intake manifold, so that with a highly dynamic control unit and optimized characteristic maps, significantly reduced fuel consumption can be achieved. ② shows the basic structure of the overall system.



② Basic structure of the gas management system in the car



③ V-model for the generic approach in the design of mechatronic systems



4 Representation of system structure in the control action plan

If you compare a purely mechanical pressure regulator having static set pressure to a mechatronic pressure regulator with variable set pressure, then in terms of its special properties over the entire load range of the downstream engine the mechatronic pressure regulator is clearly superior to the mechanical pressure regulator. The dilemma that arises with a mechanical pressure regulator is contradictory system behaviour in the partial load and full load range. At full load the resulting pressure deviation causes a steeply sloping common rail pressure. Consequently, the required maximum power of the internal combustion engine cannot be realized. In the partial load range, however, there is a common rail pressure that is far too high, which in turn is reflected in extremely poor consumption behaviour. Since the switching time of the injectors due to inertia loads and inductive switching delay is finite, too much gas flows into the intake manifold and increases the fuel consumption unnecessarily. The mechatronic gas pressure regulator helps to resolve this conflict. The gas pressure in the gas common rail is fully regulated variably between 2 to 10 bar. Consequently, the injected gas volume can be dosed very finely and is no longer subject exclusively to the restriction of finite switching times of the injectors. In the partial load range the pressure in the gas common rail is very low (2 bar) and at full load range very high (10 bar).

DESIGN AND DEVELOPMENT OF A MECHATRONIC CONTROL UNIT

The design and development of a functional mechatronic pressure and mass flow control unit, particularly with respect to the control algorithms to be determined and the proportional actuator, proved to be a complex task. First, it should be noted that the physical laws that underlie gaseous fuels and the resulting diverse needs are totally different to the currently used gasoline and diesel fuels, i.e. completely different components and system solutions are required.

The conceptual design and development of this mechatronic system was initially implemented on the basis of the known V-model for the generic approach to designing mechatronic systems, but has been adapted to the present application, ③. Based on known design methods that led to a first version of the pressure and mass flow control unit, the overall system was initially divided into subsystems with partial functions, which ensued a domain-specific physical modelling, where extensive analysis of the physical/technical basic systems, which in the current case are characterized by fluidic, mechanical, thermodynamic, electrodynamic and tribological subsystems, was the initial focus.

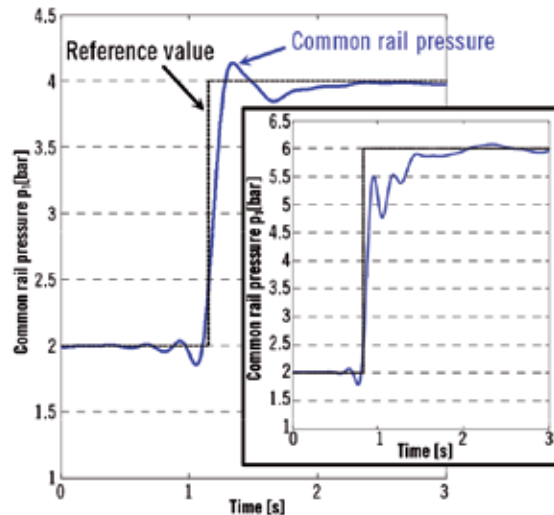
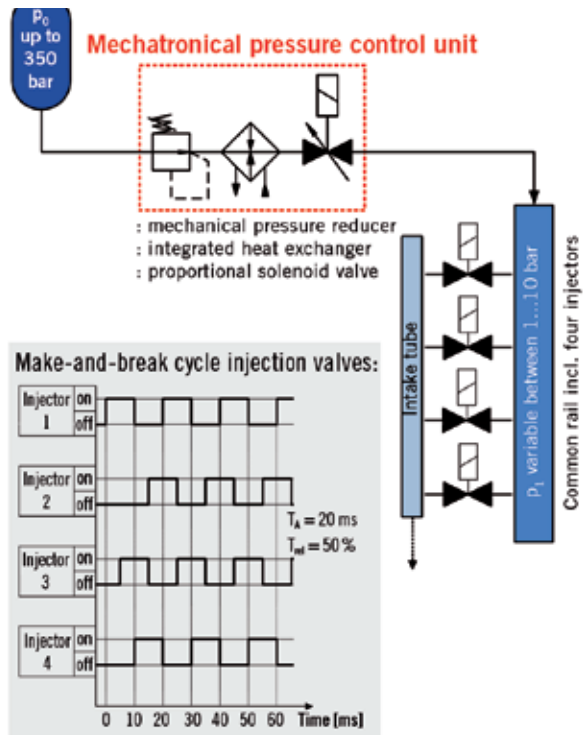
③ shows that different simulation environments are necessary for theoretical modelling. The results of the modelling/

simulation of these partial functions can then be collectively represented and simulated in the Matlab/Simulink simulation tool. Experimental tests on fabricated prototypes led to the verification/validation of the simulation model. The goal was to vary parameters so that a simulation-based optimization could be carried out. Using this approach you can achieve a significant reduction of the predevelopment time and thereby concomitant cost savings.

CONTROL ALGORITHMS AND CONTROL LOOP STRUCTURE

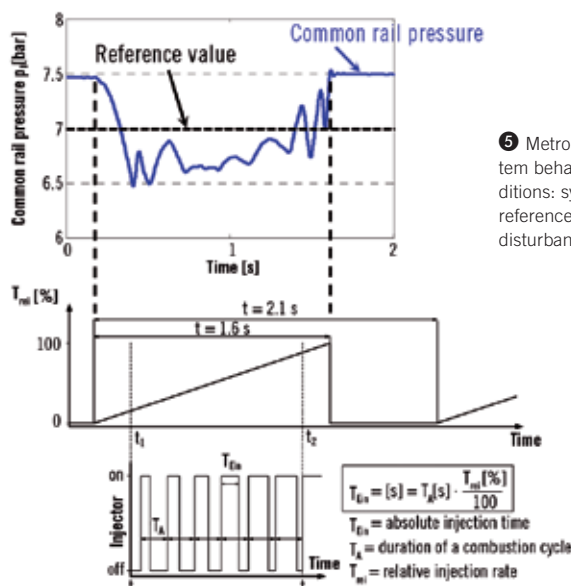
④ shows a possible control loop structure. The output of the system is the pressure in the gas common rail, which in the application shown here represents the controlled variable. This pressure is sensed by means of appropriate sensors and fed to the control process as the actual value. In the case of a control deviation, the output size of the superordinate primary control for the actuators is formed according to operating-point-dependent control algorithms with map adapted control coefficients. In the simplest case, the output signal from the controller directly represents the input of the power device.

However, in order to achieve optimal dynamic response and system stability, the switching of two auxiliary controlled variables is used. For this purpose, besides the main controlled variable pressure, there is



Characteristics of the control process variable after the jump of the reference value during make-and-break cycle of the injection valves:

- : jump of the reference value from 2 up to 4 bar
- : jump of the reference value from 2 up to 6 bar



Characteristics of the control process variable during dynamic disturbance reaction:

- : reference value = 7 bar = constant
- : linear increase of the relative injection time

⑤ Metrological examination of system behaviour in various driving conditions: system structure (top left), reference action (top right), dynamic disturbance reaction (bottom)

subordinate control of a solenoid armature stroke and the coil current. A power device with a high frequency pulse-width modulated control signal is switched between the controller assembly and the proportional solenoid valve. Since it is effectively a control with a pronounced voltage signal, the corresponding effect of the change of

the field coil resistance when heated by the subordinate current control is balanced.

The power device responds ultimately to its input value with a change to the effective coil voltage, so that the field current and hence the magnetic force can be influenced. This leads to a movement of the armature, and consequently to a

change in the free-flow, cross-sectional area of the valve. Neglecting magnetic eddy current effects and the effect of the magnetic field displacement, as well as the influence of the temperature-dependent time constants, the armature of the proportional solenoid valve responds with an overall delay of the third grade. In this respect the mechanics of the armature as a cushioned spring-mass system represents an element with a delay of the second order. In addition, there is a first order delay of the coil current of the proportional solenoid with respect to the applied voltage, which is caused by the inductance. In the form of a regulating pressure accumulator the gas common rail is the main control system in the true sense.

Since the mass flow that enters the common rail volume has a functional relationship to the free-flow, cross-sectional area of the proportional valve, the timing of mass and energy balances for the current common rail volumes are affected. The time-based pressure variation in the common rail volume is determined by input and output mass flows, exchange of energy across the system boundaries and via the conjunction of the physical quantities of mass, temperature, pressure and volume.

The determining parameter in the gas management system is the set value of the common rail pressure. The set value formation depends on several factors, such as the load of the engine or the driver's requested driving performance derived from the position of the accelerator pedal. Maps of the load requirements for the internal combustion engine are stored in the ECU unit. Furthermore, parasitic effects such as gas humidity, quality and temperature must be taken into account. These effects are also considered using separately determined compensation algorithms in the corresponding maps.

SYSTEM BEHAVIOUR

To evaluate the system behaviour, the possible driving conditions are simulated in various series of measurements, ⑤. Of particular interest here is the command and disturbance behaviour of the system. The command action reflects the progression of the actual pressure in the gas common rail after an abrupt change of set pressure, caused by changing the engine load conditions. The switching times of the injectors remain constant over the entire period. The investigation regarding the disruptive behaviour should permit a conclusion to be made about the dynamic system behaviour on successive depressions of the gas pedal and a subsequent deceleration fuel cut-off. Contrary to the realistic processes that create the desired pressure and speed depending on load, there is the simplifying assumption that the speed and the desired pressure remain constant throughout the entire process.

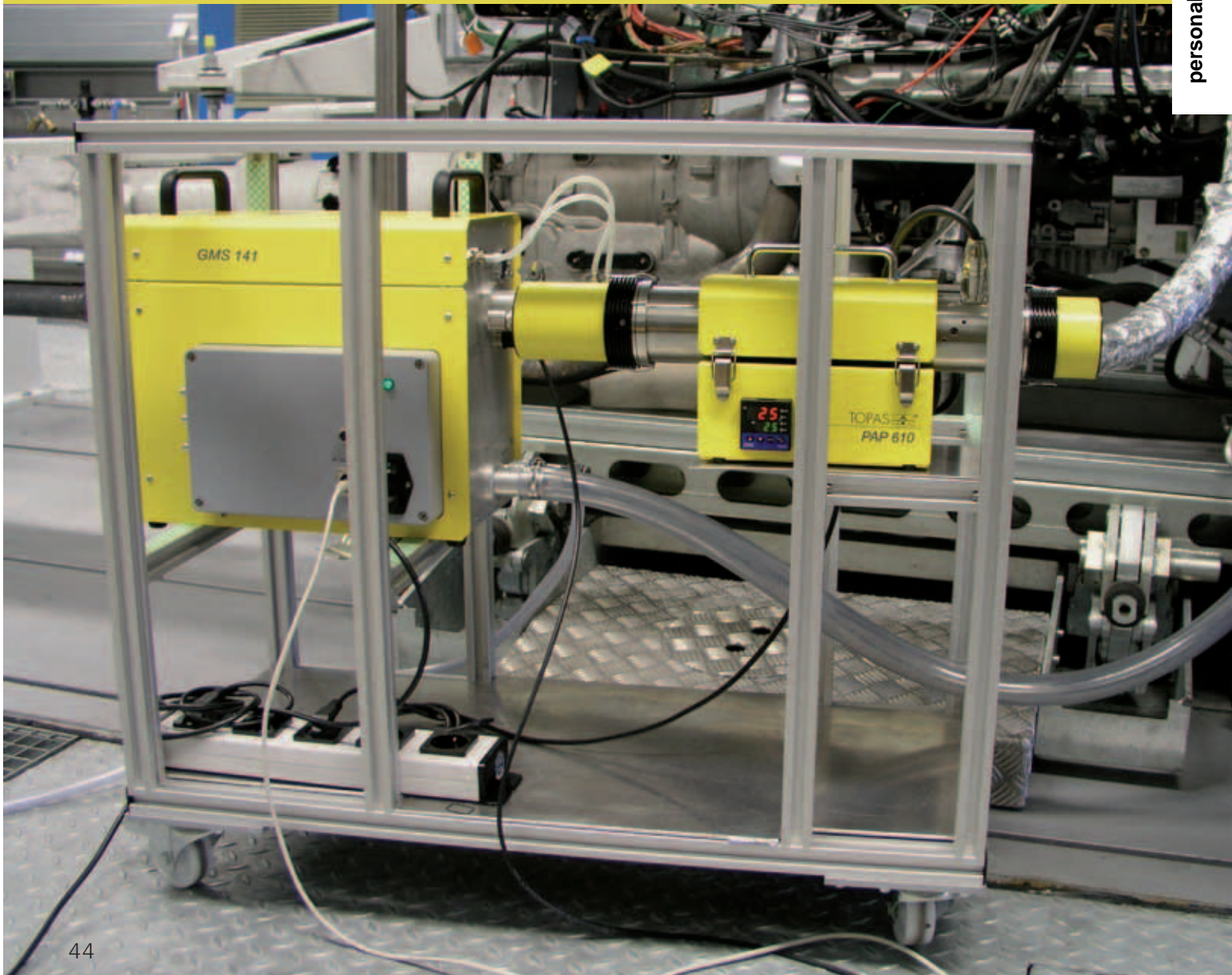
Due to the inherent non-linearity of the system, the control loop gain is a function of the operating point. Thus, in operation of the control loop with constant control parameters, operating-point-dependent instabilities can arise. With a view to optimal control dynamics, the proportional gain of the controller should not be reduced indefinitely. One approach to achieve optimum control characteristics is provided by adapting the control parameters to the respective operating point. For the mechatronic pressure and mass flow control unit, the controller parameters can be adapted in dependence on the pressure setpoint.

CONCLUSIONS AND OUTLOOK

The optimization task proved to be highly complex because the proportional control valve shows strong non-linearities due to inductance and eddy currents as well as the current limit, tribological effects, magnetic hysteresis and the free flow cross-section. This provides, in addition to the proven map-adapted PID (proportional-integral-derivative) control, a further optimization step using the possibility of an evolutionary design process for developing a fuzzy rule structure. An essential condition for the controller optimization by an evolutionary algorithm is to develop a fuzzy quality measure for evaluating the dynamic behaviour of the proportional control valve for different excitations in both the small and large signal range, which is based on characteristic parameters derived from the control response. With the help of the designed quality measure, the automated optimization of controller parameters could eventually take place via an evolutionary algorithm. These studies are currently being intensively investigated. In the near future the extent to which such approaches can improve the control behaviour of the mechatronic pressure and mass flow control unit will be demonstrated.

CRANKCASE VENTILATION INLINE MEASUREMENTS OF OIL AEROSOLS

Oily blow-by gases out of the crankcase affect the life time of parts of the engine and of the intake as well as the emission of a motor vehicle. Well-established gravimetric methods for the characterization of oil mist emissions provide comparatively poor information in spite of high costs. With the use of the inline measuring method developed by Topas, Mahle and BMW, it is possible to collect complete engine operation maps in a few hours combining it with an intelligent gravimetric procedure. Additionally, changes in particle sizes of oil droplets can be determined.



AUTHORS



DR.-ING. HARTMUT SAUTER
is Manager of Advanced Development Group at Mahle Filtersysteme GmbH in Stuttgart (Germany).



DR.-ING. DETLEF MATHIAK
is Manager of Test Methods Powertrain at BMW AG in Munich (Germany).



DIPL.-PHYS. JAN MÜLLER
is Development Engineer in the R&D Department at Topas GmbH in Dresden (Germany).



DIPL.-ING. STEPHAN LIST
is Test System Manager at Topas GmbH in Dresden (Germany).

MOTIVATION

Oily emissions of the crankcase particularly are mainly aerosols. Particle size measurements normally show a lot of droplets in the area of 1 µm size [1, 2]. The small particles are generated mainly in the piston area. Condensation, atomization at rotating shafts and spraying out of the lubricating circuit can also be origins of the emission of these oil aerosols. At charged engines, small particles can reach the crankcase via the oil return of the turbocharger. In the crankcase the particle size distribution is affected by secondary effects like decomposition or coagulation of droplets, interactions of the droplets with the wall or sedimentation. In spite of the oil mist separators used, closed crankcase ventilation systems are relevant for the total oil consumption of reciprocating engines. Due to the mandatory closed crankcase ventilation, contaminations of valves and intercoolers are possible with the consequence of reduced life time and less cooling efficiency. Oil components in the combustion also effect particle filters and catalytic converters. Regarding the total oil consumption per operation point of less than 10 g/h today, the crankcase ventilation is becoming more and more important.

Gravimetry is a quantitative analysis method for many applications. The measurement of the quantity of materials is based on the gravimetric determination of collected material. At dynamometer test benches, emissions of the closed crankcase ventilation are determined by measurements of the full aerosol flow at stationary operation conditions. Filters that are used for these measurements differ in size and material according to the engine respectively the blow-by volume flow. Usually filters of glass fibers are used. Before and after a measurement they have to be conditioned and characterized. It is nearly impossible to determine the influence of load or speed changes of the engine on the oil consumption with gravimetric methods. A lot of time is needed for the measurement of complete engine

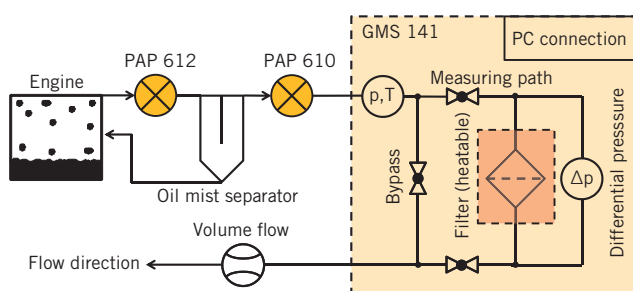
operation maps. For the determination of oil components at a low detection limit, mass spectroscopy can be used as an alternative method [3, 4].

MEASURING INSTRUMENTS AND STRATEGY OF MEASUREMENTS

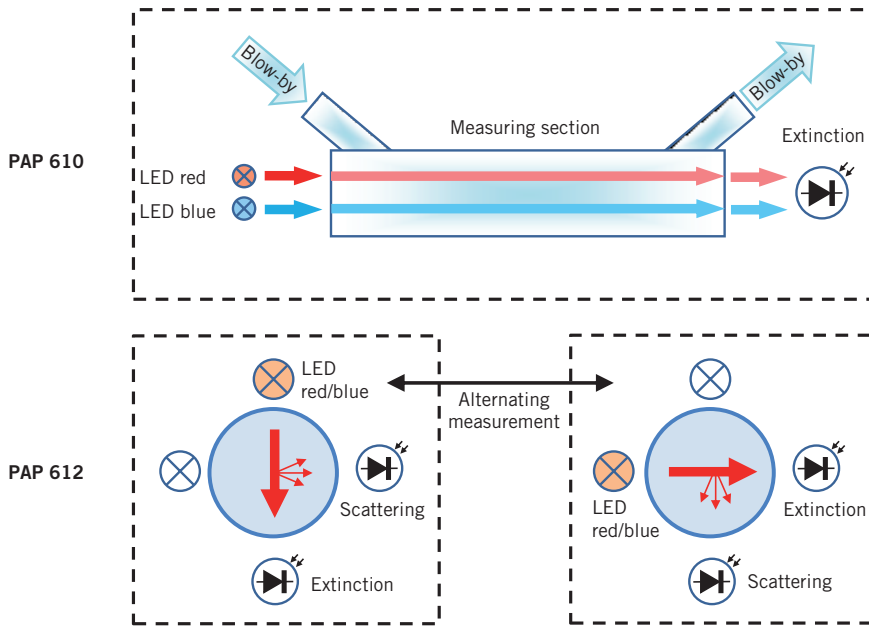
Using the measuring instruments shown in this paper, oil aerosols out of the ventilation can be characterized in a short time and with a lot of information. The new gravimetric measuring system (GMS 141), ①, allows the comfortable detection of the oil content in blow-by gases using filter blank sheets or filter cartridges directly at dynamometer test benches. Many applications like improvements of closed crankcase ventilation systems, optimization of piston geometry or the examination of the droplet generation in turbochargers are possible. The blow-by can be led through the filter housing for measurement or a bypass for conditioning the system shown in ① (yellow box). The actual load of the filter can be monitored by the differential pressure across the filter. Therefore adapted measuring times are possible. Condensation of components of the blow-by can be avoided by heating the pipes and the filter housing. After loading the filter with blow-by aerosol the samples are analyzed in the laboratory. There it is possible to characterize the composition of the blow-by in addition to the determination of the mass of the filter. Additionally, the volume flow can be determined by an orifice system during the experiment. As a result, the oil mass flow and the blow-by volume flow are connected by the mass concentration:

$$\text{EQ. 1} \quad \dot{m}_{\text{oil}} \left[\frac{\text{g}}{\text{h}} \right] = c_{\text{Oil}} \left[\frac{\text{g}}{\text{m}^3} \right] \cdot \dot{V}_{\text{blow-by}} \left[\frac{\text{m}^3}{\text{h}} \right]$$

The determination of the oil mass coming out of the crankcase directly at the dynamometer test bench was the goal of the development. Because of pulsating blow-by volume flow the developed measurement devices are integrated directly inline to the pipe system. Due to different aspects during the development of closed crankcase ventilations, two different inline photometers have been developed. They use the interaction of light with the aerosols. The concentration of oil masses can be determined after a gravimetric calibration.



① Measuring set-up for the characterization of oil mist separators



② Measuring principle of the aerosol photometers PAP 610 and PAP 612

tion. The results of the photometers were compared with a mass spectrometer and approved in laboratory and at dynamometer test bench. Because of high oil concentrations in the crankcase ventilation, only a time resolved and a qualitative comparison could be performed [3].

The process aerosol photometer PAP 610 was designed and developed for inline concentration measurements of blow-by aerosols. The measuring principle is shown in ②. The instrument uses the attenuation of light through a measuring volume caused by an aerosol. The dimensionless extinction of light describes the attenuation and is proportional to the oil concentration of the aerosol. The photometer measures the

extinction of two different wavelengths (blue: 470 nm, infrared: 875 nm). Knowing the extinction of two different wavelengths, it is possible to calculate an equivalent particle size applying the theory of Mie [5]. The ratio of both extinctions and the refractive index are an indicator for the particle size in a range of approximately 0.1 to 1.5 μm .

The PAP 612 is an inline extinction and scattered-light photometer that can be used for the detection of wall films in pipes as well as for the measurement of high drop-let concentrations. ② shows a schematic diagram of the measuring principle. The photometer particularly supports the choice of the blow-by gas sampling position of

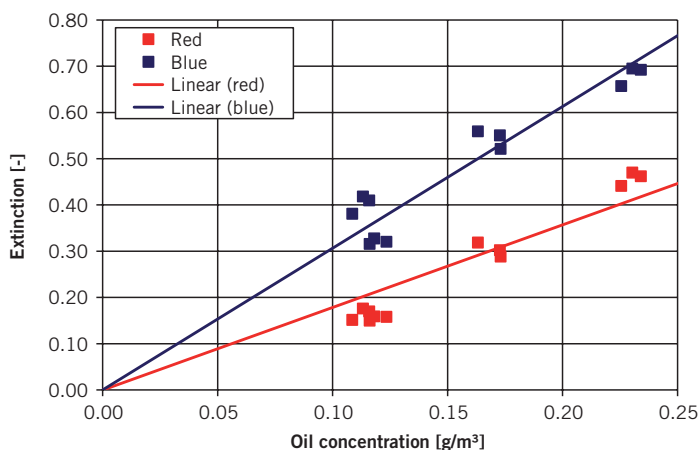
the crankcase. Due to its compact design the PAP 612 can be used in laboratory, at dynamometer test rigs on swivelling test benches and for test drives in field.

Combining the presented instruments inline as shown in ①, efficient measurements are possible. With the optical measuring instruments PAP 610 and PAP 612, the extinction and scattering intensity of the blow-by are measured permanently. The extinction shows an almost linear behavior regarding the oil concentration of the blow-by (Eq. 1). For calibration it is necessary to determine only a few sampling points gravimetrically with the GMS 141. ③ shows the extinction measured by the PAP 610 and the gravimetrically determined oil concentration. Operation points without gravimetric measurements can be interpolated by the linear regression line. The same procedure can be applied to the PAP 612. After this calibration process, the photometers PAP 610 and PAP 612 allow the determination of the oil concentration of the blow-by gases by inline measurements. Using Eq. 1 the oil mass flow can be calculated easily. The number of time-consuming gravimetric measurements is reduced significantly.

RESULTS

Subsequently some exemplarily results are presented for measurements of a gasoline engine, a truck application and a passenger car turbocharger. ④ shows the result of measurements of an operation map of a recent gasoline engine. The oil mass flow is plotted against the dimensionless engine speed and load; all values are without dimension in % and related to its respective maximum. The raw data were recorded during an automated test procedure with the PAP 612 in a few hours. Obviously there is a significant increase of the oil mass flow in particular at high loads. The load has significantly more influence on the oil mass flow than the engine speed. With the knowledge of this information, further measurements can be done efficiently.

Characterizations of diesel engines can be performed the same way. In this case, the detailed description of all measuring values will be passed on. ⑤ shows a comparison of two different piston configurations for an application of commercial vehicles. The difference can mainly be found in the concept of cooling. The cool-



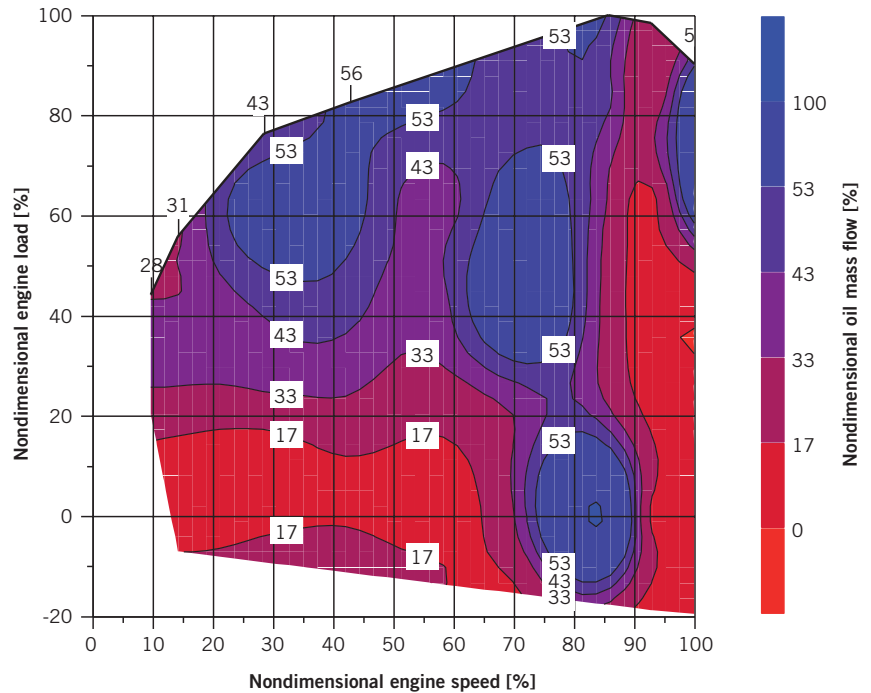
③ Calibration measurements of the extinction at different oil concentrations

ing temperature was set to a constant value during the tests. The ration of blow-by oil mass flows in % of both configurations is plotted against the dimensionless engine load and speed. One of the configurations shows significantly less oil mass flow than the other one. All measuring points are lower than 100 %. The result underlines the big influence of the cooling configuration of the pistons on the oil concentration. This is an interesting aspect of the optimizations of engines.

Besides the area of the pistons, oil aerosol can also reach the crankcase via the oil return coming from the turbocharger. The volume flow is low compared to the piston area but it contains a high concentration of oil droplets. ⑥ shows the oil concentration, the light extinction and the calculated equivalent particle size of the oil droplets for a few operation points of a small turbocharger. The results of the turbo engine show significant differences to the results of reciprocating engines: slightly bigger particles, higher concentration of oil droplets and lower oil mass flow because of the lower volume flow. The manifold interactions of oil droplets in a crankcase are the reason for the interest of this emission source.

SUMMARY

Compared to actually measuring methods used, the presented solution shows big advantages for the determination of information about blow-by gases. With dynamometer test benches, the measuring times concerning the oil consumption of the closed crankcase ventilation of an engine



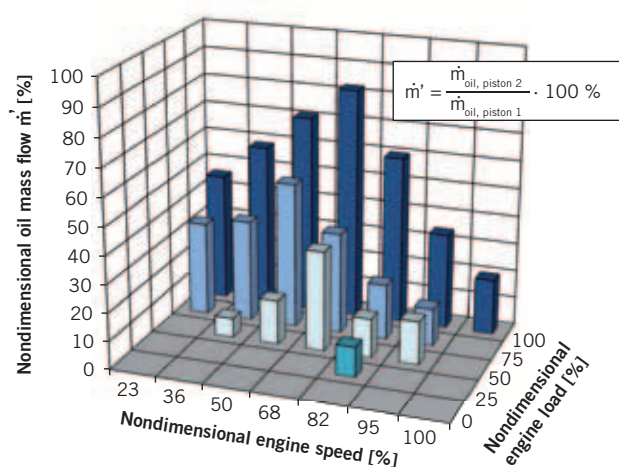
④ Gasoline engine operation map: oil mass flows in dependence on the engine load and speed

operation map can be reduced significantly. The result of these measurements can be an optimization for the choice of sampling points of closed crankcase ventilations and for the evaluation of oil mist separators. Other points of interest are the aerosol generation of turbochargers or the optimization of piston geometry.

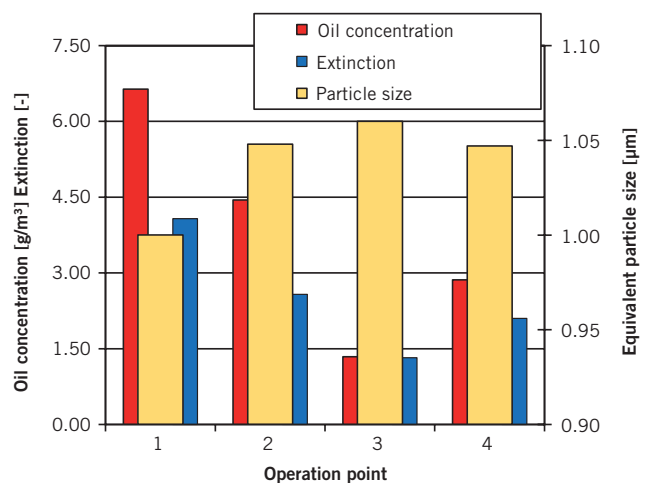
REFERENCES

- [1] Sauter, H.; Trautmann, P.: Measurement and Separation of Oil Mist Aerosols from the Crankcase Exhaust of Combustion Engines. In: MTZ world-wide 61 (2000) No. 12, pp. 18-19

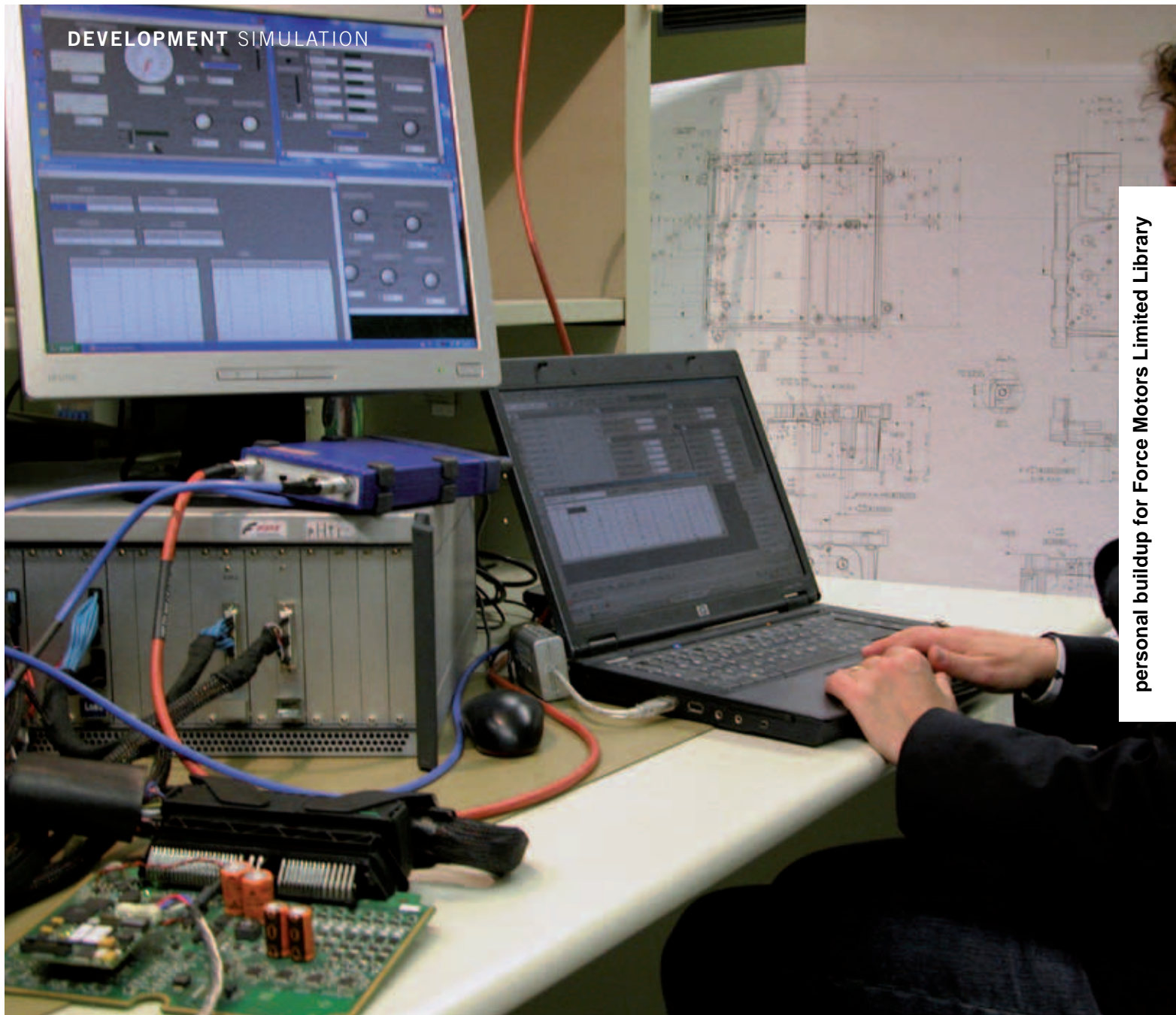
- [2] Sauter, H.: Analysen und Lösungsansätze für die Entwicklung von innovativen Kurbelgehäuseentlüftungen. Berlin: Logos, 2004
 [3] Sauter, H.; Beekmann, A.; List, S.: Online-Ölverbrauchsmessungen des Kurbelgehäuseentlüftungssystems von Otto- und Dieselmotoren. Aachener Kolloquium Fahrzeug- und Motorentechnik, 2009
 [4] Gohl, M.: Massenspektrometrisches Verfahren zur dynamischen Online-Messung der Ölemission. Düsseldorf: VDI, Fortschr.-Ber. Reihe 8 (No. 1021), 2004
 [5] Bohren, C.F.; Huffmann, D.: Absorption and Scattering of Light by Small Particles. New York: Wiley-VCH, 1998



⑤ Diesel engine: comparison of the oil mass flows with dependency on engine load and speed of two different piston configurations



⑥ Turbocharger: oil concentration, light extinction and equivalent particle sizes of operation points



HIL/SIL SYSTEM FOR THE SIMULATION OF TURBOCHARGED DIESEL ENGINES

The development of management and diagnostic systems plays a significant role in the design of powertrains, and requires suitable development and testing procedures. The University of Parma and Fiat Research Centre/Fiat Powertrain have jointly developed a Hardware-in-the-Loop system based on a PC board for the simulation of turbocharged diesel engines.

AUTHORS



PROF. ING. AGOSTINO GAMBAROTTA
is Professor of Thermal Machines and Internal Combustion Engines at the University of Parma (Italy).



DR.-ING. ANDREA RUGGIERO
is Manager of the Diesel Controls and Systems Department at Fiat Powertrain R&T in Turin (Italy).



DR.-ING. MICHELE SCIOLLA
is Coordinator of HiL Equipment Development at Fiat Powertrain R&T in Turin (Italy).



DR.-ING. GABRIELE LUCCHETTI
is Researcher and Simulation Model Developer at the University of Parma (Italy).

MOTIVATION

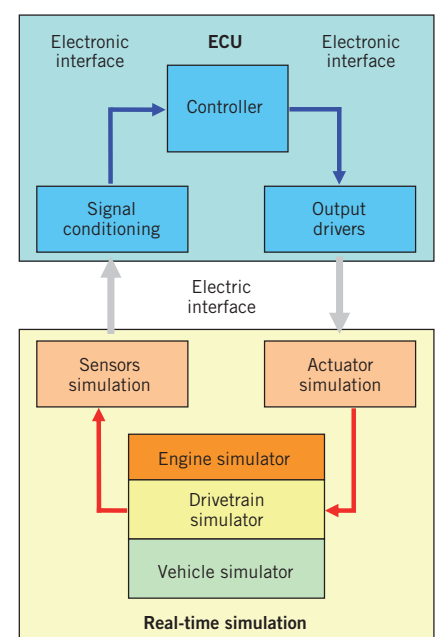
Management and diagnostic systems play a significant role in the design of current powertrains, especially when targets such as specific fuel consumption and pollutant emissions are taken into account. Mathematical models are useful tools in this field, with applications that range from the definition of optimised management systems and Hardware- and Software-in-the-Loop testing (HiL and SiL) to model-based control strategies. The University of Parma has developed a library of models for the real-time simulation of automotive engines, which is used within an original HiL system developed by Fiat Research Centre/Fiat Powertrain.

ADVANTAGES OF HiL SYSTEMS

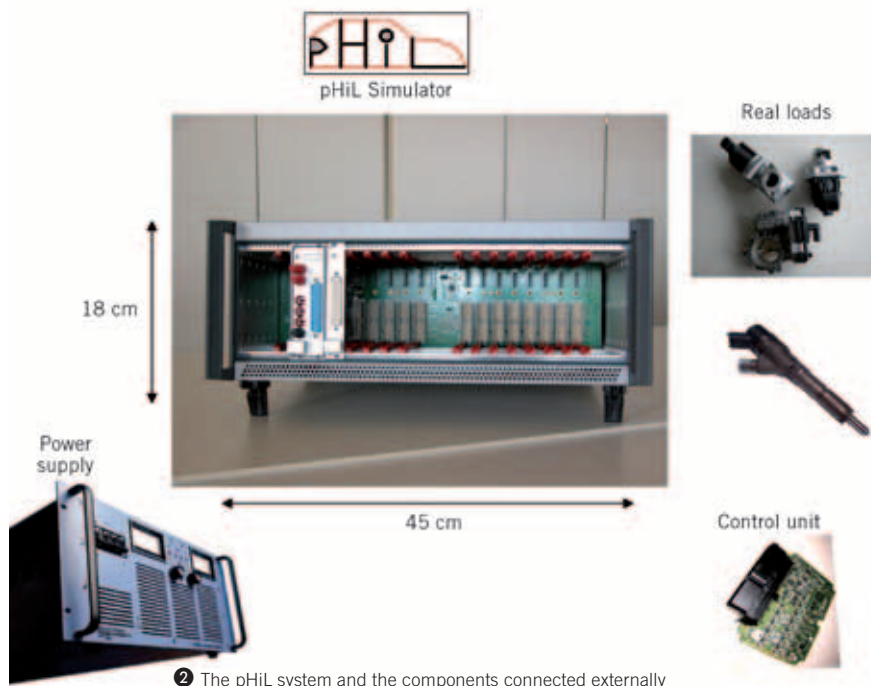
The optimisation of control systems requires suitable development and testing procedures, such as HiL, ^①, and SiL techniques that are nowadays an integral part of the design process with the aim of reducing the number of road tests [1 to 5]. Mathematical models play an important role in this field: as a typical example, HiL/SiL system allows electronic control units (ECU) to be tested by coupling them with a simulator of the controlled system. The simulation is extended by the addition of a comprehensive simulation model of the engine, powertrain and vehicle, together with a flexible I/O device. The main advantages of HiL/SiL systems are:

- : They allow control strategies to be verified at an early stage in the development phase.
- : They reduce costs and development time for prototypes.
- : They can define test cases and procedures with high repeatability.

Furthermore, HiL/SiL systems must be particularly versatile to allow different engine/powertrain configurations, thus reducing costs and development time. The adaptation of mathematical models and the related sub-systems (i.e., engine, transmission, vehicle, etc.) enable a “virtual powertrain” to be developed that is able to simulate system behaviour with good approximation



^① Schematic representation of a Hardware-in-the-Loop system (from [3])



② The pHIL system and the components connected externally

and simulation times lower than “real time”. Simplifications have to be introduced for physical/chemical processes to avoid a detailed description [1 to 5], thus leading to a combination of physical and chemical principles (white box models) and empirical relationships (black box models). This approach does not allow high-frequency phenomena to be followed (i.e., pressure wave propagation), and only averaged values of thermodynamic variables are considered (“Mean Value Models”, MVM, [1]). Considerable effort has been dedicated to developing mathematical tools to model each component and the whole powertrain, thus providing virtual prototyping of the powertrain from the very first step of the design process [1 to 3].

Models proposed in the literature for real-time engine simulation are mainly based on Quasi-Steady Flow (QSF) and Filling-and-Emptying methods (F&E) [1 to 3]. They are usually zero-dimensional, lumped-parameter, cycle-averaged models [1,3,4] that can describe low-frequency transient processes [5], but cannot describe high-frequency phenomena. Similar tools are nowadays commercially available, such as en-Dyna Themis [6], Automotive Simulation Models-AMS [7], AMESim Engine library [8], IFP HiL systems [9], real-time models based on GT-Power simulation [10], etc.

DEVELOPMENT OF A HiL SYSTEM

The hardware and software components in the described HiL (pHiL, powertrain Hardware-in-the-Loop) were developed at Fiat Research Centre/Fiat Powertrain. A significant innovation of the simulator is that a PC platform is used for the execution of both the user interface and the simulation model (tasks that are usually allocated into two separate units).

HARDWARE ARCHITECTURE

The simulator is based on a PC platform integrated into an industrial rack. It can include up to 16 modules connected to the PC platform through a cPCI connection.

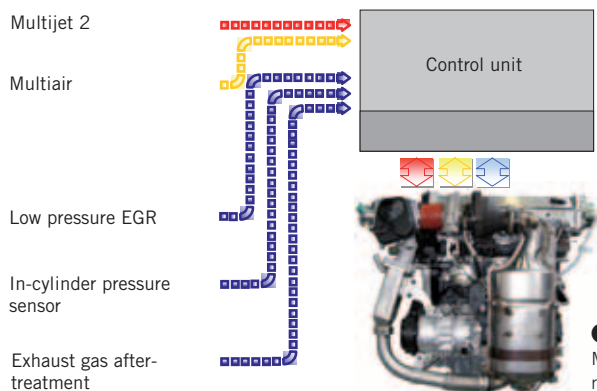
This configuration allows the emulation of complex systems with one or more ECUs. Control units are connected to the simulator through a wiring harness, and the same link is used for electrical loads. Overall dimensions are limited (45 cmx18 cmx43 cm) and therefore it can be easily used on a lab bench or desk, ②. The same PC platform is used for running both the user interface and the model of the controlled plant. Modules fitted in the rack have the same architecture, while the interface module to the control unit has been developed following a different scheme. For the presented simulator, three modules have been developed. The first one is dedicated to the power supply of the tested control unit, and is responsible for the communication channels and emulation of the signals from the crankshaft sensors. The second module is a typical general purpose I/O unit, fitted with programmable analogue inputs, channels for the emulation of active or resistive sensors, digital inputs with programmable embedded electrical loads and programmable digital and PWM outputs. The third module is used for connections to the usual automotive electrical loads (e.g., fuel injectors) and the acquisition of voltages and currents.

SOFTWARE ARCHITECTURE

The software architecture of the pHiL system is divided into three layers:

- : the Presentation Layer
- : the PCI driver and Hardware Abstraction Layer
- : the Low Level Firmware.

The Presentation Layer runs the main user interface. Each I/O port of the pHiL system can be configured and described in detail by means of physical signal char-



③ The Diesel Engine with Multi Air and Control System research project [14]

acteristics, e.g. signal type, physical range, resolution, etc. A user-friendly graphical interface allows operating parameters and I/O specifications to be set. The Hardware Abstraction Layer (HAL) guarantees the low level access to the PCI bus, and provides an easy-to-use interface to the pHIL hardware boards and easy access to each feature and each physical channel of the boards. Finally, the Low Level Firmware layer, running on each pHIL board, drives I/O signals on the boards, receiving commands from the PC interface and providing acquired data sets in return. The software interface between the Low Level Firmware and the Hardware Abstraction Layer is managed through a dual port RAM fitted in each board, where a defined data set has been used for the information exchange. A specific synchronization mechanism has been developed to avoid conflicts when accessing the dual port RAM.

Real-time operation is guaranteed by means of the Real Time Operating System running on the pHIL boards, since hardware connections allow the board to generate a periodic interrupt in order to synchronize the real-time operation of the processes running on the PC.

ACQUISITION OF CONTROL SIGNALS OF FUEL INJECTORS AND SOLENOID VALVES

In the latest generation of diesel engines, multiple injections can be actuated in a cycle. Since the engine ECU drives injectors with dedicated outputs, a specific channel of the simulator is used for each injector to send the related information to the simulation model as a 12x4 matrix, where each row contains data referring to an actuation (which is defined in terms of start, end and duration of injection). This architecture allows the acquisition of up to 12 actuations updating data at every execution step of the simulation procedure. This structure will be used in future development with crank-angle based engine models.

SIMULATION OF POWERTRAIN MODELS

For the simulation of the controlled powertrain within the pHIL, a specific Mean Value Model (MVM) has been developed using the simulation library created at the University of Parma for the real-time

simulation of automotive engines and powertrains [4, 5]. QSF and F&E approaches were used for the simulation of system components, and the library has been organised in a hierarchical structure in order to improve its portability and flexibility. Components are classified as volume components (or capacitances) and non-volume components (or resistances), the former allowing mass and energy accumulation, which is not possible in the latter. Volumes are simulated following the well-known F&E method [1] based on mass and energy conservation equations Eq. (1) and Eq. (2):

| | |
|-------|--|
| EQ. 1 | $\frac{dm}{dt} = \sum M_{in} - \sum M_{out}$ |
|-------|--|

| | |
|-------|---|
| EQ. 2 | $\frac{dT_{man}}{dt} = \frac{\sum h_{in} \cdot M_{in} - \sum h_{out} \cdot M_{out} - u \cdot \frac{dm}{dt} + \varphi}{m \cdot c_v}$ |
|-------|---|

where φ is the heat flux through walls. Non-volume components are modelled through QSF techniques, i.e., through algebraic equations. Valves and restrictions are described with Eq. (3) and Eq. (4):

| | |
|-------|---|
| EQ. 3 | $M = f_1(p_{in}, p_{out}, T_{in}, \xi)$ |
|-------|---|

| | |
|-------|---|
| EQ. 4 | $T_{out} = f_2(p_{in}, p_{out}, T_{in}, \xi)$ |
|-------|---|

which give the mass flow rate M and exit temperature T_{out} taking account of causality [1]. A similar approach was used for the compressor and turbine, with reference to reduced parameters [11]. For a fixed geometry compressor, the equations Eq. (5) and Eq. (6) were used:

| | |
|-------|----------------------------------|
| EQ. 5 | $M_{r,c} = f_1(\beta, n_{r,tc})$ |
|-------|----------------------------------|

| | |
|-------|--------------------------------|
| EQ. 6 | $n_c = f_2(M_{r,c}, n_{r,tc})$ |
|-------|--------------------------------|

where $\beta = p_{out}/p_{in}$, while the power P can be expressed in terms of compressor effi-

ciency η_c . For a variable geometry turbine (VGT), they can be rearranged as follows, Eq. (7) and Eq. (8):

| | |
|-------|---|
| EQ. 7 | $M_{nd,t} = f_1(\varepsilon, n_{nd,tc}, \xi_{VGT})$ |
|-------|---|

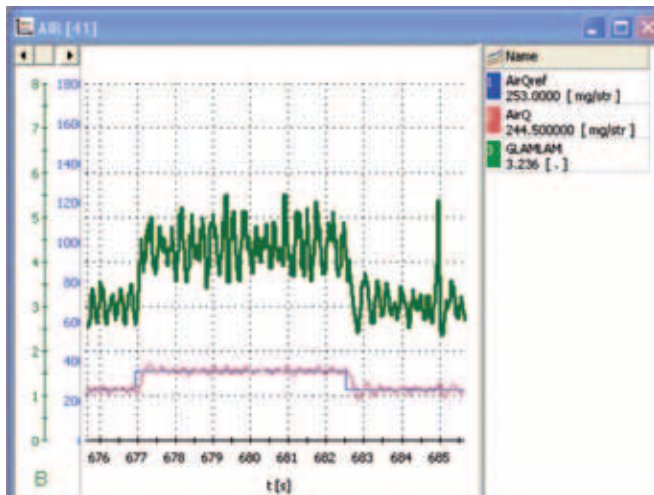
| | |
|-------|-----------------------|
| EQ. 8 | $\eta_t = f_2(u/c_s)$ |
|-------|-----------------------|

$\varepsilon_t = p_{in}/p_{out}$ and the expansion efficiency η_t are used to evaluate the turbine power. The turbocharger dynamics is modelled through the classic equation from Newton's second law. A QSF technique was used for heat exchangers (e.g., intercooler and EGR cooler), evaluating the heat flux through the efficiency ε estimated from a black-box model based on empirical correlations [12]. Combustion and in-cylinder processes are described through a simplified black-box approach: temperature rise across the cylinders ΔT_{comb} and bmep are evaluated as functions of engine speed, and fuel mass flow rate through interpolation of experimental data. The overall mass flow rate through the cylinders has been determined by means of a black-box QSF model based on the evaluation of volumetric efficiency λ_v [4, 5] corrected as suggested in [13] to take account of changes in intake temperature due to EGR.

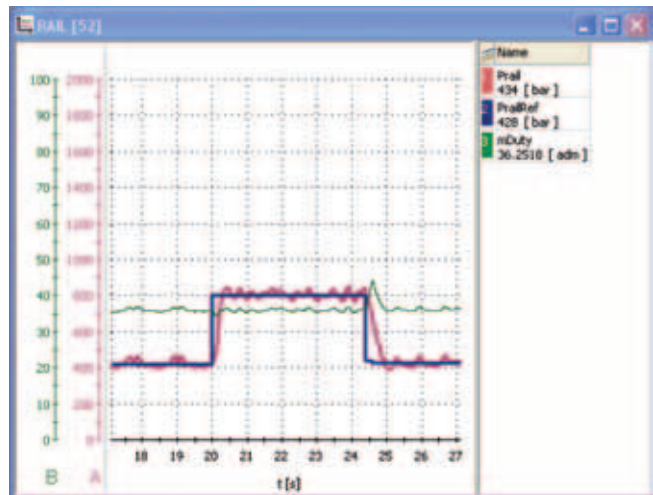
The fuel system model has been developed by taking account of the fuel rail dynamics, described by the following Eq. (9):

| | |
|-------|--|
| EQ. 9 | $p_{rail}(t) = p_{rail}(t_0) + \frac{K_{bulk}}{V_{rail}} \cdot \int_{t_0}^t (Q_{HP}(t) - Q_{inj}(t) - Q_{bf}(t) - Q_{leak}(t)) dt$ |
|-------|--|

where p_{rail} is the fuel pressure in the rail, K_{bulk} is the rail bulk modulus in [bar], V_{rail} is the rail volume in [mm³], Q_{HP} is the high pressure pump delivery in [mm³/s], Q_{inj} is the fuel flow rate through the injectors in [mm³/s], Q_{bf} is the backflow from the injectors in [mm³/s], and Q_{leak} is the flow rate in [mm³/s] due to leakages in the system. The fuel mass flow rates Q are evaluated through black-box sub-models (defined starting from experimental data).



④ Object variation (AirQref) with EGR-LP control strategy: (a) effects of step changes in air mass flow set-point (AirQ) and (b) oxygen sensor output (Glamlam)



⑤ Object variation (PrailRef) through step changes in rail fuel pressure set-point (Prail)

The vehicle model has been defined to simulate the longitudinal dynamics of a car. The classic differential equation from Newton's second law is used to simulate vehicle longitudinal dynamics: masses and inertias are reduced to the crankshaft.

A dedicated pre-processing tool has been developed in order to allow for the identification of each component sub-model from required data (measured on test bench).

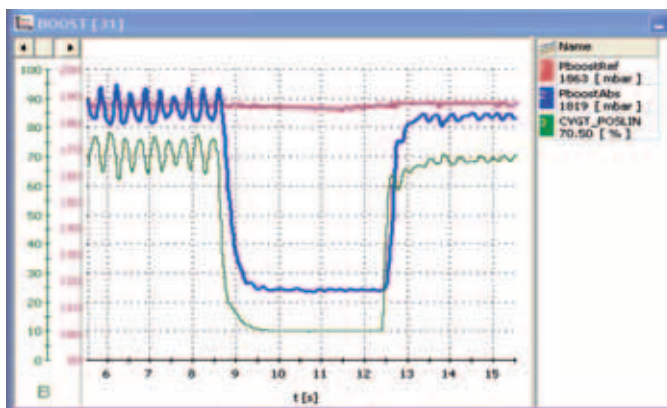
APPLICATION TO AN AUTOMOTIVE DIESEL ENGINE

The pHIL simulator is currently used at Fiat Research Centre/Fiat Powertrain within an advanced project for the development and testing of the software functions for

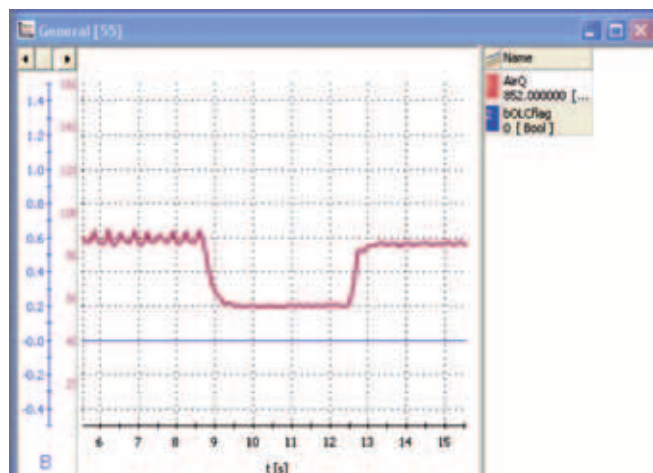
the control system of a turbocharged diesel engine with a low-pressure EGR loop and Multi Air technology, ④ [14]. The simulation model was identified starting from available data: characteristic of the turbocharger (Eq. (5) and Eq. (8)) were defined from the manufacturer's data, and for valves and restrictions (i.e., EGR), coefficients of Eq. (3) and Eq. (4) were determined from steady-state experimental data. For the evaluation of combustion process, interpolation functions were defined through a least square method, starting from experimental data. Similar data fitting techniques were used to define loss coefficients, heat exchanger efficiencies and an interpolating correlation for volumetric efficiency. The pHIL system proved its capabilities and its versatility in

the simulation of any considered transient operating conditions in "real-time". A few examples are reported in the following with reference to transients induced by changing the value of defined set points or of input parameters to the system ECU.

④ shows the effects of step changes in the air mass flow set point in terms of simulated engine air mass flow rate and linear oxygen sensor output. The system allows the behaviour of the fuel system to be simulated, ⑤. The closed-loop control properly acts on the high-pressure pump metering valve (mDuty green curve) in order to follow the desired value. The performance of the model can be further explored by acting on the turbocharger. In the example shown in ⑥,



⑥ Control variation VGT (CVGT_POSLIN): (a) boost pressure (PboostAbs) and (b) air mass flow (AirQ).



steps in the VGT actuator position (green line) are considered, leading to changes in boost pressure and in the air mass flow rate.

SUMMARY AND CONCLUSION

The hardware and software components of the HiL system presented in this paper were been developed by Fiat Research Centre/Fiat Powertrain by using a single PC platform that generates both the user interface and the simulation model. The modular configuration of the library, the flexible interfaces and identification tools for each sub-model, which were developed at the University of Parma, proved to be very useful in HiL applications, as is shown by results reported in the paper. Models for after-treatment devices in the development phase and in-cylinder processes for crank-angle simulations are now being developed.

REFERENCES

- [1] Guzzella, L.; Onder, C.H.: "Introduction to Modeling and Control of Internal Combustion Engine Systems". In: Springer-Verlag, ISBN 3-540-22274-X, 2004
- [2] Guzzella, L.; Amstutz, A.: "Control of Diesel engines". In: IEEE Trans.on Control Systems Tech., vol.18(5), 1998
- [3] Wältermann, P.: "Hardware-in-the-Loop: The Technology for Testing Electronic Controls in Automotive Engineering". In: 6th Paderborn Workshop "Designing Mechatronic Systems", Paderborn, 2009
- [4] Gambarotta, A.: "A control-oriented library for the simulation of automotive Diesel engines". 3rd International Conference on Control and Diagnostics in Automotive Applications, paper 01A3039, Sestri Levante, 7/2001
- [5] Gambarotta, A.; Lucchetti, G.; Vaja, I.: "Real-time Modelling of Transient Operation of Turbocharged Diesel Engines". Proc. IMechE Vol. 225 Part D: J. Automobile Engineering, 2011
- [6] <http://www.tesis.de/dynaware>
- [7] <http://www.dspace.de>
- [8] <http://www.amesim.com>
- [9] <http://engines-fuels.ifp.fr>
- [10] <http://www.gtisoft.com>
- [11] Watson, N.; Janota, M.S.: "Turbocharging the Internal Combustion Engine". McMillan Press, London, 1982
- [12] Kays, W.M.; London, A.L.: "Compact Heat Exchangers", McGraw-Hill, 1984
- [13] Taylor, C.F.: "The Internal Combustion Engine", 2nd edition, MIT Press, 1980
- [14] Tonetti, M.; Bernard, L.; Canino, G.; Ruggiero, A.: "MultiAir electro-hydraulic valve control technology potential on diesel engines for Euro 6 passenger car applications". international Congress on "Diesel Engines: Facing the competitiveness challenge", INSA de Rouen, France, 2010

THANKS

The authors are particularly grateful to the R&T Diesel Control SW Group and Automotive Electronics Design and Development Department at Fiat Powertrain for their significant support in the development of the HiL simulator.

PEER REVIEW ATZ | MTZ

PEER REVIEW PROCESS FOR RESEARCH ARTICLES
IN ATZ AND MTZ

STEERING COMMITTEE

| | | |
|-------------------------------------|-------------------------------------|---|
| Prof. Dr.-Ing. Lutz Eckstein | RWTH Aachen University | Institut für Kraftfahrzeuge Aachen |
| Prof. Dipl.-Des. Wolfgang Kraus | HAW Hamburg | Department Fahrzeugtechnik und Flugzeugbau |
| Prof. Dr.-Ing. Ferit Kûçûkay | Technische Universität Braunschweig | Institut für Fahrzeugtechnik |
| Prof. Dr.-Ing. Stefan Pischinger | RWTH Aachen University | Lehrstuhl für Verbrennungskraftmaschinen |
| Prof. Dr.-Ing. Hans-Christian Reuss | Universität Stuttgart | Institut für Verbrennungsmotoren und Kraftfahrwesen |
| Prof. Dr.-Ing. Ulrich Spicher | Universität Karlsruhe | Institut für Kolbenmaschinen |
| Prof. Dr.-Ing. Hans Zellbeck | Technische Universität Dresden | Lehrstuhl für Verbrennungsmotoren |

ADVISORY BOARD

| | |
|--|--|
| Prof. Dr.-Ing. Klaus Augsburg | Univ.-Ass. Dr. techn. Thomas Lauer |
| Prof. Dr.-Ing. Bernard Bäker | Prof. Dr. rer. nat. Uli Lemmer |
| Prof. Dr.-Ing. Michael Bargende | Dr. Malte Lewerenz |
| Prof. Dipl.-Ing. Dr. techn. Christian Beidl | Prof. Dr.-Ing. Markus Lienkamp |
| Dr.-Ing. Christoph Bollig | Prof. Dr. rer. nat. habil. Ulrich Maas |
| Prof. Dr. sc. techn. Konstantinos Boulouchos | Prof. Dr.-Ing. Markus Maurer |
| Prof. Dr. Dr. h.c. Manfred Broy | Prof. Dr.-Ing. Martin Meywerk |
| Prof. Dr.-Ing. Ralph Bruder | Prof. Dr.-Ing. Klaus D. Müller-Glaser |
| Dr. Gerhard Bruner | Dr. techn. Reinhard Mundl |
| Prof. Dr. rer. nat. Heiner Bubb | Prof. Dr. rer. nat. Cornelius Neumann |
| Prof. Dr. rer. nat. habil. Olaf Deutschmann | Prof. Dr.-Ing. Peter Pelz |
| Dr. techn. Arno Eichberger | Prof. Dr. techn. Ernst Pucher |
| Prof. Dr. techn. Helmut Eichseder | Dr. Jochen Rauh |
| Prof. Dr. Wilfried Eichseder | Prof. Dr.-Ing. Konrad Reif |
| Dr.-Ing. Gerald Eifler | Prof. Dr.-Ing. Stephan Rinderknecht |
| Prof. Dr.-Ing. Wolfgang Eifler | Dr.-Ing. Swen Schaub |
| Prof. Dr. rer. nat. Frank Gauterin | Prof. Dr. sc. nat. Christoph Schierz |
| Prof. Dr. techn. Bernhard Geringer | Prof. Dr. rer.-nat. Christof Schulz |
| Prof. Dr.-Ing. Uwe Grebe | Prof. Dr. rer. nat. Andy Schürr |
| Dr. mont. Christoph Guster | Prof. Dr.-Ing. Ulrich Seiffert |
| Prof. Dr.-Ing. Holger Hanselka | Prof. Dr.-Ing. Hermann J. Stadtfeld |
| Prof. Dr.-Ing. Horst Harndorf | Prof. Dr. techn. Hermann Steffan |
| Prof. Dr. techn. Wolfgang Hirschberg | Prof. Dr.-Ing. Wolfgang Steiger |
| Univ.-Doz. Dr. techn. Peter Hofmann | Prof. Dr.-Ing. Peter Steinberg |
| Prof. Dr.-Ing. Bernd-Robert Höhn | Prof. Dr.-Ing. Christoph Stiller |
| Prof. Dr. rer. nat. Peter Holstein | Dr.-Ing. Peter Stommel |
| Dr. techn. Heidelinde Holzer | Dr.-Ing. Ralph Sundermeier |
| Prof. Dr.-Ing. habil. Werner Hufenbach | Prof. Dr.-Ing. Wolfgang Thiemann |
| Prof. Dr.-Ing. Armin Huß | Prof. Dr.-Ing. Helmut Tschöke |
| Prof. Dr.-Ing. Roland Kasper | Dr.-Ing. Pim van der Jagt |
| Prof. Dr.-Ing. Tran Quoc Khanh | Prof. Dr.-Ing. Georg Wachtmeister |
| Dr. Philip Köhn | Prof. Dr.-Ing. Jochen Wiedemann |
| Prof. Dr.-Ing. Ulrich Konigorski | Prof. Dr. techn. Andreas Wimmer |
| Dr. Oliver Kröcher | Prof. Dr. rer. nat. Hermann Winner |
| Prof. Dr.-Ing. Peter Krug | Prof. Dr. med. habil. Hartmut Witte |
| Dr. Christian Krüger | |

Scientific articles of universities in ATZ Automobiltechnische Zeitschrift and MTZ Motortechnische Zeitschrift are subject to a proofing method, the so-called peer review process. Articles accepted by the editors are reviewed by experts from research and industry before publication. For the reader, the peer review process further enhances the quality of the magazines' content on a national and international level. For authors in the institutes, it provides a scientifically recognised publication platform.

In the ATZ | MTZ Peer Review Process, once the editors has received an article, it is reviewed by two experts from the Advisory Board. If these experts do not reach a unanimous agreement, a member of the Steering Committee acts as an arbitrator. Following the experts' recommended corrections and subsequent editing by the author, the article is accepted.

In 2008, the peer review process utilized by ATZ and MTZ was presented by the WKM (Wissenschaftliche Gesellschaft für Kraftfahrzeug- und Motorentechnik e. V. / German Professional Association for Automotive and Motor Engineering) to the DFG (Deutsche Forschungsgemeinschaft / German Research Foundation) for official recognition.



Founded 1939 by Prof. Dr.-Ing. E. h. Heinrich Buschmann and
Dr.-Ing. E. h. Prosper L'Orange

02 | 2012 – February 2012 – Volume 73

Springer Vieweg | Springer Fachmedien Wiesbaden GmbH

P. O. Box 15 46 · 65173 Wiesbaden · Germany | Abraham-Lincoln-Straße 46 · 65189 Wiesbaden · Germany
Amtsgericht Wiesbaden, HRB 9754, USt-IdNr. DE811148419

Managing Directors Dr. Ralf Birkelbach (Chairman), Armin Gross, Albrecht Schirmacher | **Director Advertising** Armin Gross

Director Marketing + Individual Sales Rolf-Günther Hobbeling | **Director Production** Christian Staral

SCIENTIFIC ADVISORY BOARD

Prof. Dr.-Ing. Michael Bargende
Universität Stuttgart

Prof. Dr. techn. Christian Beidl
TU Darmstadt

Dr.-Ing. Ulrich Dohle
Tognum AG

Dr. Klaus Egger

Dipl.-Ing. Dietmar Goericke
Forschungsvereinigung
Verbrennungskraftmaschinen e.V.

Prof. Dr.-Ing. Uwe-Dieter Grebe
GM Powertrain

Prof. Dr. Jens Hadler
Volkswagen AG

Dipl.-Ing. Thorsten Herdan
VDMA-Fachverband Motoren
und Systeme

Prof. Dr.-Ing. Heinz K. Junker
Mahle GmbH

Dipl.-Ing. Peter Langen
BMW AG

Prof. Dr. Hans Peter Lenz
ÖVK

Prof. Dr. h. c. Helmut List
AVL List GmbH

Dr.-Ing. Ralf Marquard
Deutz AG

Dipl.-Ing. Wolfgang Maus
Emitec Gesellschaft für
Emissionstechnologie mbH

Prof. Dr.-Ing. Stefan Pischinger
FEV GmbH

Prof. Dr. Hans-Peter Schmalzl
APC – Advanced Propulsion
Concepts Mannheim GmbH

Prof. Dr.-Ing. Ulrich Seiffert
TU Braunschweig

Prof. Dr.-Ing. Ulrich Spicher
WKM

EDITORS-IN-CHARGE

Dr. Johannes Liebl, Wolfgang Siebenpfeiffer

EDITORIAL STAFF

EDITOR-IN-CHIEF

Johannes Winterhagen (win)
phone +49 611 7878-342 · fax +49 611 7878-462
johannes.winterhagen@springer.com

VICE EDITOR-IN-CHIEF

Ruben Danisch (rd)
phone +49 611 7878-393 · fax +49 611 7878-462
ruben.danisch@springer.com

CHIEF-ON-DUTY

Kirsten Beckmann M. A. (kb)
phone +49 611 7878-343 · fax +49 611 7878-462
kirsten.beckmann@springer.com

SECTIONS

Electrics, Electronics
Markus Schöttle (scho)
phone +49 611 7878-257 · fax +49 611 7878-462
markus.schoettle@springer.com

Engine
Ruben Danisch (rd)
phone +49 611 7878-393 · fax +49 611 7878-462
ruben.danisch@springer.com

Production, Materials
Stefan Schlott (hlo)
phone +49 8726 9675972
Redaktion_Schlott@gmx.net

Service, Event Calendar
Martina Schraad (mas)
phone +49 611 7878-276 · fax +49 611 7878-462
martina.schraad@springer.com

Research, Transmission
Dipl.-Ing. Michael Reichenbach (rei)
phone +49 611 7878-341 · fax +49 611 7878-462
michael.reichenbach@springer.com

Dipl.-Ing. (FH) Moritz-York von Hohenenthal (mvh)
phone +49 611 7878-278 · fax +49 611 7878-462
moritz.von.hohenenthal@springer.com

PERMANENT CONTRIBUTORS

Richard Backhaus (rb), Andreas Burkert (ab),
Prof. Dr.-Ing. Stefan Breuer (sb), Dipl.-Ing. (FH)
Andreas Fuchs (fu), Jürgen Grandel (gl), Ulrich
Knorra (kno), Prof. Dr.-Ing. Fred Schäfer (fs),
Roland Schedel (rs)

ENGLISH LANGUAGE CONSULTANT

Paul Willin (pw)

ONLINE | ELECTRONIC MEDIA

Managing Editor
Gernot Goppelt (gg)
phone +49 611 7878-121 · fax +49 611 7878-462
gernot.goppelt@springer.com

Editorial Staff
Caterina Schröder (cs)
phone +49 611 7878-190 · fax +49 611 7878-462
caterina.schroeder@springer.com

Katrin Pudenz M. A. (pu)
phone +49 6172 301-288 · fax +49 6172 301-299
redaktion@kpz-publishing.com

SPECIAL PROJECTS

Managing Editor
Markus Bereszewski (mb)
phone +49 611 7878-122 · fax +49 611 7878-462
markus.bereszewski@springer.com

Editorial Staff

Christiane Brüninghaus (chb)
phone +49 611 7878-136 · fax +49 611 7878-462
christiane.brueninghaus@springer.com

ASSISTANCE

Christiane Imhof
phone +49 611 7878-154 · fax +49 611 7878-462
christiane.imhof@springer.com

Marlena Strugala
phone +49 611 7878-180 · fax +49 611 7878-462
marlena.strugala@springer.com

ADDRESS

Abraham-Lincoln-Straße 46 · 65189 Wiesbaden
P. O. Box 1546 · 65173 Wiesbaden, Germany
redaktion@ATZonline.de

MARKETING | OFFPRINTS

PRODUCT MANAGEMENT AUTOMOTIVE MEDIA

Sabrina Brokopp
phone +49 611 7878-192 · fax +49 611 7878-407
sabrina.brokopp@springer.com

OFFPRINTS

Martin Leopold
phone +49 2642 9075-96 · fax +49 2642 9075-97
leopold@medien-kontor.de

ADVERTISING

HEAD OF SALES MANAGEMENT

Britta Dolch
phone +49 611 7878-323 · fax +49 611 7878-140
britta.dolch@best-ad-media.de

KEY ACCOUNT MANAGEMENT

Rouven Bastian
phone +49 611 7878-399 · fax +49 611 7878-140
rouven.bastian@best-ad-media.de

SALES MANAGEMENT

Volker Hesedenz
phone +49 611 7878-269 · fax +49 611 7878-140
volker.hesedenz@best-ad-media.de

MEDIA SALES

Frank Nagel
phone +49 611 7878-395 · fax +49 611 7878-140
frank.nagel@best-ad-media.de

DISPLAY AD MANAGER

Petra Steffen-Munsberg
phone +49 611 7878-164 · fax +49 611 7878-443
petra.steffen-munsberg@best-ad-media.de

AD PRICES

Advertising ratecard from October 2011

PRODUCTION | LAYOUT

Heiko Köllner
phone +49 611 7878-177 · fax +49 611 7878-464
heiko.koellner@springer.com

YOUR HOTLINE TO MTZ

Editorial Staff

☎ +49 611 7878-393

Customer Service

☎ +49 6221 345-4303

Advertising

☎ +49 611 7878-395

SUBSCRIPTIONS

Springer Customer Service Center GmbH
Haberstraße 7 · 69126 Heidelberg · Germany
phone +49 6221 345-4303 · fax +49 6221 345-4229
Monday to Friday, 8 a.m. to 6 p.m.
springervieweg-service@springer.com

SUBSCRIPTION CONDITIONS

The eMagazine appears 11 times a year at an annual subscription rate 199 € for private persons and 299 € for companies. Special rate for students on proof of status in the form of current registration certificate 98 €. Special rate for VDI/ÖVK members on proof of status in the form of current member certificate 172 €. Special rate for studying VDI members on proof of status in the form of current registration and member certificate 71 €. Annual subscription rate for combination MTZworldwide (eMagazine) and MTZ (print) 398 €. All prices include VAT at 7%. Every subscription comes with access to the ATZonline archive. However, access is only available for the individual subscription holder. To obtain access for your entire company/library/organisation, please contact Rüdiger Schwenk (ruediger.schwenk@springer.com or phone +49 611 7878-357). The subscription can be cancelled in written form at any time with effect from the next available issue.

HINTS FOR AUTHORS

All manuscripts should be sent directly to the editors. By submitting photographs and drawings the sender releases the publishers from claims by third parties. Only works not yet published in Germany or abroad can generally be accepted for publication. The manuscripts must not be offered for publication to other journals simultaneously. In accepting the manuscript the publisher acquires the right to produce royalty-free offprints. The journal and all articles and figures are protected by copyright. Any utilisation beyond the strict limits of the copyright law without permission of the publisher is illegal. This applies particularly to duplications, translations, microfilming and storage and processing in electronic systems.

© Springer Vieweg |
Springer Fachmedien Wiesbaden GmbH,
Wiesbaden 2012

Springer Vieweg is a brand of Springer DE. Springer DE is part of Springer Science+Business Media.

AUTHORS

**DIPL.-ING.****HANS-PHILIPP WALTHER**

is Scientific Employee at the Institute for Internal Combustion Engines at the Technische Universität in Munich (Germany).

**MSC. MECH. ENG.****STÉPHANIE SCHLATTER**

is Scientific Employee at the Aerothermochemistry and Combustion Systems Laboratory at the Swiss Federal Institute of Technology Zurich (Switzerland).

**PROF. DR.-ING.****GEORG WACHTMEISTER**

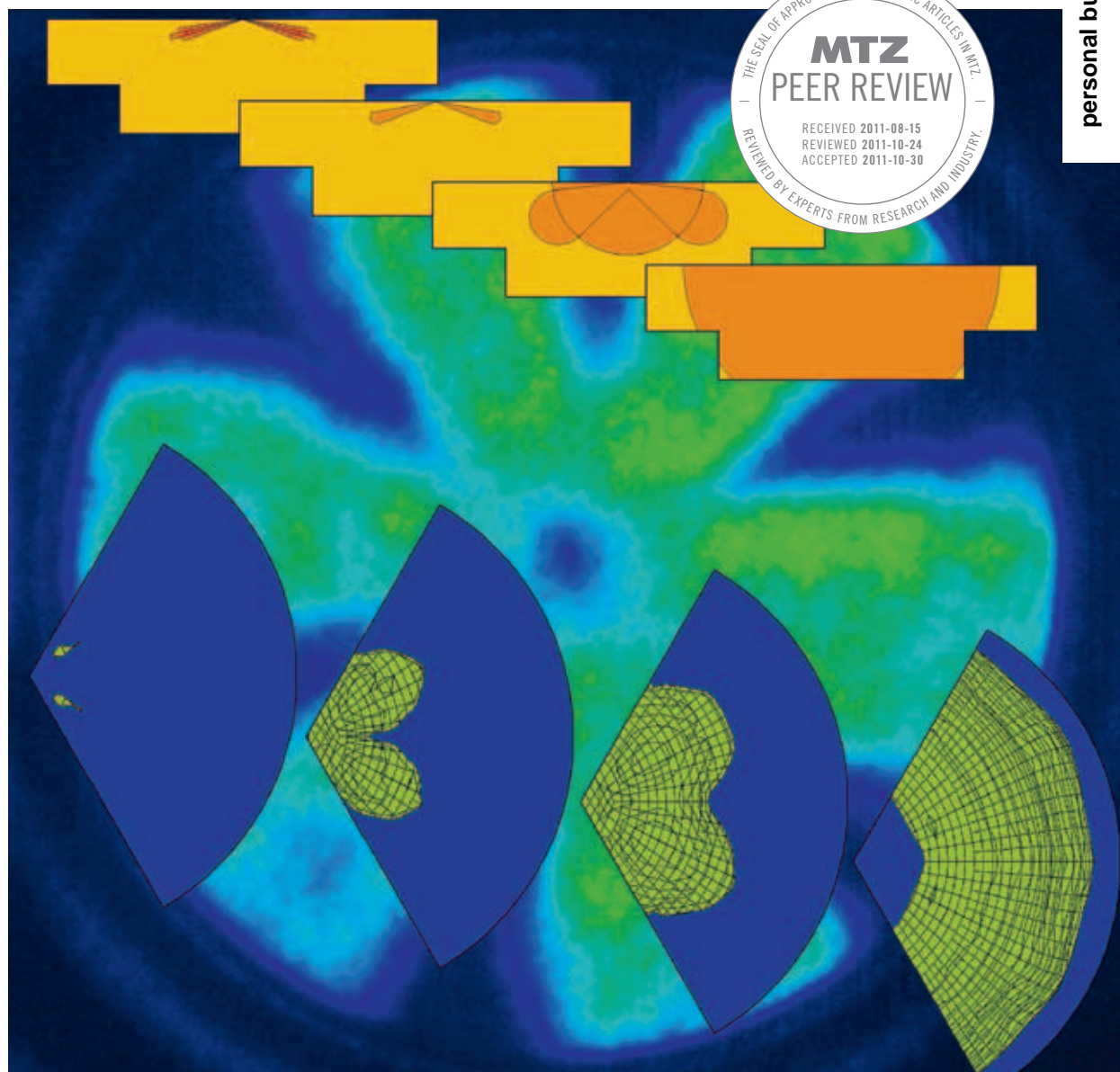
is Director of the Institute for Internal Combustion Engines at Technische Universität in Munich (Germany).

**PROF. DR. SC. TECHN.****KONSTANTINOS BOULOCHOS**

is Director of the Aerothermochemistry and Combustion Systems Laboratory at the Swiss Federal Institute of Technology Zurich (Switzerland).

COMBUSTION MODELS FOR LEAN-BURN GAS ENGINES WITH PILOT INJECTION

Efficient development of Combustion Engines requires detailed models which reliably predict engine behavior over a broad range of operating conditions. Within the framework of an FVV research project two combustion models were developed at two research centers: At the Aerothermochemistry and Combustion Systems Laboratory (LAV) of the Swiss Federal Institute of Technology Zurich (ETH) a model for 3D CFD Simulations was developed. At the Institute of Combustion Engines (LVK) of the Technische Universität München (TUM) a phenomenological model for engine cycle simulations was developed. Both models are validated by means of a large number of experiments from an optically accessible single stroke free floating piston engine at LAV and a modified heavy-duty single cylinder engine at LVK.

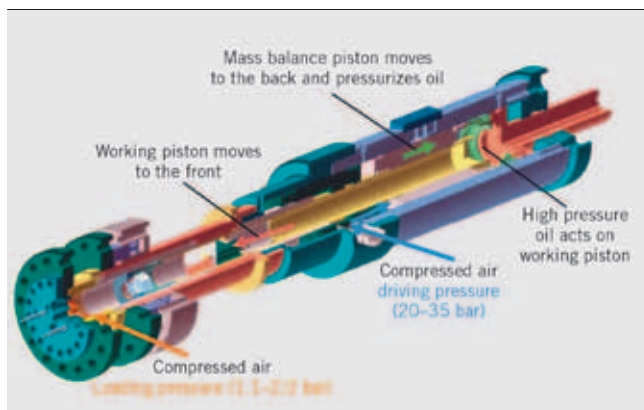


| | |
|---|---|
| 1 | INTRODUCTION |
| 2 | SINGLE STROKE RAPID COMPRESSION MACHINE |
| 3 | COMBUSTION ENGINE EXPERIMENTS |
| 4 | SIMULATION MODELS |
| 5 | SUMMARY |

1 INTRODUCTION

Gas engines with pilot injection are a promising concept regarding future demands for the reduction of CO₂ emissions as well as pollutants like NO_x and PM. Although widely used in marine [2] and stationary large bore engines, premixed combustion of a homogeneous methane/air mixture ignited by a small pilot spray involves complex processes which are not fully understood and still largely optimized by trial and error procedures. For the optimization of corresponding combustion engines a better understanding of the fundamental processes and the availability of appropriate simulation models is essential. Existing models developed specifically for premixed combustion ignited by means of conventional spark plugs cannot be used as there are major differences especially during the ignition and early combustion phases when employing pilot injection. Therefore two combustion models were developed to simulate the combustion process of gas engines with pilot injection.

Experimental data from both an optically accessible test rig and a modified heavy-duty engine have been used for model development and validation and provide valuable insight with respect to processes occurring in dual-fuel combustion.



① Working principle of the ETH Zurich Single Stroke Machine

| | |
|-------------------------------|---|
| BORE | D = 84 mm |
| STROKE | Continuously, 120 mm–250 mm |
| COMPRESSION RATIO ϵ | Continuously, 5–30 |
| PISTON | Top hat piston bowl, depth 4 mm, d = 52 mm (window) |
| CYLINDER HEAD | Flat, with two injectors |
| DIESEL PILOT INJECTION SYSTEM | Bosch Common rail system, 2 nd generation, IAV FI2RE |

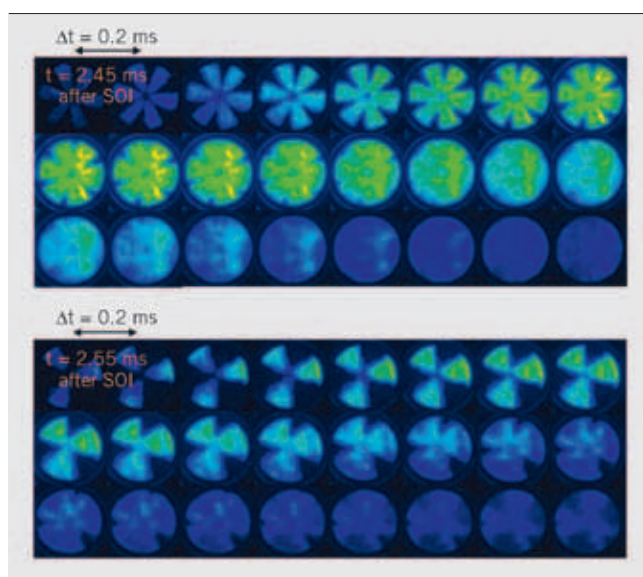
② Relevant parameters for the experiments on the single stroke engine

2 SINGLE STROKE RAPID COMPRESSION MACHINE

The measurements were carried out on a free floating piston single stroke machine (SSM) with a bore of 84 mm and which features a variable stroke and, as a consequence, a variable compression ratio. Combined with an easily interchangeable cylinder head, and a piston equipped with a large quartz window, the SSM constitutes a highly flexible test rig in terms of optical access, operating conditions and modifiability. An overview of the characteristic specifications of the machine can be found in ① and ②. The piston is driven by pressurized air acting indirectly on the working piston therefore the stroke of the machine can be adjusted by choosing the loading to driving pressure ratio. A detailed description of the working principle can be found in [3].

Pictures with an intensified high speed camera with OH-filter were acquired at a frequency of 10 kHz during ignition and combustion. The machine parameters for the experiments were chosen according to the engine experiments at LVK/TU Munich described in detail below. The observation domain of the SSM is appropriate for the investigation of the autoignition process of the diesel pilot and the subsequent early flame development phase of the premixed flame. The ratio of loading to driving pressure and temperatures of cylinder liner, piston and cylinder head in the SSM were chosen to result in the same pressure and temperature conditions of the mixture at TDC as in the test engine at LVK.

The optical recordings of the chemiluminescence for both nozzle configurations show ignition and combustion of the pilot spray and the methane-air charge, as shown in ③ for an air/fuel ratio of $\lambda_{CH_4} = 1.5$. Methane which is entrained into the pilot spray or is close to the spray, is ignited by the heat released from the autoigniting pilot spray. Subsequent premixed flame propagation can be observed originating from these autoignition spots. Even for very lean mixtures (up to $\lambda_{CH_4} = 2.7$, results not shown) the same initial flame shape could be observed, although under such lean conditions no flame propagation in the unburnt mixture can be sustained.



③ OH-Chemiluminescence three-hole injector (top) and six-hole injector (bottom) for $\lambda_{CH_4} = 1.5$

To be able to investigate micro pilot injections, the amount of injected fuel mass had to be further reduced. Therefore, based on the original six-hole nozzle geometry, a three-hole nozzle was manufactured by blocking half of the original nozzle holes (my means of welding). To increase the predictability of the developed combustion models, both nozzle geometries were analyzed with an Injection Rate Analyzer produced by IAV applying different injection parameters. The obtained information about total injected mass and time resolved evolution of the mass flow rate through the injector was used to improve the spray related boundary conditions in the simulation.

3 COMBUSTION ENGINE EXPERIMENTS

At LVK, experiments were carried out using a single cylinder research engine. The measurement data such as cylinder pressure and combustion rate were used for the adjustment of the model parameters and the validation of the phenomenological model. The research engine, a modified engine based on an MTU type 396, ④, has formerly been used for research projects on Otto gas engines with spark plug ignition and scavenged pre-chamber ignition. It was equipped with the same pilot injection system that was used on the single stroke machine at LAV ETH Zurich. During the experimental testing each operating parameter was varied singularly in order to investigate its influence on the combustion. Unlike the experiments on the single stroke rapid compression machine, the influence of different pilot fuels, e.g. rape oil, and several different gases could be investigated in the engine experiments.

4 SIMULATION MODELS

On the basis of the experimental results two combustion models were developed. Both share the concept of splitting the whole combustion process in two separate regimes namely the autoignition and combustion of the pilot spray and the subsequent premixed combustion of the methane-air charge.

4.1 CFD COMBUSTION MODEL

The computational mesh corresponds to a sector of 120° which allows the modeling of the three-hole nozzle as well as the six-hole geometry using the same grid. Mesh motion is performed following a measured piston position trace from the experiments (due to the absence of crank related piston kinematics).

A standard two-equation model with default parameters is employed for turbulence, namely the $k-\epsilon$ RNG model [4]. For spray atomization, Huh's model [5] is used and droplet secondary breakup is treated by the Reitz-Diwakar [6] model. Further details regarding the governing equations and the standard parameters can be found in [7].

Premixed combustion of the methane-air charge and flame propagation was modeled using the Weller model [8, 9] for partially premixed regimes. It is a flame area model in which the wrinkling factor describes the flame surface together with a regress variable. The laminar flame speed is determined following the approach of Gülder [10]. All governing equations can be found in [7].

Auto ignition and combustion of the pilot spray is modeled using a 2D CMC approach (Conditional Moment Closure). Details regarding the governing equations can be found in [11, 12]; while fur-

| | |
|-------------------|---|
| BORE | D=165 mm |
| STROKE | s = 185 mm |
| DISPLACEMENT | $V_H = 3960 \text{ cm}^3$ |
| COMPRESSION RATIO | $\epsilon = 10.65 \dots 12.05$ |
| MAXIMUM PRESSURE | $p_{\max} = 150 \text{ bar}$ |
| SPEED | $n_{\max} = 1800 \text{ rpm}$ |
| SWIRL | Shrouded valve in inlet duct (optional) |
| PISTON SHAPES | Omega, lense and flat |
| GAS SUPPLY | Timed gas injection close to the inlet duct |

④ Technical data of the MTU 396 test engine

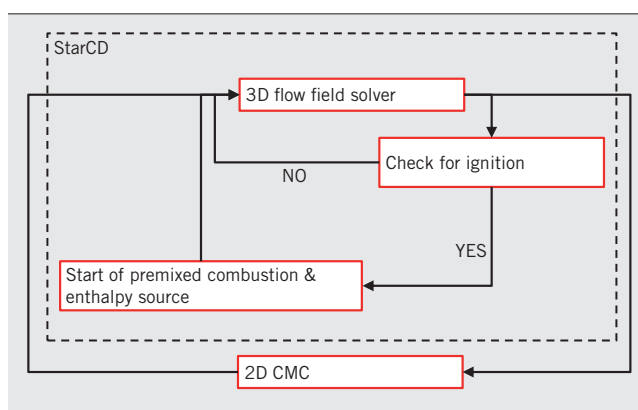
ther information concerning the interfacing with the CFD solver and the numerical procedure is documented in [13, 14]. The applied reaction mechanism for n-heptane consists of 22 species and 18 reaction steps as proposed in [15] including methane as a reactive component, allowing the modeling of the influence of methane on the ignition behavior of the pilot spray.

The hot spots computed by the CMC model serve as ignition sources for the premixed combustion model, a coupling through user coded subroutines was realized. A check for ignition is performed in every time-step and for every cell of the computational domain. If ignition in the CMC model has occurred, premixed combustion is started in these ignition cells together with an enthalpy source modeling the energy released by the ignition processes. ⑤ shows schematically the structure and working principle of the full model, for which further documentation can be found in [16].

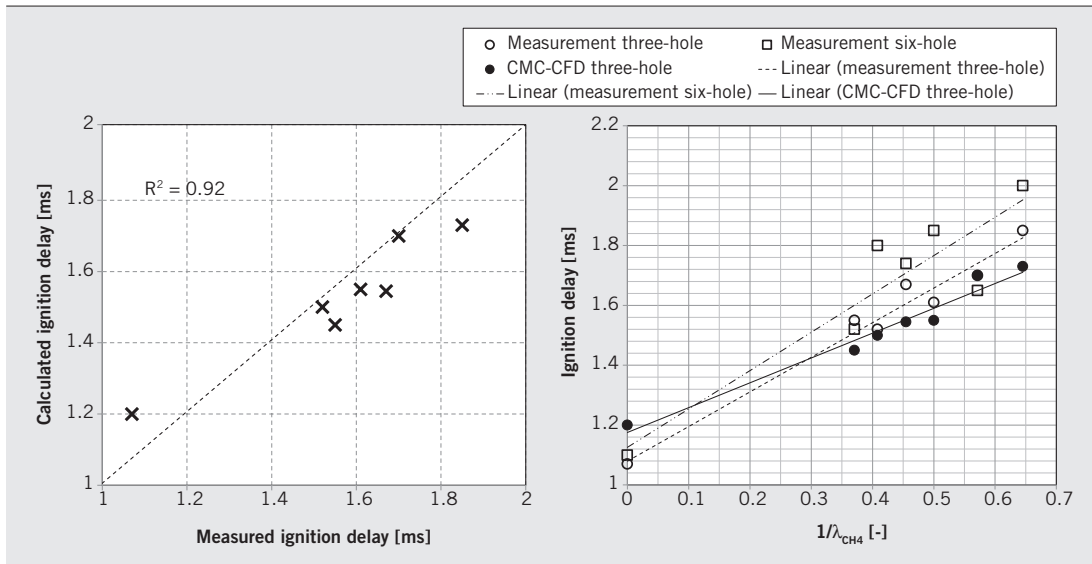
The optical results from the EHT experiments are used for validation of the combustion simulation. By using a detailed reaction mechanism together with the described coupling, calibration of the combustion model is not necessary since it contains no tuning parameter. Comparison of the values for the ignition delay computed and measured in a regression plot, ⑥ (left), shows excellent agreement of the coupled model with the experimental data.

The ignition delay of the pilot spray tends to increase with the amount of premixed methane in the ambient gas mixture, ⑥ (right). This has been observed in several studies before [17-19].

The 2D spatial OH chemiluminescence imaging data (line of sight along the cylinder axis direction) provides time resolved in-



⑤ Coupling of the full CFD combustion model



⑥ Comparison of computed and measured ignition delay in a regression plot (left) and as a function of the amount of premixed methane in the surrounding gas mixture (right)

formation on the ignition location and subsequent combustion, allowing for comparison of the recorded images with the calculated iso-surface of the flame front. The latter is characterized by the change in the regress variable which changes from a value of 1.0 in the unburnt to 0 in the burnt gases at the flame front position. ⑦ shows the evolution of the OH distribution and the iso-surface of the regress variable at a value of 0.3 for an air/fuel ratio of $\lambda_{CH_4}=1.5$. The shape of the initial flame kernel is predicted well

by the simulation and the propagation of the flames towards the injector location in the center is also well captured.

4.2 PHENOMENOLOGICAL MODEL

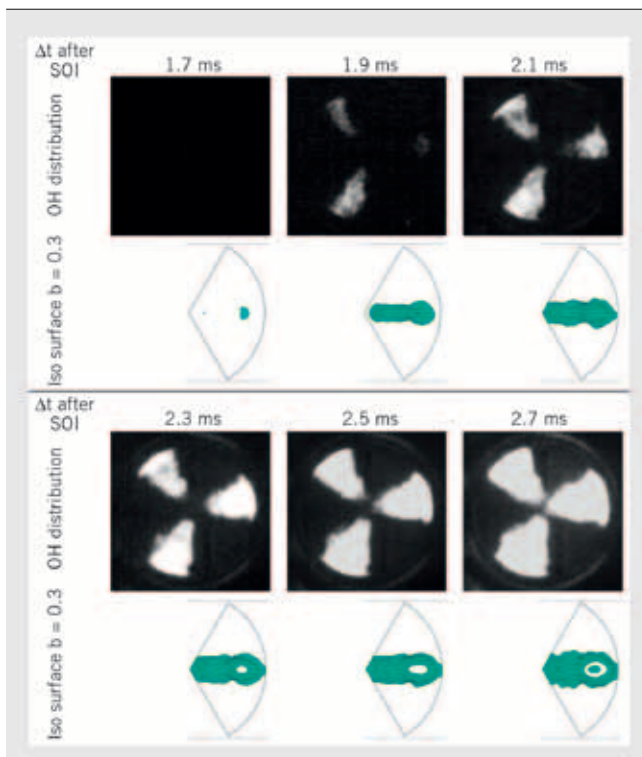
The basis for the phenomenological model were the combustion models for spark plug ignition and scavenged pre-chamber ignition developed at the LVK [20]. These are two zone combustion models that distinguish between burned and unburned gas zone, ⑧. The models additionally contain a flame zone that thermodynamically is a part of the unburned gas zone [20].

The mass within the flame is calculated by integrating the mass flows in and out of the flame zone.

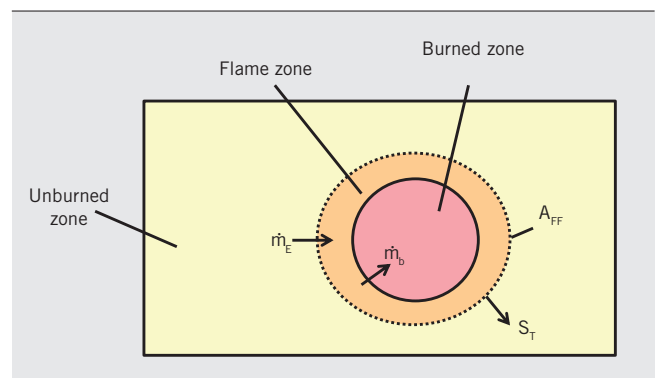
$$\text{EQ. 1} \quad \dot{m}_F = \int (\dot{m}_E - \dot{m}_b) dt$$

The mass flow out of the flame zone depends on its mass m_F , a characteristic burning time T_L and a model constant C_F :

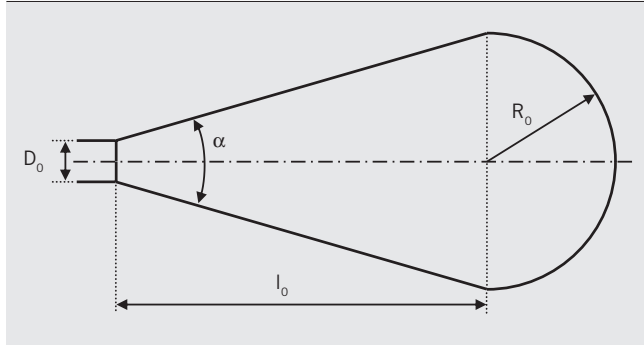
$$\text{EQ. 2} \quad \frac{dm_b}{dt} = C_F \cdot \frac{m_F}{T_L}$$



⑦ Evolution of the mean OH distribution and computed iso surface for $b=0.3$ for a λ_{CH_4} value of 1.5



⑧ Concept of the model for premixed flames



⑨ Assumed shape of the flame jet for the computation of volume and surface [Auer]

The calculation of the mass flow into the flame zone is based on the propagation of the flame front area A_{FF} with the turbulent burning velocity s_T into the unburned zone with the density ρ_u .

$$\text{EQ. 3} \quad \frac{dm_E}{dt} = \rho_u \cdot A_{FF} \cdot s_T$$

For the application of such a model for combustion engines with pilot injection two major submodels need to be modified. These are the modeling of the ignition delay and the propagation of the flame front in the early stages of the premixed combustion.

Based on the optical measurement data, ③, it is assumed that the combustion starts with jet shaped flames. From there the flame fronts propagate into the unburned region and finally overlap. To model this linear transition from the flame jets to the spherical flame front is chosen. As the penetration depth l_{K0} of the pilot fuel spray is larger than that of the flame jets for the scavenged pre-chamber, the linear transition takes effect for a longer period.

$$\text{EQ. 4} \quad A_{FF} = \left(1 - \frac{r_{flame}(\rho)}{l_{K0}}\right) \cdot A_{FF_jet} + \left(1 - \frac{r_{flame}(\rho)}{l_{K0}}\right) \cdot A_{FF_hemispherical}$$

The geometrical shape of the flame jet is necessary for the calculation of the surface area. It is assumed that it consists of a truncated cone and a hemisphere, ⑨. Thus the surface of the flame jet can be calculated during the combustion calculation while the flame front of the hemisphere is calculated in a preprocessing step and stored into a flame front area map.

As long as the flame zone is smaller than the maximum spray region unburned pilot fuel influences the pre-mixed combustion of the gas-air-mixture. This is accounted for by a model parameter that has an influence on the flame speed. The turbulence parameters were adjusted in a way that for the standard injector $C_s = 1$.

$$\text{EQ. 5} \quad S_{eff} = C_s \cdot s_T$$

When simulating the setup with a three-hole injector it was seen that $C_s = 1.5$ leads to good results. It is assumed that the difference in the combustion behavior is due to the different spray break-up of the injectors, which is characterized by the Weber number. Comparing the actual Weber numbers of the two injectors

it can be seen, that the quotient of the square roots of the Weber numbers leads to the applied value. For the validation of this equation more experiments with different nozzle geometries would be necessary.

$$\text{EQ. 6} \quad C_s = \sqrt{\frac{We_{3-hole}}{We_{6-hole}}}$$

More experiments with different injector nozzle geometries would be necessary to investigate the extent of validity of this equation.

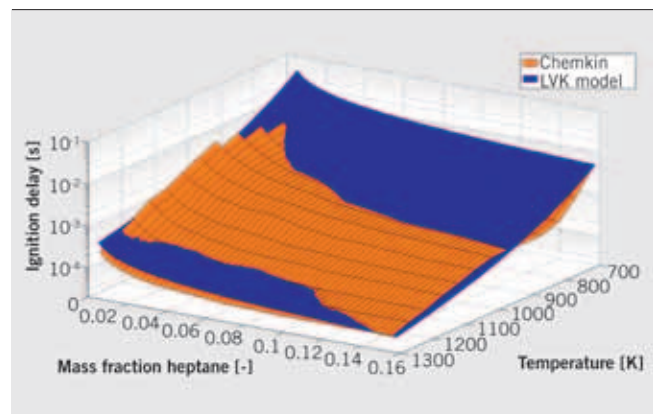
Modeling the ignition delay leads to more substantial changes to the combustion model. As the injection is of dominating importance a parcel model [21, 22] was used. Within this model the spray is divided into discrete parcels which composition changes after a distinct break-up time due to entrainment and evaporation. The state of each parcel is computed for each time step as temperature and composition form the basis for the calculation of the ignition delay. A one step mechanism was developed, ⑩, based on chemical reaction kinetics calculations with Chemkin using different reaction mechanisms [23, 24]. w_{Diesel} is the mass fraction of Diesel fuel within a parcel.

$$\text{EQ. 7} \quad \tau_{ZV} = c_1 \cdot \frac{1}{\lambda_{Gas-air-mixture} \cdot p_{Cyl}^{1.19} \cdot \chi_{Diesel}^{-0.65} \cdot e^{\frac{c_2}{T}}}$$

To account for the non-constant boundary conditions an ignition integral is computed according to the models for Diesel engines. Thus the condition for ignition can be described as

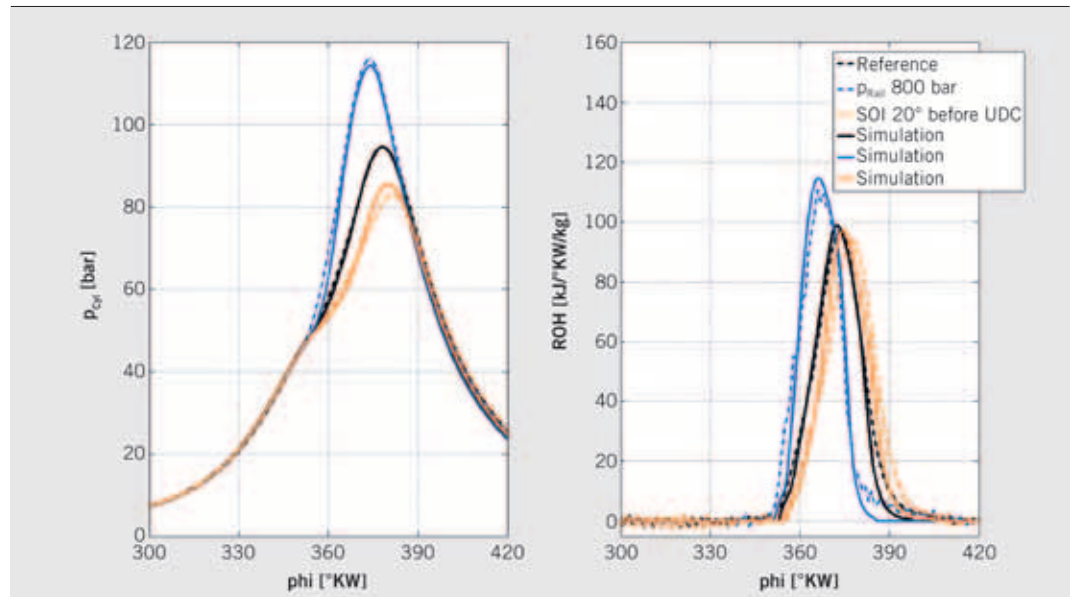
$$\text{EQ. 8} \quad \int_0^t \frac{1}{\tau_{ZV}} dt \geq 1$$

The results of the calculations are compared to operating data of the research engine for the final validation of the combustion model. As is typical for phenomenological models the parameters of the combustion model were adjusted to a single reference point which is presented in black in the figures. As an example different injection parameters are simulated using the phenomenological model, ⑩, and compared to measurement data. Moreover the influence of the configuration of the injector on the combustion



⑩ Comparison of ignition delays calculated with Chemkin and the one step mechanism created for the phenomenological combustion model, $p = 40$ bar, $\lambda = 1.66$

11 Results of the variation of rail pressure and start of injection on cylinder pressure and combustion rate starting from the reference point: duration of injection 350 μ s, start of injection 25° before TDC, $p_{\text{Rail}}=400$ bar, $p_L=1.04$ barR, $\lambda=1.5$

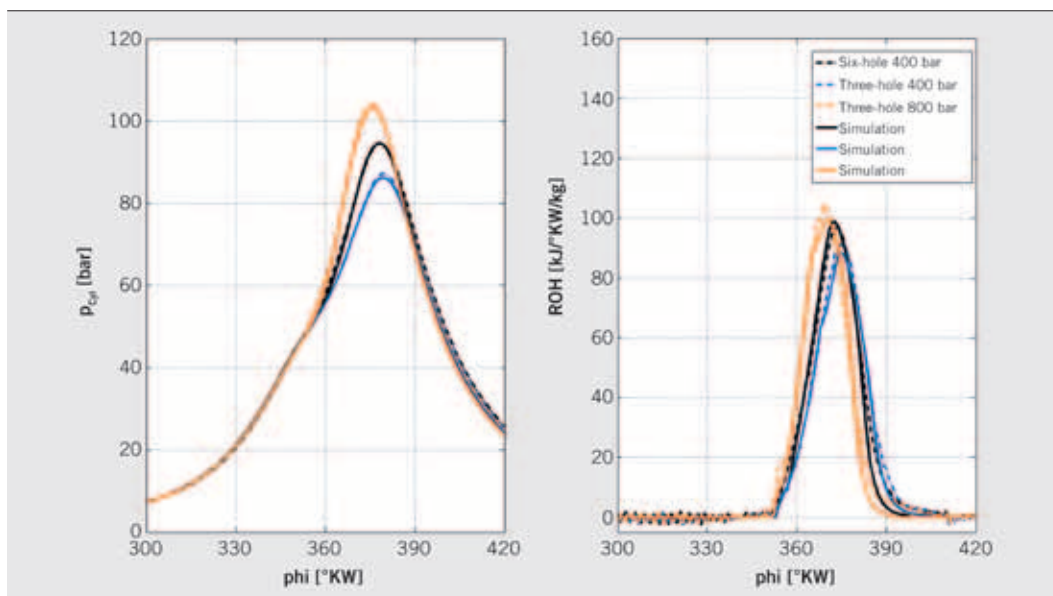


model is shown, 12. Based on the configuration for the reference point an operating point using the three-hole nozzle was computed. An additional operating point using the three-hole nozzle with a raised injection pressure of 800 bar shows that the simulation results for the applied value of $C_s=1.5$ are coherent.

Further variations of the boundary conditions [1] show that the model is capable of predicting the engine operating behavior for a multitude of parameters, e.g. loading pressure, injection duration and compression ratio. When applying the model to the use of different pilot fuels and gases it can be concluded that the pilot fuel and its break up behavior have a dominant influence on the first half of the combustion. As the shape of the piston has a major influence on the flow and especially the turbulence within the combustion chamber optimization in this research area requires 3D CFD calculations.

5 SUMMARY

Two models for lean-burn premixed gas engines with pilot injection were developed based on data from an optically accessible test rig and from a modified heavy-duty single cylinder engine. The first can be used for combustion simulation within the framework of 3D CFD solvers whereas the second model is of a phenomenological nature and can be employed in work cycle simulations. Both share the concept of using different models for the computation of injection and self-ignition on the one hand and premixed combustion on the other. The models are based on substantial experimental data, mainly carried out using a single stroke free floating piston test rig and a modified single-cylinder research engine. Thus the fundamental processes dominating the ignition



12 Simulation of the three-hole injector nozzle for different rail pressures based on the simulation of the reference point: duration of injection 350 μ s, start of injection 25° before TDC, $p_{\text{Rail}}=400$ bar, $p_L=1.04$ barR, $\lambda=1.5$

and flame propagation phase could be investigated. Moreover the test data was used for the adjustment and the validation of the combustion models.

It was shown that with both models it is well possible to predict the combustion behavior under different operating conditions. Moreover the results of the research project improve the understanding of the ongoing physical and chemical processes as well as the influence of the internal engine processes on combustion.

REFERENCES

- [1] Walther, H.-Ph.; Schlatter, S.; Wachtmeister, G.; Boulouchos, K.: Bericht zum FVV-Vorhaben Nr. 960, Frankfurt am Main, 2011
- [2] Troberg, M.; Delneri, D.: Roadmap zur Erfüllung der Tier-III-Abgasnorm für Schiffsmotoren. In: MTZ 71 (2010), Nr. 06, S. 394-401
- [3] Escher, A.; Wright, Y. M.; Boulouchos, K.: Visualisierung, thermodynamische Analyse und Simulation von neuen Brennverfahren in einem optisch zugänglichen Versuchsträger. 11. Tagung „Der Arbeitsprozess des Verbrennungsmotors“ (2007), Graz, Austria
- [4] Yakhot, V., Smith, L.M.: The Renormalization Group, The ϵ -Expansion and Derivation of Turbulence Models. Journ. Sci. Comp. (1992) 7, pp. 35-61
- [5] Huh, K. Y.; Gosman, A. D.: A phenomenological model of diesel spray atomization. Proc. Int. Conf. on Multiphase Flows (1991), Tsukuba, Japan
- [6] Reitz, R.D.; Diwakar, R.: Effect of drop breakup on fuel sprays. SAE Technical Paper 860469
- [7] STAR-CD Methodology guide Version 4.12
- [8] Weller, H. G.; Uslu, S.; Gosman, A.D.; Maly, R. R.; Herweg, R.; Heel, B.: Prediction of Combustion in Homogeneous-Charge Spark-Ignition Engines. 3rd Int. Symp. On Diagnostics and Modelling of Combustion in Internal Combustion Engines (1994), Yokohama, Japan
- [9] Heel, B.; Maly, R.; Weller, H. G.; Gosman, A.D.: Validation of SI combustion model over range of speed, load, equivalence ratio and spark timing. Proc. 4th Int. Symp. On Diagnostics and Modeling of Combustion in Internal Combustion Engines (1998), pp. 255-260, Kyoto, Japan
- [10] Gülder, Ö.L.: Turbulent premixed flame propagation models for different combustion regimes. Symp. Int. Comb. (1991) 23, pp. 743-750
- [11] Bilger, R.: Conditional moment closure for turbulent reacting flows. Phys. Fluids A, 5, pp. 436-444
- [12] Klimenko, A. Y.: Multicomponent diffusion of various admixtures in turbulent flow. Fluid Mech. 25, pp. 327-334
- [13] Wright, Y.M.; De Paola G.; Boulouchos, K.; Mastorakos, E.: Simulations of spray auto-ignition and flame establishment with twodimensional CMC, Combustion and Flame 143, pp. 402-419, 2005
- [14] De Paola G.; Mastorakos E.; Wright Y. M.; Boulouchos K.: Diesel Engine Simulations with Multi-Dimensional Conditional Moment Closure, Combustion Science and Technology, Volume 180, Issue 5, pp. 883 - 899, 2008
- [15] Liu, S.; Hewson, J. C.; Chen, J. H.; Pitsch, H.: Effect of strain rate on high-pressure non-premixed n-heptane autoignition in counterflow. Combust. Flame (2004) 137, pp. 320-339
- [16] Schlatter, S.; Wright, Y. M.; Schneider, B.; Boulouchos, K.: Proceedings of the 7th Dessau Gas Engine Conference, Dessau, Germany, 2011
- [17] Karim, G.A.: Combustion in Gas Fueled Compression Ignition Engines of the Dual Fuel Type. ASME J. Eng. Gas Turbines and Power (2003) 125, pp. 827-836
- [18] Liu, Z.; Karim, G. A.: The Ignition Delay Period in Dual Fuel Engines. SAE paper 950466
- [19] Mbarawa, M.: A correlation for Estimation of Ignition Delay of Dual Fuel Combustion Based on Constant Volume Combustion Vessel Experiments. R & D Journal (2003) incorporated into The SA Mechanical Engineer 19, pp. 17-22
- [20] Auer, M.: Erstellung phänomenologischer Modelle zur Vorausberechnung des Brennverlaufes von Magerkonzept-Gasmotoren, München, Technische Universität, Dissertation, 2010
- [21] Stiesch, G.: Phänomenologisches Multizonen-Modell der Verbrennung und Schadstoffbildung im Dieselmotor. Düsseldorf, VDI Verlag, 1999
- [22] Thoma, M.: Modellierung der Voreinspritzung bei dieselmotorischer Verbrennung, Düsseldorf, VDI Verlag, 2004
- [23] Engine-Research-Center: Engine Research Center, University of Wisconsin – Madison, Chemical Reaction Mechanisms. Online, Zitat vom: 7. September 2010, <http://www.erc.wisc.edu/chemicalreaction.php>
- [24] Center-for-Energy-Research: University of California, Center for Energy Research, Combustion Division, 2010, Zitat vom: 7. September 2010, <http://www-mae.ucsd.edu/~combustion/cermech/index.html>

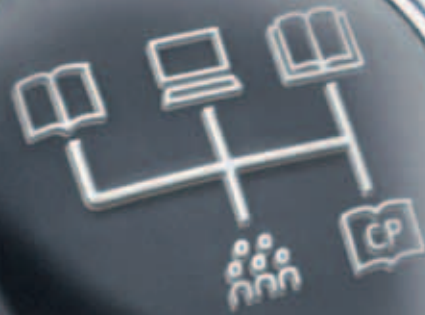
THANKS

This investigation was performed in the context of a research project (No. 960) by the Forschungsvereinigung Verbrennungskraftmaschinen e.V. (FVV, Frankfurt), which was accompanied and supported by a working group populated by representatives of industry. The authors would like to express their thanks to the working group and its leader, Dr.-Ing. Ioannis Vlaskos of Ricardo Deutschland GmbH, for substantial support and finances provided for the fuel gases.

The project (Nr. 15590 N) was encouraged by the Federation of Industrial Research Associations (AiF) under patronage of the Federal Ministry of Economics and Technology (BMWi) as well as by the Swiss Federal Office of Energy (BfE-Nr. 102668).

The Best for Your Communication. On the right track.

personal buildup for Force Motors Limited Library



Best Ad Media spreads your message via professional journals, online solutions and textbooks | Specialised books in print and e-book form, events and other media formats tailored to your individual needs. As part of the renowned specialised publisher Springer Fachmedien Wiesbaden GmbH we help you reach decision-making target groups in business, technology and society. All the solutions for your communication needs - at your fingertips!

www.best-ad-media.de

Richtig schalten.



AUTHORS



DR.-ING. DIRK GOSSLAU
is responsible for
Research Projects at the
Chair for Automotive
Technology and Drives
at the BTU Cottbus
(Germany).



**PROF. DR.-ING.
PETER STEINBERG**
is Head of the Chair for
Automotive Technology
and Drives at the
BTU Cottbus (Germany).

PREDICTIVE COOLING SYSTEM CONTROL TO REDUCE FUEL CONSUMPTION

In this post by the BTU Cottbus, a predictive component is added to the cooling system control. It considers the behavior of the driver and the vehicle environment. Basic idea is the use of the thermal inertia of components and fluids, to raise the average component temperatures, without exceeding the standard peak temperatures. Significant fuel consumption savings have been identified with the predictive control, which can be realized without additional sensors/actuators.



| | |
|---|---|
| 1 | INTRODUCTION: STEADY STATE AND TRANSIENT TEMPERATURE BEHAVIOR |
| 2 | PREDICTIVE THERMAL MANAGEMENT |
| 3 | COOLING SYSTEM CONTROL AND RESULTS |
| 4 | CONCLUSION AND OUTLOOK |

1 INTRODUCTION: STEADY STATE AND TRANSIENT TEMPERATURE BEHAVIOR

One of the design points of cooling system is heat transfer in the maximum effective horsepower point. The cooling system is oversized for the heat dissipation in partial load and at low speeds and thus adjusts to low component temperatures, see left diagram in ❶. The coolant and thus the device temperature is raised, can be potential of fuel consumption saved without further measures, as shown in ❷ on the right diagram.

Due to the usual system pressure boundaries the coolant temperatures can't be set higher than about 115 °C. This results in a certain value of heat removal, depending on coolant pump speed. This value can't be underrun. There is a minimum flow rate necessary to avoid the handling of (deliberate) local bubble boiling in film boiling and thus the formation of insulating vapor layers with hotspots. For stationary operation the coolant and thus component temperatures so not to raise without serious changes to the cooling system.

The theoretically possible consumption benefits by raising the average temperature of the components were determined on engine test bench, and are shown in ❷. The amount of air needed decreases during increasing mechanical efficiency with increasing temperature. Two effects are responsible for the lower air effort. On the one hand, thermal de-throttling takes place with increasing temperature, on the other hand, the air intake at the same collector temperature in the cylinder at higher temperatures of the parts is heated more than in the series. This means higher compression end temperatures with less necessary fresh-air mass. The

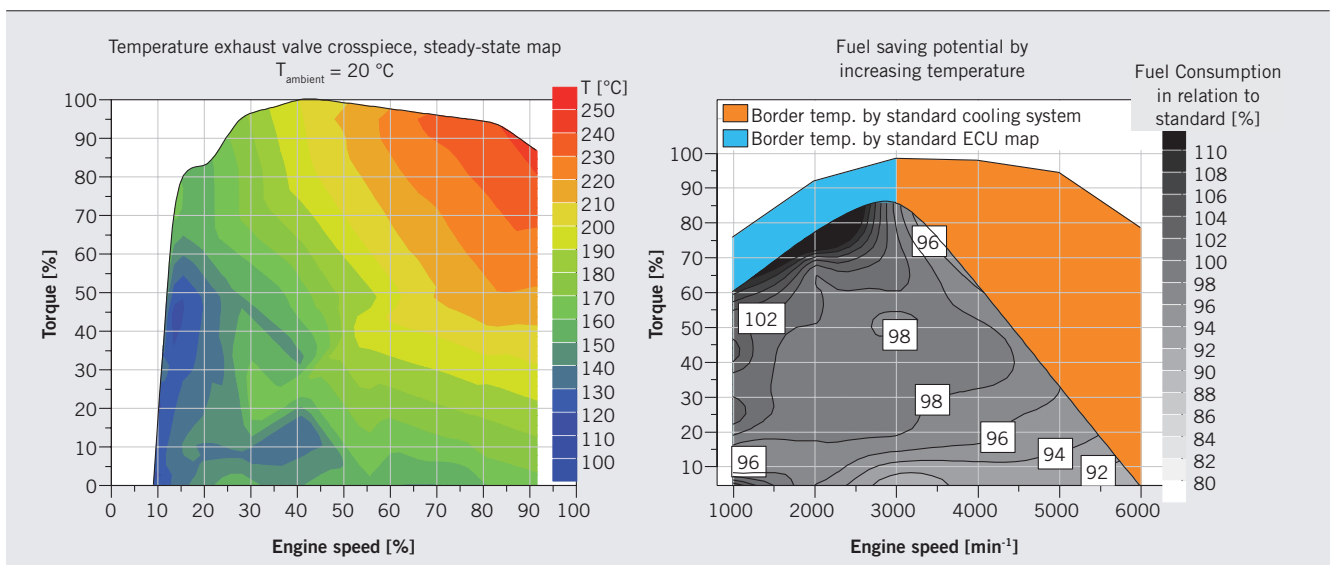
compression work decreases. The higher temperature level leads to faster burning and reaching a higher peak pressure. There is therefore an approach to the constant-volume cycle. These laws apply in the entire engine map, however, hardly a temperature increase is possible at high speeds and loads.

Component temperature gradients, which are mainly load and speed dependent arise in real road trip. A quiet and a dynamic driver on each same track are compared in ❸. Despite the average of performance requirement of the dynamic driver is four times higher as the the value of the calm driver is, nearly same average component temperature is set. With high performance requirements the cooling system large coolant flow rates and low temperature adjusts so, that the component border temperatures at sustained high load would not exceeded. Reduces the load quickly; as is the case on extra urban roads and in cities; is the temperature of the component then to significantly lower values than for example in steady state operation. This has strong cooling of the engine in this low-load phase and only slow heating with short pulses of load result. Target of a predictive controller is the estimate of expected heat coupling from combustion and friction and the cooling potential expected.

2 PREDICTIVE THERMAL MANAGEMENT

2.1 BASIC IDEA

A forward-looking component is to be provided to the ECU, in particular to the cooling system controller. This is to make the fuzzy estimation of heat removal expected and the cooling potential expected. Thus, the controller has the ability to compare between the two and on the basis of the current, calculated and the precomputed parts temperature set at least need cooling performance. This should highly dynamic processes, for example in the taking on a highway or the rapid overtaking occur, lead as long as not to increase the cooling performance, use up the cooling component protection must start. The driving conditions are influenced mainly by the driver, track type and -profile, and the traffic environ-



❶ Standard component temperatures (left) and potential for fuel consumption by raising the temperature of the coolant (right)

ment, ④. Each driving state reflects a combination of all factors with each discrete values. Based on the data of the various factors, it should be possible to compare the current with the prospective values of cooling requirement and cooling potential. In addition to the reduction of specific fuel consumption as a result of higher component temperatures, a consumption advantage by the lower average drive power of coolant pump and fan is to expect.

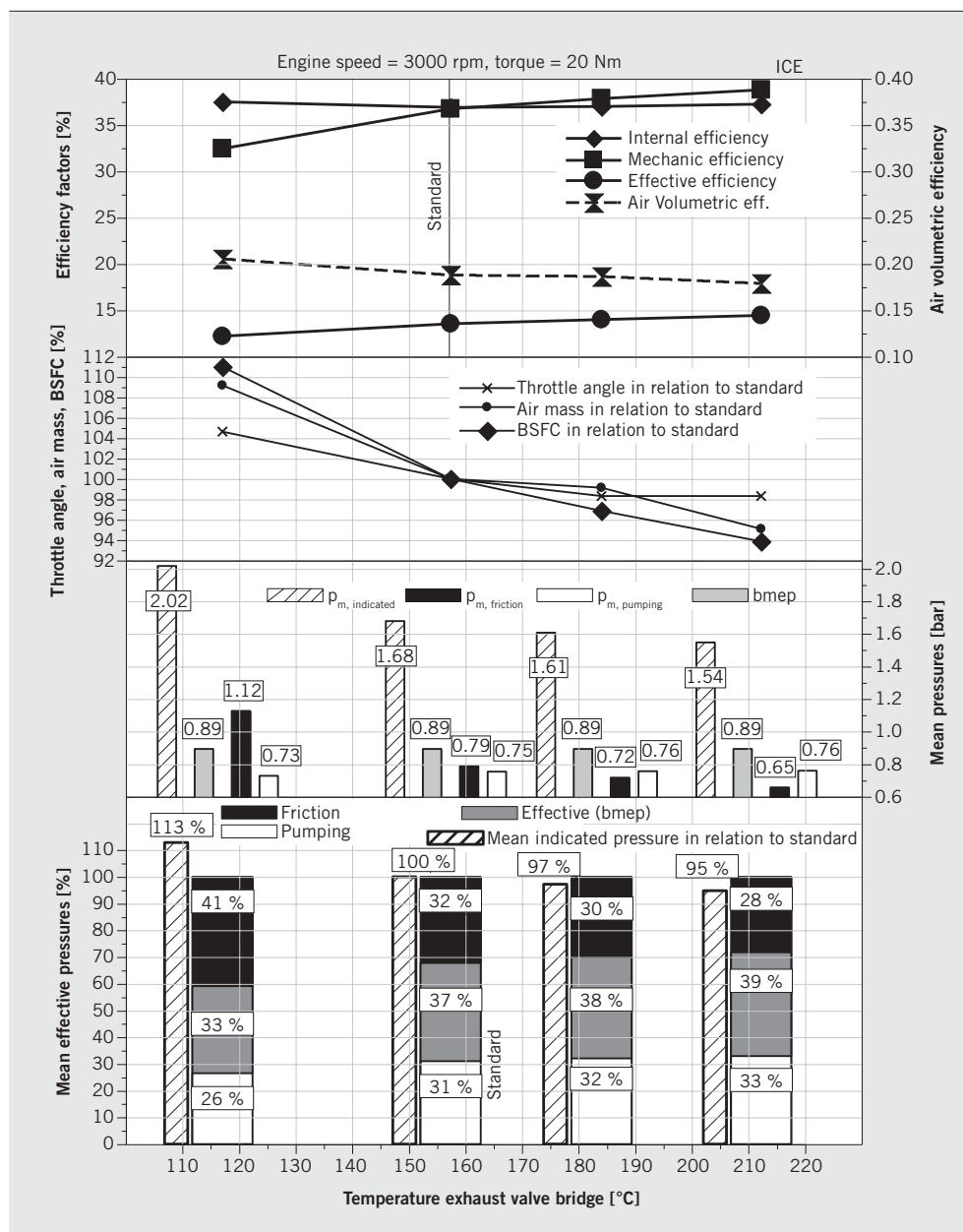
2.2 RELEVANCE AREAS OF PREDICTIVE THERMAL MANAGEMENT

Knowledge of the frequency distribution of the driving conditions and the resulting frequently engine operating points is useful for the assessment of practicable consumption potential. To do this, field tests were carried out with several people on public roads. There were also data from the engine-CAN and vehicle-CAN meas-

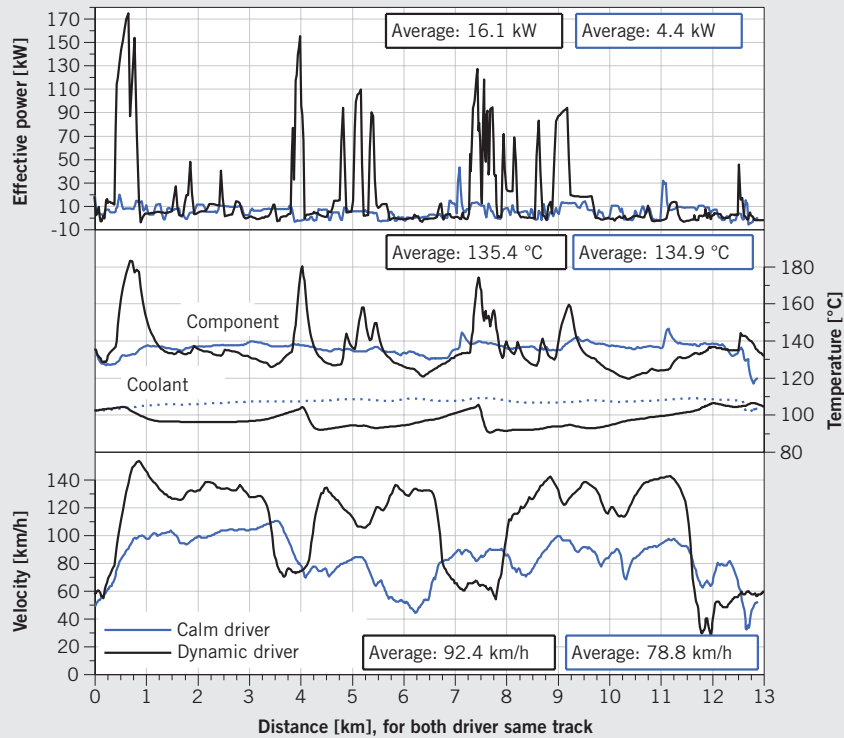
ured to transfer driving test values to the dynamic engine test bench to handle the calibration of predictive controller for cooling system under realistic conditions.

The following statements can be derived from the frequency distribution is shown in ⑤:

- : Idle represents the most common point of operation with a 12 % share, the second most common point of operation is at 13 % of load and 23.6 % of maximum engine speed.
- : The vehicle was operated in more than 80 % of all run-time components in lower partial load at low speeds, the full load rate is 2 %.
- : A very calm driver in the city is represented approximately with the NEDC.
- : Real ride a temperature of 126 °C in the cylinder bar adjusts in the most common operating point, steady state, however, of 144 °C. Considered engine the fuel consumption potential hid-



② Calibration and thermodynamic parameters at change of component temperature



3 Comparison of a calm and a dynamic driver on the extra urban roads

den alone in the dynamics is at a temperature elevation of 18 K at around 2 %.

In cities is driven with low load in a relatively broad speed range, on country roads with slightly higher loads in narrow speed range and on motorways with medium-sized loads in an once again narrower speed range. Dynamic driver widen the load as well as the speed ranges from calm.

Thus, raising the average component temperatures in the lower and middle section of engine map can cover most of the actual operating conditions of the engine.

2.3 TYPE DETECTION

The predictive control of cooling system is dependent on the knowledge of the type of driver and the type of road. The driver type provides information about the dynamics of the engine performance requirement and thus of generation of heat. The road type describes the average level of performance requirement and generation of heat. The road type must be complemented by a detection of inclination and gradient rides. They mean an offset of effective power output in positive or negative direction. Journeys with maximum payload or towable mass can be depicted so also. To achieve the type of detections without additional sensors, only data of the standard existing in-vehicle control units were analyzed. Navigation data were not included.

To set the maximum time intervals for decisions of the cooling system controller, the time constants in the test with corresponding application of the standard cooling system controller have been identified.

The road type was distinguished in town, road and motorway. Here, not the actual topographical accuracy, but the figure of the respective operating status is important. The road type variables to recognize quickly and reliably on the one hand the operation corresponding to the three track types, on the other hand to avoid fast back and fro between the types.

From the variety of the available variables were the meaningful with the help of a hypothesis matrix selected and combined by subsequent classification. Most expressive for the distinction of the three types of track the variables proved gear, engine speed, driving pedal angle, injection volume, yaw angle and brake application.

For the resulting variable SE_{10s} , typical value ranges for each type of track were determined by frequency distribution.

Using value queries a variable can be made now track type ST, which arises from the mean value of each variable and the route recognition SE_{10s} and takes only values between -2 for cities and +4 for motorways. Each variable is represented twice, on the one hand direct, on the other hand indirectly by SE_{10s} , each weighted in ST. As a result, a misinterpretation can be minimized, for example if a variable lights atypical values. As an example rolling at high speed idle that listed, the size of SE_{10s} take negative values by very small values for the $n_{standard engine}$, and a value of 0 for gang-
norm. This would lead to the classification as urban track. The individual review of the variable and SE_{10s} and the subsequent averaging falls ST only to values for extra urban road. This is shown in 6 for downshifting from 6th gear in the 3rd represented at 120 km/h, see values at t=1890 to 1895s.

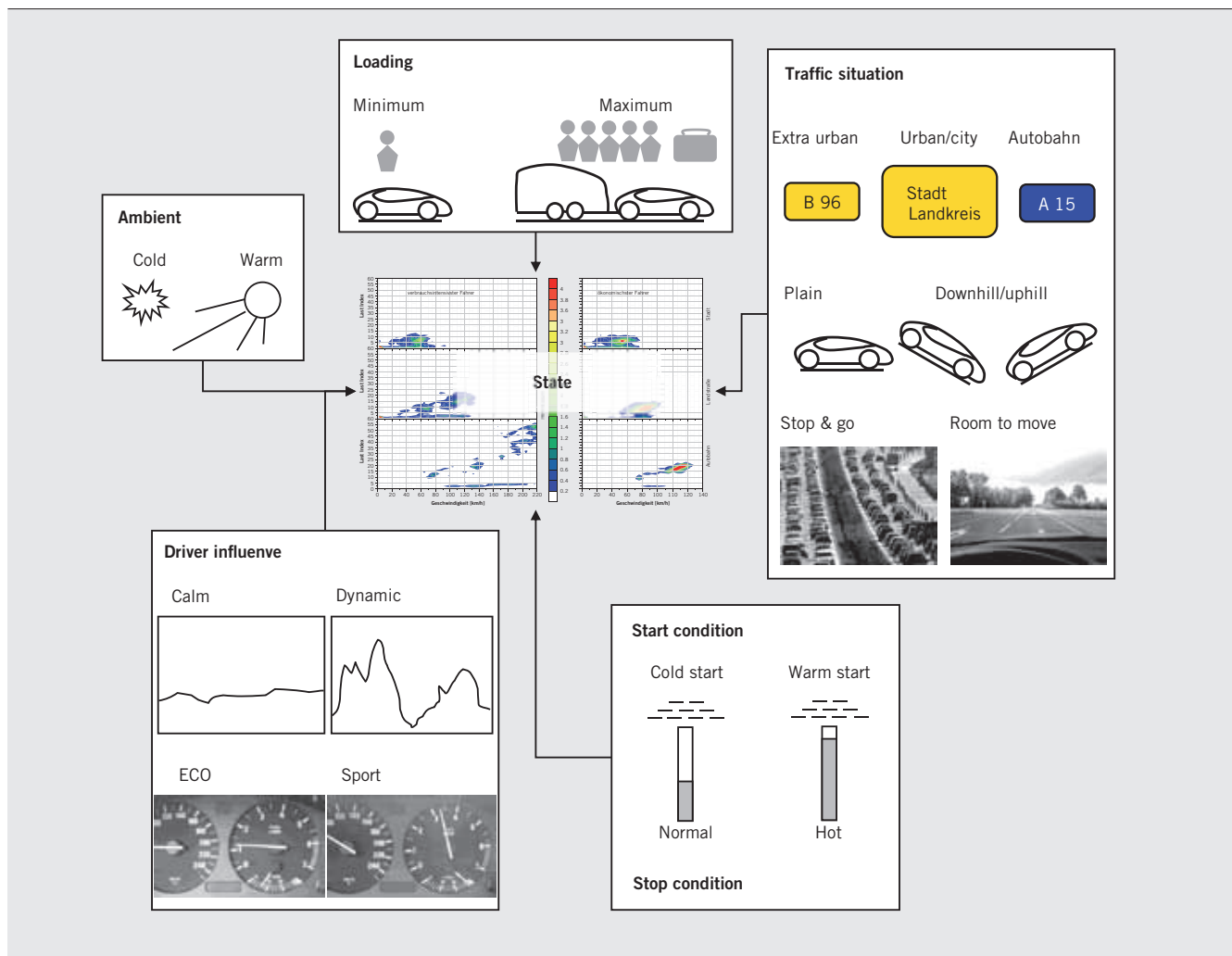
By including the speed hit accuracy arise between 71 and 81 % with respect to the topographical track types. Here, it should again be noted, not the topographic road type transition, but the driving state dragging modified by the driver to be meaningful for heat removal and cooling potential.

Uphill driving is determined by means of comparison of the delivered power to the wheels with the drag equation. The wheel performance obtained from the engine torque model, the engine speed, as well as test bench correlated towing performance corrections was compared with the necessary drag performance resulting from the drag equation. Gradients are reliably detected with this method and exactly reproduced on approximate, $0,5^\circ$. On downhill driving, it is important to distinguish between braking and downhill. While the signal of the brake application delivers a clear statement, but does not reflect the strength of the brake application. Therefore, a finding a match based on the averaged longitudinal acceleration and the position of the driving pedal was carried out. Thus, downhill rides can be reliably identified, a statement about the gradient angle cannot be made however.

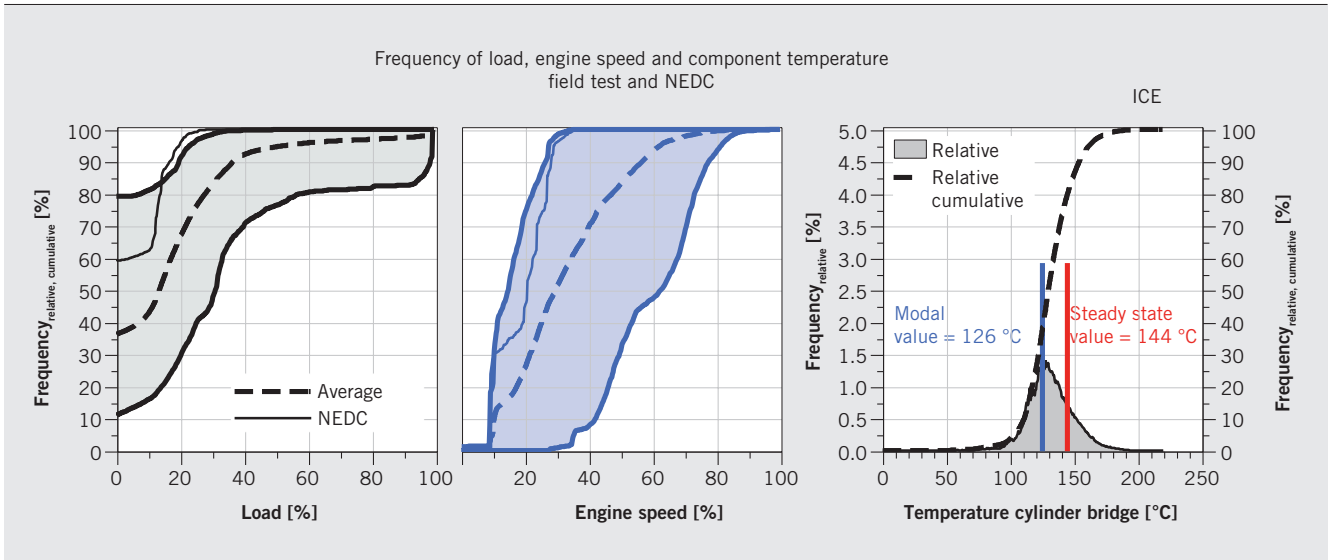
The driver type variable is intended to influence the rapidness of cooling system controller. Information about changing ampli-

tudes, their gradient and the frequency of the quantities affecting the generation of heat and cooling potential are necessary. Engine performance proved it most appropriate, the entries of the heat from combustion and friction are included in it. Drive power, required for a specific driving state, only dependent on the vehicle and the drag coefficients. With enough long viewing time, the value for the set performance for all driver types adopts similar values, for example in urban driving are about 2 to 5 kW required for the considered vehicle. However, the necessary times are too long for the cooling system control. It is interesting for the assignment of a particular driver to the range of the total surveyed drivers as an average adjusted performance is realized.

⑦ shows significant differences for five drivers (which are all examined drivers representative) in the performance requirement. Driver 2 provides a high performance and switches with high frequency. The current variation of the mean moving about 60 s moves often at values of 50 to 100 kW. This driver can be described as very dynamically with high performance requirements. Driver 4 provides a very low performance on average. The variation of the mean moving about 60 s maximum 25 kW of long fields but only 0 to 5 kW. This driver can be considered to be calm with low load re-



④ Influences on the observed and predicted driving state

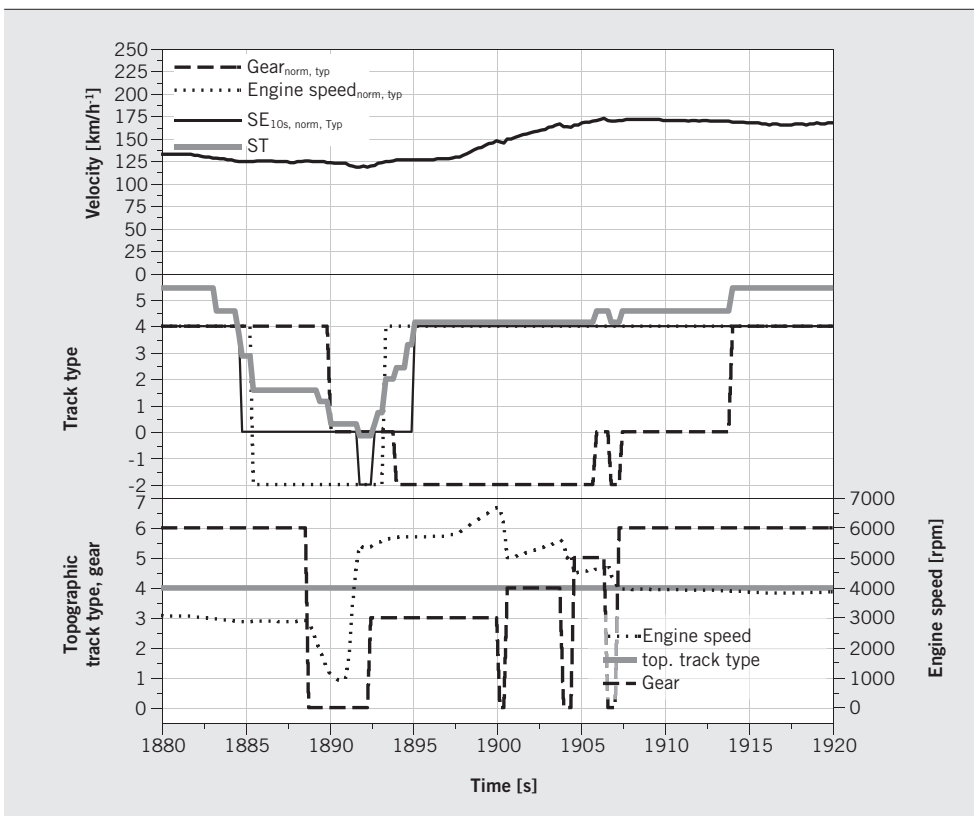


5 Frequency of load, speed and component temperature from field tests

quest. The interval of 60 s for the moving average proved a most appropriate, on the one hand the individual driver differences clearly highlight and on the other hand the time constants of the cooling system does not meet, which would lead a thermostatic regulation similar to oscillations in the course of the temperature.

The gradient of the driving pedal angular speed often used for the driver type assessment for adaptive automatic transmission

controls [1] was also investigated for its suitability as a vivacious driver assessment. The comparison of the current deviation from moving mean about 60 s for this size with the which drag power showed that misinterpretations are possible when using the driving pedal angle due to lack of information about the generation of heat, that when using the drag power as a raw value does not occur.



6 Downshift at 120 km/h, history of the individual variable mappings

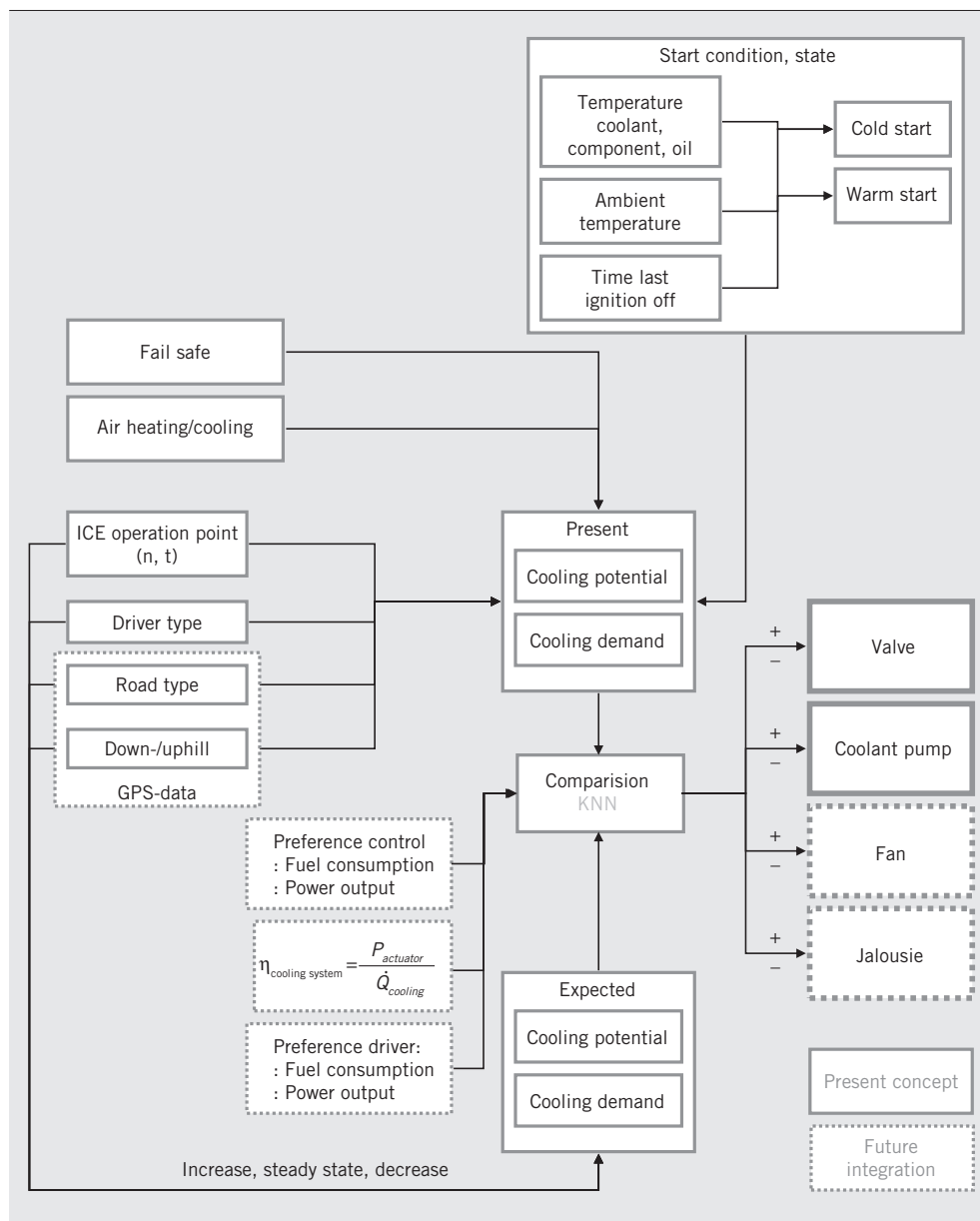
The classification of the type of driver is done using analog value ranges from the combination of the set effective power and the current variation of the moving mean of it. Both enter into with the frequency of their occurrence in the classification.

3 COOLING SYSTEM CONTROL AND RESULTS

The concept of control shown in ❸ compares the heat removal to be expected with the cooling potential expected and takes deci-



❷ Current variation of the moving mean about 60 s of the effective brake power, five drivers on FTA circuit



8 Concept of predictive cooling system controller

sions on the regulation of coolant pump and mapped thermostat afterwards. The road type predicts the expected range and the driver type the kind of performance requirements.

The controller concept was adapted on engine test bench with real driving profiles from the field tests. This was an in-vehicle used identical engine used. To cover the consumption statements, every attempt was driven three times under identical environmental conditions.

The comparison of dynamic and calm drivers on road trip (each same section), each with the standard ECU map of cooling system control compared with predictively applied regulation to the test is shown in 9.

The average temperatures of the parts from the calm driver increased to 4 K and from the dynamic driver raised to 15 K. Component temperatures reached maximum about 10 K higher than in standard map, however, are still far from the component border

temperature. Consumption was reduced by 0.25 % for the calm driver and 1 % for the dynamic driver.

In urban driving, 10, a temperature increase to 26 K succeeds in dynamic driving. This leads to a fuel saving of 3 %. In a calm driving, about 5 K be achieved higher temperatures, however, did not lead to any significant benefit of consumption.

4 CONCLUSION AND OUTLOOK

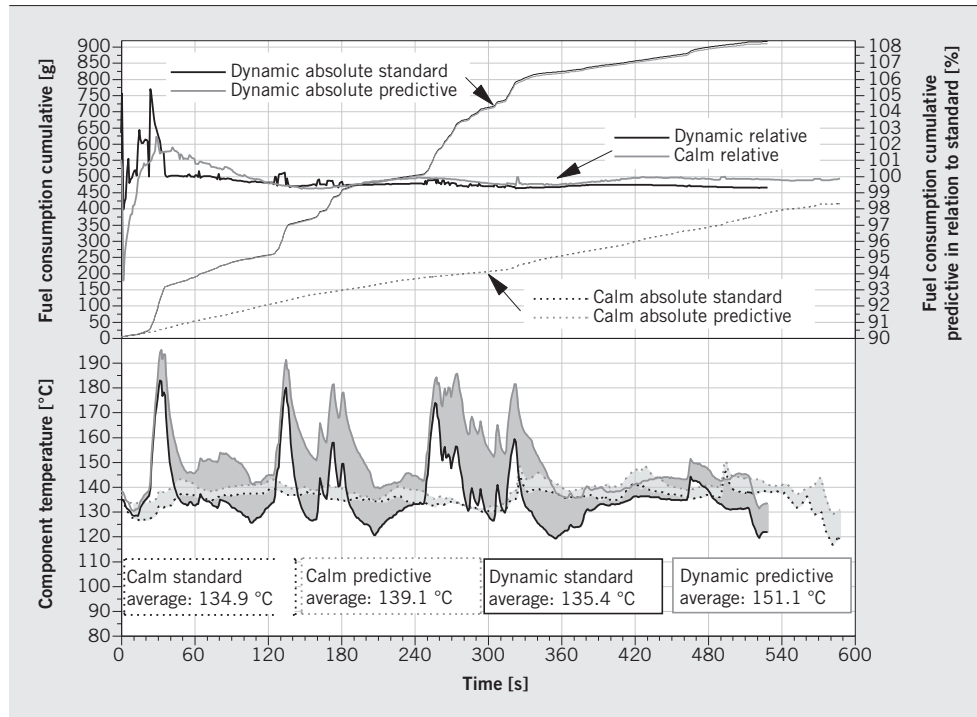
With the predictive cooling system control significant advantages can be achieved by raising the middle component temperatures. The shown potential is achieved only by taking advantage of the dynamics in the vehicle and the heat storage capacities in components and fluids. The comparison of currently existing heat input and cooling potential with the predicted values is the base of the controller. Road types, profiles and driver types are used, the

values of them are generated by classification and consideration of the frequencies from variables of ECU.

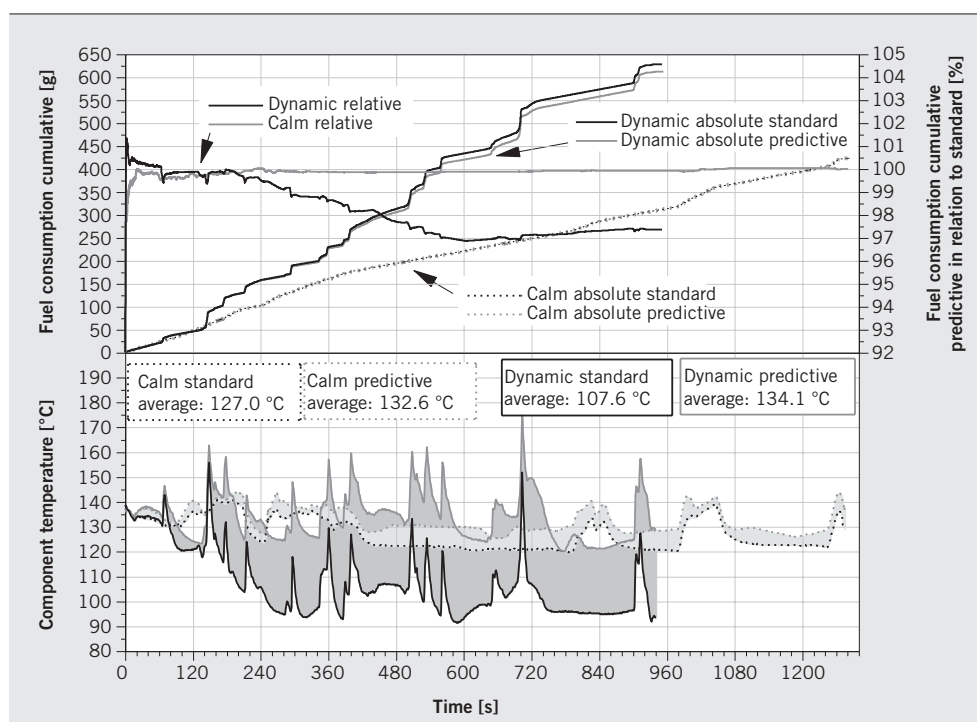
The potential for fuel consumption each is the minimum for the examined driving states and driving situations. The full potential of forward-looking control requires the use of artificial neural network (KNN) as the controller. It results from the demand to set optimum component temperatures for every driver in every situation

on all road types. These cases can be operated with conventional controls only with appropriate safety margin to the component temperature or with a not manageable calibration work.

The system can be further improved by a quick three-way valve replaces the standard map-controlled thermostat. In particular the closing of conventional thermostats is directly dependent on the coolant flow rate and the temperature of the coolant at the



9 Component temperatures and fuel consumption in the standard calibration and predictive calibration, dynamic and a calm driver on extra urban road, part of FTA circuit on engine test bench



10 Component temperatures and fuel consumption in the standard calibration and predictive calibration, dynamic and a calm driver on urban road, part of FTA circuit on engine test bench

wax cartridge, the thermostat closes so when faster removal of load too slowly.

Contrary to reduce fuel consumption improve filling by fast coolant and component temperature reduction is when the controller expected high performance requirements. However, it is to be expected, insofar as the benefit of filling in the performance is noticeable with very good acceptance.

REFERENCES

- [1] Küçükay, F.; Renoth, F.: Intelligente Steuerung von Automatikgetrieben durch den Einsatz der Elektronik. In: ATZ 96 (1994), No.4, pp. 228-235
- [2] Neunzig, D.; Benmimoun, A.: Potenziale der vorausschauenden Fahrerassistenz zur Reduktion des Kraftstoffverbrauches; 11. Aachener Kolloquium Fahrzeug- und Motorentechnik 2002; Vol. 2, pp. 1205-1238
- [3] Beßlein, W.: Verminderung der Schadstoffemissionen und des Kraftstoffverbrauches, insbesondere während der Warmlaufphase und im unteren Leistungsbereich, bei einem schnelllaufenden Viertakt-Diesel-Direkteinspritzer durch variable Heißkühlung; 1985; Forschungsberichte Verbrennungskraftmaschinen/1982/M86022054363 Report
- [4] Betz, J. et al.: Entwicklung von Motorkühlsystemen bei erhöhten Anforderungen an transiente Bedingungen; Internationales Wiener Motorensymposium, 22-Fortschritt-Berichte VDI, Reihe 12: Verkehrstechnik/Fahrzeugtechnik/2001/20011001009 Beitrag (conference)
- [5] Bronstein, A.; Semendjajew, B.: Taschenbuch der Mathematik; Verlag Harri Deutsch, Thun Frankfurt/M.; 1989
- [6] Goßlau, D.; Steinberg, P.: Heat Management for an IC Engine in Consideration of Driver Behaviour and surrounding Area of the Car; FISITA 2004 World Automotive Congress, Barcelona; 2004; Paper Code F2004F433-paper
- [7] Goßlau, D.: Vorausschauende Kühlsystemregelung, Diss. BTU Cottbus, Shaker Verlag, Aachen 2009